Application of the Local Mode Model to CH-Stretching Overtone Spectra of Substituted Benzenes and Related Compounds: Analysis of Structurally and Conformationally Inequivalent CH Bonds

by

Kathleen M. Gough

A Thesis Submitted to
the Faculty of Graduate Studies
of the University of Manitoba
in partial fulfillment of
the requirements of the degree
Doctor of Philosphy

Winnipeg, Manitoba

February 1984

APPLICATION OF THE LOCAL MODE MODEL TO CH-STRETCHING OVERTONE SPECTRA OF SUBSTITUTED BENZENES AND RELATED COMPOUNDS: ANALYSIS OF STRUCTURALLY AND CONFORMATIONALLY INEQUIVALENT CH BONDS

BY

KATHLEEN M. GOUGH

A thesis submitted to the Faculty of Graduate Studies of the University of Manitoba in partial fulfillment of the requirements of the degree of

DOCTOR OF PHILOSPHY

© 1984

Permission has been granted to the LIBRARY OF THE UNIVERSITY OF MANITOBA to lend or sell copies of this thesis, to the NATIONAL LIBRARY OF CANADA to microfilm this thesis and to lend or sell copies of the film, and UNIVERSITY MICROFILMS to publish an abstract of this thesis.

The author reserves other publication rights, and neither the thesis nor extensive extracts from it may be printed or otherwise reproduced without the author's written permission.

Abstract

CH-stretching overtone spectra of substituted benzenes in the liquid (Δv = 2-7) and gas (Δv = 2-5) phases were obtained. The spectra were analyzed according to the local mode model, in which molecules behave as if all vibrational quanta were deposited in a single one of a set of equivalent CH oscillators. The overtone spectra of molecules containing structurally and conformationally inequivalent CH bonds have resolved peaks which exhibit the behaviour of a set of uncoupled anharmonic diatomic oscillators.

The spectra were obtained with Cary 14, Cary 219 or Beckman 5270 spectrophotometers. All overtone bands were digitized, manually or electronically, and analyzed with band fitting programs on Nicolet 1180 or 1280 data systems.

Partly resolved peaks due to vibrational excitation of inequivalent CH (CD) bonds were observed and assigned in the liquid phase spectra of nitrobenzene, 3,4,5-tri-, 2,3,4,5-tetra- and penta-deuteronitrobenzene, and in the gas phase spectra of mono, 1,2-di- and 1,3-difluorobenzene. The gas phase spectra of 1,4-di-, 1,3,5-tri-, 1,2,3,4-, 1,2,3,5-, and 1,2,4,5-tetrafluorobenzene exhibited only single peaks at each overtone. The existence of inequivalent CH bonds in a series of halogenated benzenes was inferred from the analysis of liquid phase spectral shifts and linewidths, and of gas phase spectra for α,α,α-trifluorotoluene. CH bond lengths decrease with increasing proximity to these substituents, due to their sigma electron withdrawing and pi electron donating properties. The bond length changes and their relationship to electron redistribution were supported by molecular orbital geometry optimization at STO-3G and 4-21G levels.

Aryl and methyl CH bands were well resolved in the gas phase spectra of toluene and the xylenes. Overtone vibrations of structurally inequivalent aryl and conformationally inequivalent methyl CH bonds were also observed and assigned, again supported by STO-3G and 4-21G calculations. Increasing involvement in hyperconjugation causes an increase in methyl CH bond length on rotation from 0° to 90° to the ring plane.

Overtones of ethylenic and methylenic CH bonds were resolved in the gas phase spectra of 1,3- and 1,4-cyclohexadiene. The 1,3-isomer is twisted; the methylenic CH bonds have axial/equatorial character. The 1,4-isomer is planar; the four methylenic CH bonds are equivalent.

Overtones of conformationally inequivalent methyl CH bonds were observed in the liquid and gas phase spectra of anisole.

List of Publications and Theses

1. K.M. Gough and B.R. Henry, "Overtone Spectral Investigation of Substituent Induced Bond Length Changes in Gas Phase Fluorinated Benzenes and their Correlation with Ab Initio STO-3G and 4-21G Calculations", J. Am. Chem. Soc., 106, 2781-7 (1984).
2. K.M. Gough and B.R. Henry, "Gas Phase Overtone Spectral Investigation of Inequivalent Aryl and Alkyl CH Bonds in Toluene and the Xylenes", J. Phys. Chem., 88, 1298-1302 (1984).
3. K.M. Gough and B.R. Henry, "The CH-Stretching Overtone Spectra of Nitrobenzene and its Deuterated Derivatives: Assignment of the ortho-CH", J. Phys. Chem. 87, 3804-5 (1983).
4. K.M. Gough and B.R. Henry, "The CH-Stretching Overtone Spectra of Nitro- and Halo-Substituted Benzenes: A Local Mode Investigation of Substituent Effects", J. Phys. Chem. 87, 3433-41 (1983).
5. K.M. Gough and B.R. Henry, "Applications of the Local Mode Model to CH Bond Length Changes, Molecular Conformations and Vibrational Dynamics", in PHOTOCHEMISTRY AND PHOTOBIOLOGY: Proceedings of the International Conference, January 5-10, 1983, University of Alexandria, Egypt, Vols. I & II, A.H. Zewail, ed., (Harwood Academic Publishers, Chur, Switzerland, 1983).
6. J.J. Oren, K.M. Gough and H.D. Gesser, "The Solvent Extraction of Fe(III) from Acidic Chloride Solutions by Open-Cell Polyurethane Foam Sponge (OCPUFS)", Can. J. Chem. 57, 2032-36 (1979).
7. H.D. Gesser, G.A. Horsefall, K.M. Gough and B. Krawchuk, "Transport of Metal Complex Chlorides Through Plastic Film Membrane", Nature 268, 323 (1977).

8. K.M. Gough, "The Extraction and Recovery of Phthalates from Water by the Use of Polyurethane Foam", M. Sc. Thesis, University of Manitoba, 1976.

9. K.M. Gough and H.D. Gesser, "The Extraction and Recovery of Phthalates from Water by the Use of Polyurethane Foam", J. Chromatog. 115, 383-90 (1975).

Acknowledgements

Many people have given me their time, advice, assistance and encouragement while this thesis was in preparation. I would like to name some of them here.

First of all, I must thank Morgan, my son, who, though he may not yet realize it, has been an inspiration and a tower of strength. He has far more confidence in me than I have had in myself, as children will, and it has kept me going. I also thank my husband, Tim Wildman, for his unflagging support, not to mention numerous discussions from quantum chemistry to the meaning of life. There are also my friends, especially Sylvia, Carol, Donna and Hilary. With each of them I have spent many long evenings, sharing our hopes and fears, and sipping wine or endless cups of tea.

I would like to thank Bryan Henry for his patience, understanding and good guidance that have made this thesis possible. No one could ask for a better supervisor.

I would like to thank Dr. Ted Schaefer for many useful discussions, particularly on the toluene problem, and Dr. Norman Hunter for advice on the deuterated nitrobenzene synthesis, and the use of some potassium t-butoxide. I would also like to thank Dr. Willem Siebrand for making it possible for me to complete the computer calculations at the National Research Council, and for several interesting discussions.

I am grateful to Dr. Frank Hruska for permission to use the Nicolet 1180 system, and to Kirk Marat for teaching me how to use the programs and for continuing assistance with both the Nicolet 1180 and 1280. I would like to thank Dr. Tim Wildman and Rudy Sebastien for

help with the GAUSSIAN programs, and Rudy also for running NMR analyses on several of the samples.

I am very grateful to Allan Tarr and Mike Sowa for interesting discussions on the work as it progressed, and for assistance in completing this thesis at a distance.

I am grateful to the University of Manitoba for the financial assistance of a postgraduate fellowship.

Finally, I would like to express my thanks to Diane Vallieres and Sue Farrell who have done such an excellent job of typing this manuscript.

Table of Contents

Table of Contents (cont'd)

Table of Contents (cont'd)

Table of Contents (cont'd)

List of Tables

List of Tables

List of Tables

List of Tables

List of Figures

List of Figures (cont'd)

List of Figures (cont'd)

List of Figures (cont'd)

List of Figures (cont'd)

List of Figures (cont'd)

List of Figures (cont'd)

Index of Equations

CHAPTER 1

INTRODUCTION

i) The Local Mode Model

The CH-stretching vibrations are unique among the fundamental vibrations of hydrocarbons in that they occur at relatively high frequencies (~3000 cm^{-1}) and do not couple strongly with the other motions of the molecule. At the fundamental level, there is coupling between the CH-stretching vibrations of individual CH bonds. In other words, at the fundamental level they are satisfactorily analyzed in terms of the normal mode model.[1,2] Before modern instrumentation made possible the detailed study of fundamental spectra, before the normal mode model had been introduced, overtones of the CH-stretching vibrations were observed in the near IR by photographic techniques. In 1929, Ellis[3] described the quasi-diatomic character of the benzene CH-stretching overtone series from $\Delta v = 3$ to 8, where Δv is the number of vibrational stretching quanta. The overtone frequency for $\Delta v = n$, ν^n, could be obtained from a simple anharmonic oscillator expression

$$\nu^n = 3083\ n - 57.5\ n^2 \qquad (1)$$

He found that the vibrations of different types of CH oscillators occurred at different characteristic frequencies, and he associated these frequencies with the dissociation energies of the individual CH bonds. In 1933, Freymann[4] presented the results of a major investigation of the CH-stretching overtone spectra for many types of CH bonds. He too observed a shift in the position of the overtone maxima which corresponded to the type of CH bond: aryl, alkyl, etc., and to the presence of substituents in the molecule. In particular, he considered: the effect of chain length in saturated hydrocarbons; degree of saturation; effects of isomerism; substituents on benzene, and the electric dipole moment; hydrogen bonding in (O-H) containing

molecules; and the effect of temperature on frequency and intensity. In 1940, Kempter[5] reported the CH-stretching overtone spectra of benzene and benzene derivatives in the liquid phase, in the regions corresponding to $\Delta v = 3$ to 5. In the spectra of benzene, toluene, p-xylene and mesitylene he observed multiple absorption maxima at each overtone region which he, like Ellis[3], assigned to aryl and alkyl CH oscillators. He found that the intensity of the bands assigned to the aryl or alkyl CH bonds increased linearly with the number of aryl or alkyl CH bonds present, although the aryl bands were intrinsically more intense. The overtones of nitro-, chloro-, and ethylbenzene, phenol, styrene, polystyrene and benzoic acid were also analyzed.

In 1941, Suhrmann and Klein[6] reported the CH-stretching overtone spectra of fifty-three hydrocarbons including normal and cycloalkanes, and derivatives thereof, benzene and derivatives, as well as some ethers and ketones, at $\Delta v = 3$ and 4. Once again, peaks were identified whose frequencies were characteristic of the different types of CH bonds present in the molecules. This work was chiefly concerned with intensities, and the authors accepted the variation in frequency with bond type as a useful empirical phenomenon. Inequivalent CH bonds gave rise to resolved or partially resolved overtone absorptions in the spectra of some ethers and dioxane, as well as alkyl substituted benzenes.

In 1950, Suhrmann[7] extended the regions studied to include $\Delta v = 1$ to 6. He found that, as expected, the overtone peak maxima of chloroform could be described by the equation for an anharmonic oscillator, and determined the harmonic frequency and anharmonicity constant by a least squares fit of the overtone frequencies to the

expression for a diatomic, anharmonic oscillator. The shift in the frequency of the overtone maxima of several molecules, relative to cyclohexane, was measured. He deduced that the frequency shift was a direct result of the different electron affinities of the substituents. $CHC\ell_3$, $CH_2C\ell_2$, several chloroethanes and ethenes, as well as benzene and substituted benzenes were studied. It was assumed that the different electron affinities produced varying field effects which altered the CH bond strength. The positions of the overtone maxima were shifted to higher frequencies for stronger CH bonds. This interpretation was similar to that in the earlier work by Ellis[3], although the latter was not referenced.

Many other papers appeared in the literature during the period 1920-1940, on these subjects. It was an accepted experimental observation that inequivalent CH bonds gave rise to resolved peaks in the overtone spectra. The common conclusions regarding substituent effects were that they depended on the electron affinity of the substituent, that with an increase in the latter the CH bond became stronger, and that the overtone vibrations of the stronger CH bonds appeared at higher frequencies.

The CH-stretching overtone vibrations became an area of interest again when their importance as receptors of energy in non-radiative transitions was recognized by Siebrand et al.[8,9,10] Martin and Kalantar[11] attempted to apply normal mode formalism to their analysis, rather than the simple quasi-diatomic oscillator approach. They suggested that the benzene overtones consisted of one quantum of the ν_{20} (e_{1u}) mode plus one or more quanta of the ν_2 (a_{1g}) mode.

The local mode interpretation was first introduced by Henry and Siebrand in 1968[12]. They proposed that the CH-stretching overtones in polyatomic molecules corresponded to Morse diatomic anharmonic oscillators. In particular, the dissociation of a single bond in a polyatomic molecule can be better represented in this picture than in the normal mode model. The equation for the local mode model was written as

$$E = \sum_i (v_i + \tfrac{1}{2})\hbar\omega_i + \sum_{i>j}\sum c_{ij}\hbar\omega_{ij} + \sum_{i\geq j}\sum (v_i + \tfrac{1}{2})(v_j + \tfrac{1}{2})\hbar X_{ij}$$

$$= E_o + \sum_i v_i\hbar\omega_i^o + \sum_{i>j}\sum c_{ij}\hbar\omega_{ij}^o + \sum_{i\geq j}\sum v_i v_j \hbar X_{ij} \qquad (2)$$

where v_i is the vibrational quantum number, ω_i is the frequency of the i^{th} local mode, the X_{ij} are the local model anharmonicity constants, and the $c_{ij}^o\hbar\omega_{ij}^o$ are harmonic coupling terms, with c_{ij} of the order of $(v_i v_j)^{\frac{1}{2}}$ and ω_{ij}^o of the order of $(\omega_K^o - \omega_L^o)$. The subscripts K and L refer to the corresponding normal modes. (The vibrational energy could also be written in terms of normal modes). The harmonic coupling could be assumed to be small, and could be neglected, as were the off-diagonal anharmonicity constants X_{ij} $(i \neq j)$. For a set of equivalent oscillators the X_{ii} terms would be equal. Thus, eq. 2 represented a set of weakly coupled local modes. The value of X_{ii} could be obtained spectroscopically. The equivalence of the normal and local representations of the vibrational energy was then exploited to yield values for all of the normal mode anharmonicity constants. In the normal mode representation, the off-diagonal terms are consistently much larger than the diagonal terms. However, it was considered to be essential to retain the normal mode aspect of the analysis and to seek a description of the overtone bands in terms of an appropriately weighted combination of allowed normal modes.

Hayward and Henry[13] showed that the local mode model was the description of choice for the large amplitude CH stretching vibrations. The bandshape calculated in terms of anharmonic normal mode components was necessarily broad and complex, in contrast to the experimental spectra which exhibited essentially a single narrow peak at each overtone. The peak maxima corresponded to the excitation of the most anharmonic vibration, with all of the energy deposited in a single oscillator. The parameters in the simple local mode equation

$$\Delta E_{o \rightarrow v} = \omega v + X v^2 \qquad (3)$$

were shown to be sufficient to describe the vibrations up to $\Delta v = 7$ for CH_4, $CH_3C\ell$, $CH_2C\ell_2$, $CHC\ell_3$, C_2H_6, C_6H_6, $C_6H_5CH_3$ and $C_6H_4(CH_3)_2$. Here, ω is the local mode frequency and X is the diagonal local mode anharmonicity constant. It was noted that the frequencies of the local mode band maxima at $\Delta v = 5$ correlated well with ν_{CH}^{iso} [14], the fundamental stretching frequency of a CH bond in a molecule where all the hydrogens but one have been replaced by deuterium. It was also noted that the overtones of the aryl and methyl CH oscillators in toluene and the xylenes were resolved, and could be described by eq. 3[13b].

Various aspects of the local mode description have since received extensive attention. In particular, the intensity and the time evolution of the local mode vibrations have been investigated by many groups[15-19]. While these topics are important to the development and understanding of the local mode model, they are not particularly relevant to this work.

The local mode parameters, ω and X, have been found to display characteristic variations with bond type and environment. The magnitude of ω varies with bond strength and length. This has been established empirically by McKean[20] and co-workers for ν_{CH}^{iso}, and by Wong and Moore[21] and by Mizugai and Katayama[22] at $\Delta v = 6$, but the discussion of their work belongs more properly with the discussion of CH bond lengths and is deferred until Chapter 4.

The value of X has been found to depend in part on the environment of the CH bond. Where inter- or intramolecular crowding is such as to restrict large amplitude vibrational motion, the magnitude of X decreases, that is, the oscillator is constrained to behave in a more harmonic fashion. A decrease in X, related to high viscosity was first observed by Greenley and Henry[23] in the overtone spectrum of 3-methylpentane. A similar decrease in X due to steric hindrance, was later found for a series of methyl-substituted alkanes[24,25].

The only significant change to the local mode model has been the inclusion of symmetry[26-28]. For the simplest case of two equivalent CH oscillators in a molecule excited with v quanta of energy, it is necessary to take symmetrized combinations of the initially degenerate states $|v,0\rangle$ and $|0,v\rangle$

$$|v,0\rangle_{\pm} = \frac{1}{\sqrt{2}} (|v,0\rangle \pm |0,v\rangle) \qquad (4)$$

In general, only $|m \pm 1, n \mp 1\rangle$ states can couple to the state $|m,n\rangle$, so that of the pure local mode states only $|1,0\rangle$ and $|0,1\rangle$ couple directly. At higher overtones the two oscillators remain essentially uncoupled and degenerate. The overtone spectra of the dihalomethanes were fully analyzed within the terms of this model[28].

ii) Introduction to the Problem

The main thrust of this work has been to attempt to understand the variations observed in the CH-stretching overtone spectra of some substituted benzene compounds. The spectra have been analyzed following the local mode model introduced by Henry and Siebrand[12], and modified to its present form by Hayward and Henry[13] and by Mortensen et al.[28] It was anticipated that the changes in the spectra could be interpreted in terms of the electronic effects of the substituents. The most important independently determined experimental parameters related to the electronic effect are the substituent parameters of Taft[29], and especially σ_I, the inductive part of the Hammett sigma[30]. Initially, correlations were sought between the substituent parameters and the shift in the position of the overtone maxima relative to benzene, for a given overtone, in the liquid phase. As the work developed, the correlations were extended to include the results of ab initio molecular orbital calculations with complete geometry optimization. In particular, the predicted changes in the CH bond lengths and in the electron distribution upon substitution were related to the observed frequency shifts in the gas phase overtone spectra.

Because of the variation of ω and X with bond type and environment, it is possible to distinguish overtones of conformationally inequivalent CH bonds[31,32]. Evidence of conformational differences was examined in the gas phase overtone spectra of the methyl groups in toluene and the xylenes, and in the spectra of 1,3- and 1,4-cyclohexadiene.

Little mention of the early studies on CH-stretching overtones has been made in the recent local mode literature. Because several of the very early papers contain information which is particularly relevant to this work, some of them have been reviewed in the introduction. Others are referred to in the chapters where the data are related to the present spectra. In this context, the local mode model can be seen as a natural development and a more sophisticated, fundamentally acceptable description of a well known phenomenon.

CHAPTER 2

EXPERIMENTAL

i) Materials

Most of the compounds to be studied were available commercially at 97+ to 99+% purity and were used without further purification, with the following exceptions.

1,4-dichlorobenzene, 1,3,5-trichlorobenzene and 1,3,5-tribromobenzene were purified by recrystallizing twice from spectral grade carbon tetrachloride (Fisher, spectranalyzed). Iodobenzene was fractionally distilled at reduced pressure, and the fraction boiling at 105-107°C was used.

Nitrobenzene was first passed through a column of Woelm alumina, and then fractionally distilled at reduced pressure. The third fraction, boiling range 149.5-150°C, was used. The nitrobenzene had been found to contain a small amount of highly coloured (green) impurity, which absorbed strongly in the spectral region corresponding to $\Delta v = 4$ and 5. After purification this impurity had been reduced to a negligible level.

Partially deuterated nitrobenzene was synthesized as described in the next section.

ii) 3,4,5-tri- and 2,3,4,5-tetradeuteronitrobenzene

Fully deuterated nitrobenzene was obtained commercially (Aldrich, 99+%). The partially deuterated compounds were prepared by a modification of the technique described by Guthrie and Wesley[33]. All glassware was cleaned and dried overnight at 100°C. Dry tert-butyl alcohol was obtained from distillation over sodium (boiling range 79-83°C) under a stream of dry argon, and stored under dry argon. A 0.47 M solvent base was prepared by the addition of 4.3 g potassium tert-butoxide to 75 mℓ dry tert-butyl alcohol, in a 250 mℓ, three-neck round bottom flask. One neck was connected to the dry argon supply, the central one was fitted with a condenser open to the atmosphere via a $CaSO_4$ drying tube, and the third closed with a rubber septum. The solvent base mixture was warmed and stirred for two hours to completely dissolve the base. Pentadeuteronitrobenzene (13 mℓ) was injected via the septum, and the reaction mixture was stirred and refluxed for 6 hours. The reaction was quenched with 60 mℓ hexane-water (1:1). The hexane layer was washed three times with water, dried over anhydrous Na_2SO_4 and transferred to a clean flask. Most of the solvent was removed by distillation. The pressure was reduced and the product obtained by fractional distillation (b.pt. 150°C).

Mass spectral analysis showed that the product was a 1:2:1 mixture of penta-, tetra-, and trideuteronitrobenzene. From ^1H NMR, it was found that the protons were present only at the ortho positions.

iii) Sample preparation

a) Liquids and solids

Samples were placed in cells of various lengths from 0.10 to 10.0 cm. The longer path lengths were used for the less intense, higher overtones, and for solutions. Several of the halogenated benzenes were solid at room temperature. These were dissolved in spectral quality carbon tetrachloride, and the spectra of the solutions were recorded. The spectrum of pure carbon tetrachloride was recorded and was found to have no absorptions in the region of the CH-stretching overtones. To test whether there were spectral shifts due to a solvent effect, the spectrum of pure chlorobenzene was compared with that of chlorobenzene in carbon tetrachloride. There were no discernible differences.

Sample concentration in the carbon tetrachloride was not determined. Most of the solids were only poorly soluble in it, and a saturated solution was prepared. In all cases, the intent was to have as much sample in solution as possible, in order to obtain a good signal to noise ratio.

b) Gas phase spectra

Room temperature

A variable path length gas cell (Wilkes Scientific Corp., South Norwalk, CT, Model 5720) was used. In a typical experiment, the gas cell was connected to a vacuum line and pumped down. The sample was placed in a flask, connected to the vacuum line, and evacuated with several freeze-pump-thaw cycles. The gas cell and sample flask were isolated together on the vacuum line, and the stopcocks to each were opened to allow the vapour to diffuse into the gas cell. The cell was then sealed, disconnected, and mounted in the spectrophotometer. Background spectra were recorded from the empty gas cell before and after as a check against contamination.

Elevated temperature

A heating jacket for the gas cell was made by wrapping the length of the cell body with half inch copper tubing. The gas cell, evacuated, was first mounted in the correct position in the spectrophotometer. The temperature was raised, and kept constant, by circulation of water from a constant temperature heating bath, (Haake, Berlin) through the tubing. To minimize heat loss and help stabilize the system, the cell was wrapped in several layers of black cloth, and allowed to equilibrate for 2-3 hours before spectra were recorded.

In a typical experiment, background spectra were recorded from the evaluated flask in the regions corresponding to $\Delta v = 2$, 3, 4, and 5. The sample was placed in a 50 mℓ round bottom flask fitted with a stopcock and swagelock connections, degassed, and connected to the gas cell inlet. As the gas cell had usually been heated to 86°C, the

sample in the flask was warmed with a hot water bath to 75-80°C. With stopcock and gas cell inlet valve open, the absorption signal in the $\Delta v = 2$ region was monitored until sufficient vapour had been introduced to give a signal of between 0.5 and 1.0 absorbance units. The spectrum at $\Delta v = 2$ was recorded.

Where possible, more sample was introduced before the higher overtone spectra were recorded, as the intensity typically falls off by an order of magnitude at each successive overtone. For $\Delta v = 4$ and 5, the absorption was very weak, and several spectral scans were accumulated (Ch. 2, section iv). After all overtone spectra were recorded, the cell was evacuated, and the background spectra recorded again. Where several scans had been recorded for a given overtone, an equal number of background spectra were also recorded. It was not possible to automate the recording of spectra in the same spectral region because of mechanical limitations in the spectrophotometer. A typical scan required between 20 and 45 minutes, so a reasonable number of scans accumulated for signal averaging was about ten.

The path length was varied from 0.75 to 14.25 m depending on the overtone and the sample involved. Details are included where the spectra are presented. The slitwidth and baseline changed at each path length, the latter rising and sloping more with increased length. It was necessary to use a neutral density filter in the reference beam to bring the spectra onto scale. As this reduced the light intensity considerably, the instrument automatically increased the slitwidth, so that the resolution at $\Delta v = 5$, was only 2 to 4 cm^{-1}.

iv) Spectrophotometers: Data Collection and Treatment

Over the course of this work, several spectrophotometers were used, and the means of obtaining and treating data varied accordingly.

The liquid phase spectra of nitrobenzene and the halogenated benzenes were recorded on a Cary 14 with a 0-2 or a 0.0-0.2 absorbance slidewire, for Δv = 2, 3, and 4, a Cary 219 with scale expansions from 0.0-0.5 to 0.0-0.1 for Δv = 5, 6 and 7, or on a Beckman 5270 with scale expansions from 0.0-3.0 to 0.0-0.01, for Δv = 2 to 7. All gas phase spectra were recorded on the Beckman 5270 spectrophotometer.

Cary 14

The Cary 14 produced an absorption profile on chart paper; the spectrum was linear in wavelength. The spectra were digitized manually, 5 Å intervals between data points, and the data converted to a linear energy scale (3 to 6 cm^{-1} intervals between data points) with the program CONVERT[34]. The converted, digitized spectra were then entered into a Nicolet 1180 data system, and analyzed with a standard curve analysis program (CAP). This is a simple band-fitting procedure in which the experimental spectrum is simulated as a sum of Lorentzian peaks. The input parameters consist of the position, intensity and linewidth of each peak as well as the position and slope of the baseline. The number of peaks used in the band fit are chosen at the operator's discretion, up to a maximum of twenty peaks. In practice, only those peaks which were resolved, partially resolved, or appeared as prominent shoulders were simulated. It was also possible to add in Gaussian character, but for these spectra there was little change in the results even with the inclusion of up to 25% Gaussian.

Each of these parameters was varied interactively, while the experimental and calculated band envelopes were displayed on a CRT. The quality of fit was determined from the size of the rms deviation, and by a visual comparison of the match between experimental and calculated spectra, which were plotted out with a Bruker WH-90DS plotter.

The CAP also calculated approximate peak areas as the product of the full width at half maximum and the intensity. The calculated area, and its percentage of the total area were listed in the output for each peak. In this text, either the percentage area or the relative area is reported. The relative areas were determined from the ratio of the areas of the peaks of interest, for cases where the spectra contained peaks from a variety of sources.

Cary 219

The Cary 219 had a printer which produced the digitized absorbance at equal wavelength intervals. These data points were converted to be linear in energy and analyzed with CAP as for the Cary 14 data.

Beckman 5270

A digital signal could be recorded from the Beckman 5270 in two ways. Initially, it was recorded from the digital absorbance display onto cassette (DCR/10, William Palmer Ind., Los Angeles, CA) and later transferred to a Nicolet 1280 system for analysis. Eventually a direct link between the Beckman digital absorbance display and the Nicolet 1280 was constructed, and the digitized spectra could be recorded directly into the Nicolet memory. The data points were

collected at fixed wavelength intervals, and immediately converted to be linear in energy, at 1.22 cm^{-1} intervals, in the Nicolet file. The latter interval was set in the software, for the entire spectral range of 5000-20000 cm^{-1}. Instrumental slitwidth, and the data point collection intervals, varied with the spectral region. At $\Delta\nu = 5$, for some gas phase spectra, the slitwidth and data point collection intervals were, unavoidably, slightly greater than the energy intervals. The relevant data for the gas phase spectra of some fluorinated benzenes are given in Table I. Where the slitwidth exceeded the energy data point interval of 1.22 cm^{-1}, a Gaussian (FWHM = slitwidth) was folded into the experimental absorbance profile. This would cause a small increase in the observed linewidth, but was not corrected for in the data treatment.

Background spectra were subtracted from sample spectra, and the corrected data stored on disc. To signal average, the data files for each of the scans were added into one file, and an equal number of background scans were subtracted. It was necessary to subtract an equal number of background scans, as the noise level was the same in both sample and background spectra.

The experimental spectra were again decomposed with a Nicolet curve analysis program which fitted Lorentzian peaks to the experimental data. As with the Nicolet 1180 system, up to 100% Gaussian character could be included, but again this was added, not folded in. The value of the rms deviation, and visual comparison of the experimental and calculated curves were used to evaluate the quality of the band fit. Experimental and calculated curves were plotted with the Nicolet Zeta digital plotter. The calculated band envelopes were also stored on disc.

Table I. Data Collection Parameters for Overtone Spectra of Some Gas Phase Fluorinated Benzenes

Molelcule	Overtone	Slitwidth (cm^{-1})	Data Collection Interval (cm^{-1})	Path Length[a] (m)
fluorobenzene	2	0.05	0.27-0.30	12.75
	3	0.07-0.08	0.56-0.66	12.75
	4	0.4-1.0	1.0-1.1	12.75
	5	3.0-1.7	1.8-2.1	6.75
1,2-difluorobenzene	2	0.05	0.27-0.30	9.75
	3	0.15	0.56-0.66	12.75
	4	0.4-1.0	1.0-1.1	12.75
	5	3.2-2.3	1.8-2.1	8.25
1,3-difluorobenzene	2	0.05	0.27-3.0	9.75
	3	0.4-0.6	0.56-0.66	14.25
	4	0.3-0.9	1.0-1.1	14.25
	5	0.2-0.1	0.3-0.4	9.75
1,4-difluorobenzene	2	0.05	0.27-0.30	9.75
	3	~0.5	0.56-0.66	9.75
	4	0.4-1.0	1.0-1.1	9.75
	5	3.4	1.8-2.1	8.25

[a]The spectra at $\Delta v = 5$ were recorded at a later date, and because of technical problems with the cell it was not possible to record at longer path lengths or narrower slitwidths in some cases.

All of the experimental spectra presented in this work have been plotted with the WH-90DS (Cary 14 and Cary 219) or the Nicolet Zeta (Beckman 5270) plotters, after treatment as described above. For brevity, the figure captions identify only the spectrophotometer used to record the data.

v) Molecular Orbital Calculations

a) Programs

The GAUSSIAN70[35] program and the MONSTERGAUSS[36] program, a version of GAUSSIAN80[37] with some modifications[39] were used to perform ab initio molecular orbital calculations with full geometry optimization. With the GAUSSIAN70 program, it was only possible to optimize the geometric parameters sequentially, so that for full optimization most parameters were optimized twice. This procedure was lengthy: about ten hours of computer time were required to optimize fluorobenzene with the STO-3G basis set (vide infra), on an Amdahl 470/V7. The MONSTERGAUSS program was used for the remaining fluorobenzenes. This program is more efficient since it employs a force gradient method[39], in which all parameters are optimized simultaneously. The fully optimized geometry of 1,3-difluorobenzene, at the STO-3G level was obtained in 65 minutes on an IBM370/3033. The IBM computer itself is about as fast as the Amdahl.

b) Basis sets

The STO-3G[40] and 4-21G[41,42] basis sets were employed. The former is a minimum basis set which provides one atomic orbital per orbital on an atom, each expanded as three Gaussians. In this basis there would be one atomic orbital on hydrogen and five on carbon, with common coefficients and exponents for orbitals with the same principal quantum number. Calculations at this level were completed more rapidly than at the 4-21G level, but the results were correspondingly poorer. Full geometry optimization produced CH bond lengths to within about ±0.005 Å of the spectroscopically determined values, r_o.

The 4-21G basis set is an extended, split valence basis. Inner shell atomic orbitals are again represented by one atomic orbital each, expanded as four Gaussians. Valence shell atomic orbitals are represented by two atomic orbitals, expanded as two and one Gaussian, respectively. Once again the same coefficients and exponents are used for atomic orbitals with the same principal quantum number. In this basis set, a hydrogen atom has two atomic orbitals, and a carbon atom has nine. The total number of Gaussians used increases only marginally, but the use of different exponents and coefficients in the valence shell orbitals results in a greater sensitivity to the bonding interactions. The CH bond lengths calculated with this basis set, while smaller in magnitude than the accepted r_e (equilibrium bond length) values, appear to model small variations (±0.001 to 0.002 Å) very well[41,43] (vide infra).

It was not always possible to perform geometry optimization at the 4-21G level because of size limitations. For example, at the 4-21G level, nitrobenzene is described by ninety-one atomic orbitals, but the MONSTERGAUSS program can only accomodate a maximum of ninety.

The results of 4-21G geometry optimization have recently been published by Boggs et al. for benzene[44], mono-, 1-3-di-, 1,3,5-tri and pentafluorobenzene[45], and toluene[46]. These geometries with the exception of pentafluorobenzene, were used in the MONSTERGAUSS program, in single runs, to obtain information about the variation in the electron population distribution. Small differences exist between the 4-21G basis set used by Boggs et al.[41,44-46] and that used in the MONSTERGAUSS program. In the latter, developed by Pople et al.[42], the coefficients and exponents of the Gaussians used to expand the valence shell atomic orbitals are those optimized for the 6-21G basis set. Those used by Boggs[41] were optimized differently, and vary by 2 or 3% from the values obtained by Pople et al. Because of this, minor differences occur in the values of the electron populations and the energies of the molecules as calculated with MONSTERGAUSS compared to those of Boggs et al.[44-46]

The fully optimized geometries of 1,2- and 1,4-difluorobenzene had not been calculated for the 4-21G level. These geometry optimizations were performed for this work, along with the STO-3G geometry optimizations of numerous other molecules. These results appear in Chapter 4.

CHAPTER 3

CH-STRETCHING OVERTONE SPECTRA OF SUBSTITUTED BENZENES IN THE LIQUID PHASE

i) Earlier Work

As noted in Chapter 1, in the very early studies on the CH-stretching overtone spectra[3-7] the unique correspondence between overtone stretching frequency and bond length was an accepted empirical phenomenon. In 1927, Barnes and Fulweiler[47] reported $\Delta v = 4$ for benzene and seven alkyl-substituted derivatives: toluene, o, m- and p-xylene, mesitylene, ethylbenzene and m-plus p-diethylbenzene (mixture). They attempted to correlate the shift in the aryl CH-stretching overtone maximum with the substituent mass.

In 1932, Freyman[48] showed that if substituents other than alkyl were considered the frequency shift correlated, not with the mass, but, with the electric dipole moment of the molecule, and the electronegativity of the substituent. At the same time, Allard[49] independently proposed that a frequency shift could be anticipated, due to the interaction of electric dipoles within the molecule.

In 1938, Barchewitz[50] examined the overtone spectra of several substituted benzenes in the $\Delta v = 4$ and $\Delta v = 5$ region. Apart from the frequency shift, he observed a doubling in the overtone bands of nitrobenzene, and the para-substituted fluoro-, chloro-, bromo- and nitrotoluenes. In the case of nitrobenzene, which had also been observed by Freymann[48] at $\Delta v = 3$, the doubling was attributed to some reduction in the molecular symmetry. For the substituted toluenes, it was assumed that the CH bonds responded to the electric dipole nearest them, thus two responded to the CH_3 influence, and two to the para substitutent.

As noted in the introduction, Kempter[5], and Suhrmann and Klein[6] also looked at substituted benzenes, but they were chiefly

interested in intensity. The separation of aryl and alkyl CH overtones was well known.

The overtone spectra of substituted benzenes have received attention again in the last seven years. The liquid phase overtone spectra of toluene and the xylenes were re-examined[13,51,52]. The gas phase overtone spectra of these molecules were recorded for this work, and the results appear in Chapter 4, section (ii).

Mizugai and Katayama[53] studied $\Delta v = 6$ of thirty mono-substituted benzenes using thermal lensing spectroscopy. They measured the shifts in the positions of the overtone maxima and correlated these values with σ_I, the inductive part of the Hammett sigma[30]. They concluded that an increase in the sigma electron-withdrawing power of the substituent resulted in shorter, stronger CH bonds. The decrease in bond length and increase in bond strength was manifested as a shift of the overtone peak maximum to a higher frequency. This was also demonstrated by these authors in a study on some heterocyclics[22]. For disubstituted molecules[54], they too observed either an asymmetry in the bandshape, or, in some cases, partially resolved doublets. The assignment made was similar to that of Barchewitz[50], i.e., the peak which appeared at or near the frequency of the peak in the spectrum of the monosubstituted compound was assigned as the overtone of the CH oscillator ortho to that substituent. Where the inequivalent CH oscillators gave rise only to an asymmetric band, it was found that the frequency shift was roughly proportional to the sum of the σ_I values of the two substituents.

ii) Nitrobenzene

The liquid phase CH-stretching overtone spectra of nitrobenzene were recorded in the regions corresponding to Δv = 3 to 6, (Figs. 1 and 2). For the pair of curves at each overtone, the upper spectrum is the digitized data from the Cary 14, converted to be linear in energy, and plotted with the Bruker WH-90DS plotter. The lower spectrum in each pair is the calculated band envelope from the Nicolet 1180 curve analysis program. The positions of the peak maxima from the CAP results and the relative areas are given in Table II. The local mode parameters calculated from these peak positions and eq. 3 are given in Table III.

The earlier assignment of the nitrobenzene doublet[50] was incorrect, while that of the para-substituted toluenes was correct. In accordance with the observations of Mizugai and Katayama[53,54], the considerable sigma electron withdrawing powers of the NO_2 group should produce a shift of the overtone maximum(a) to higher frequencies, at each overtone. It was assumed that this influence varied with the position of the CH oscillator relative to the NO_2 group. Thus the CH bonds <u>ortho</u> to the substituent would experience the greatest influence and these overtones would appear at much higher frequencies than those of the CH bonds <u>meta</u> and <u>para</u>. The calculated shifts in frequency ($\Delta\bar{\nu}$) relative to benzene are shown in Table II, for each calculated peak at each overtone. The higher frequency peak in each overtone band is assigned to the CH-stretching overtone of the <u>ortho</u> CH bonds; the lower frequency peak, to the <u>meta</u> and <u>para</u> CH bonds.

Three other factors supported this assignment, to some extent. First, the ratio of the peak areas at Δv = 3 is about 3:2

Figure 1

The calculated and experimentally observed CH-stretching overtone spectra of nitrobenzene, $\Delta v = 3$ (lower curves) and $\Delta v = 4$ (upper curves). Experimental spectra were obtained in the liquid phase at room temperature with the Cary 14. The lower curve of each pair is the calculated band envelope. Ordinate: arbitrary linear absorption units.

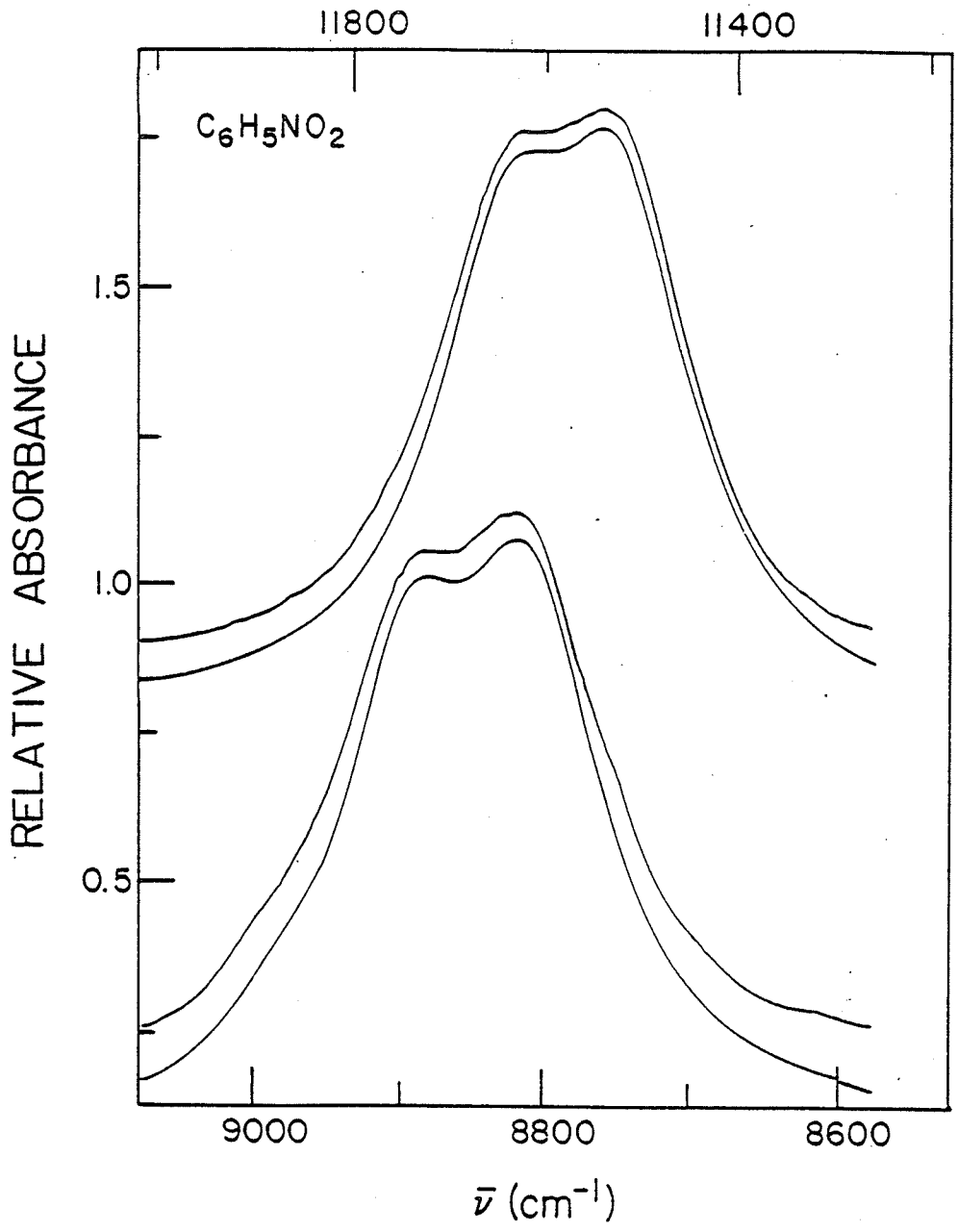
11800
11400
$C_6H_5NO_2$
1.5
1.0
0.5
RELATIVE ABSORBANCE
9000
8800
8600
$\bar{\nu}$ (cm^{-1})

Figure 2

The calculated and experimentally observed CH-stretching overtone spectra of nitrobenzene, $\Delta v = 5$ (lower curves) and $\Delta v = 6$ (upper curves). Experimental spectra were obtained in the liquid phase at room temperature with the Cary 14. The lower curve of each pair is the calculated band envelope. Ordinate: arbitrary linear absorption units.

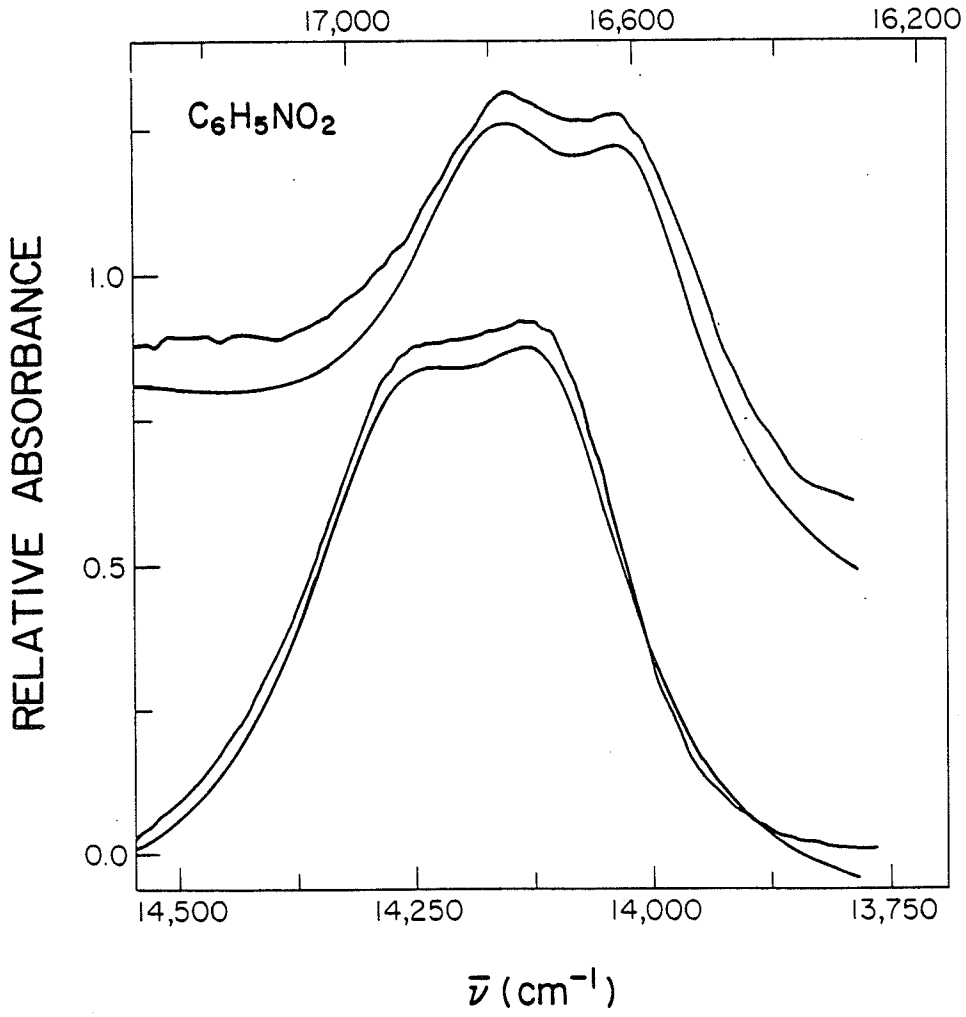
17,000
16,600
16,200
$C_6H_5NO_2$
RELATIVE ABSORBANCE
1.0
0.5
0.0
14,500
14,250
14,000
13,750
$\bar{\nu}$ (cm^{-1})

Table II. Parameters from the Curve Analysis of the Nitrobenzene CH-Stretching Overtone Spectra

Δv	Assignment	$\bar{\nu}_{max}$ (cm^{-1})	FWHM (cm^{-1})	Relative Area	$\Delta\bar{\nu}$ [a] (cm^{-1})
3	ortho	8898	100	2.0	139
	meta, para	8815	124	3.4	55
4	ortho	11634	188	2.0	192
	meta, para	11515	163	1.8	71
5	ortho	14274	237	2.0	259
	meta, para	14112	218	1.9	97
6	ortho	16795	289	2.0	328
	meta, para	16596	220	1.3	128

[a]Shift in position of overtone maximum relative to benzene, Ref. 55.

Table III. Local Mode Parameters for Nitrobenzene

Assignment	ω (cm^{-1})	X (cm^{-1})	r
ortho	3132 ±2	-55.5 ±0.5	-0.99992
meta, para	3109 ±3	-57.3 ±0.5	-0.99991

(Table II), for low: high frequency peaks. This ratio gradually changes and is reversed at the higher overtones. However, in liquid phase spectra there is typically an increased asymmetry to the high energy side, due in part to unresolved local mode combinations. The occurrence of a sloping baseline at $\Delta v = 5$ and 6 presented a further complication, as the ratio of the areas was very sensitive to the estimated position and slope of the baseline. Finally, the relative intensity of bands does not necessarily correspond to the relative number of CH oscillators of a given type. For example, in cyclohexane[32,56] the peaks associated with the equatorial CH bonds are about twice the intensity of the peaks associated with the axial CH bonds. In the n-alkanes, the methyl peaks are more intense than the methylene peaks on a per hydrogen basis[22,57]. Thus, while the ratio of the areas at $\Delta v = 3$ should be a better indicator than at $\Delta v = 6$, and supports the assignment here, peak areas cannot be considered as a reliable parameter for peak assignment.

A second factor is the magnitude of the diagonal local mode anharmonicity, X, (Table III). The magnitude of this parameter decreases when steric hindrance or increased viscosity restricts large amplitude vibrations[23-25]. The magnitude of X for the high frequency peak is significantly lower than that for the low frequency peak. This fact can be interpreted as the result of steric hindrance imposed by the NO_2 group on the ortho CH bonds.

Finally, the spectra of nitrobenzene were studied in conjunction with the overtone spectra of nineteen other substituted benzenes (see Chapter 3, section (iv)). Following the approach of Mizugai and Katayama[53], the frequency shifts of the peak maxima

relative to benzene, $\Delta\bar{\nu}$, were plotted against the value of σ_I. The shift of the lower frequency peak followed the correlation with σ_I established for the band maxima of the other compounds. Since σ_I is empirically determined only for the meta and para positions, this correlation supported the assignment of the lower frequency peak to the excitation of meta and para CH bonds.

This assignment was later confirmed by the analysis of the deuterated and partially-deuterated nitrobenzene overtone spectra, described in the next section.

iii) Deuterated and Partially Deuterated Nitrobenzene

The assignment of the peaks in the overtone spectra of nitrobenzene was very important to the interpretation of much of the gas phase data (Chapter 4). The evidence supporting the assignment was not conclusive, and further evidence was sought.

The technique of isolating CH bonds by partial deuteration in order to examine the "isolated" fundamental CH stretching frequency has been used extensively by McKean and co-workers[20]. For this study, the ortho CH bonds were effectively isolated by substituting protons at the ortho positions of fully deuterated nitrobenzene (Chapter 2, section (ii)).

Figure 3 shows the liquid phase overtone spectra of pentadeuteronitrobenzene, and the product mixture, which consisted of a 1:2:1 mix of unreacted pentadeuteronitrobenzene, 2,3,4,5-tetradeutero- and 3,4,5-trideuteronitrobenzene, in the region corresponding to $\Delta v = 3$ (CD). The results of the curve deconvolution are given in Table IV. The spectrum of the pentadeuteronitrobenzene has the same appearance as that of nitrobenzene at $\Delta v = 3$ (CH), (Figure 3). It is a partially resolved doublet and the ratio of the deconvoluted peak areas, low to high frequency, is 3:2. In the spectrum of the mixture, the high frequency peak has decreased, so that the ratio of the areas is now 3:1. This is precisely the change in intensity expected on the basis of the mass spectral analysis, provided that the high frequency peak corresponds to the ortho CH oscillator.

The spectra of nitrobenzene, the product mixture, and pentadeuteronitrobenzene in the $\Delta v = 3$ (CH) region are shown in Figure 4. The results of the deconvolution of these spectra appear in

Figure 3

The liquid phase overtone spectra of pentadeuteronitrobenzene (upper spectrum) and of a 1:2:1 mixture of 3,4,5-tri-, 2,3,4,5-tetra- and pentadeuteronitrobenzene (lower spectrum), at room temperature in the region of $\Delta v = 3$ (CD); 2 cm pathlength, recorded with the Beckman 5270.

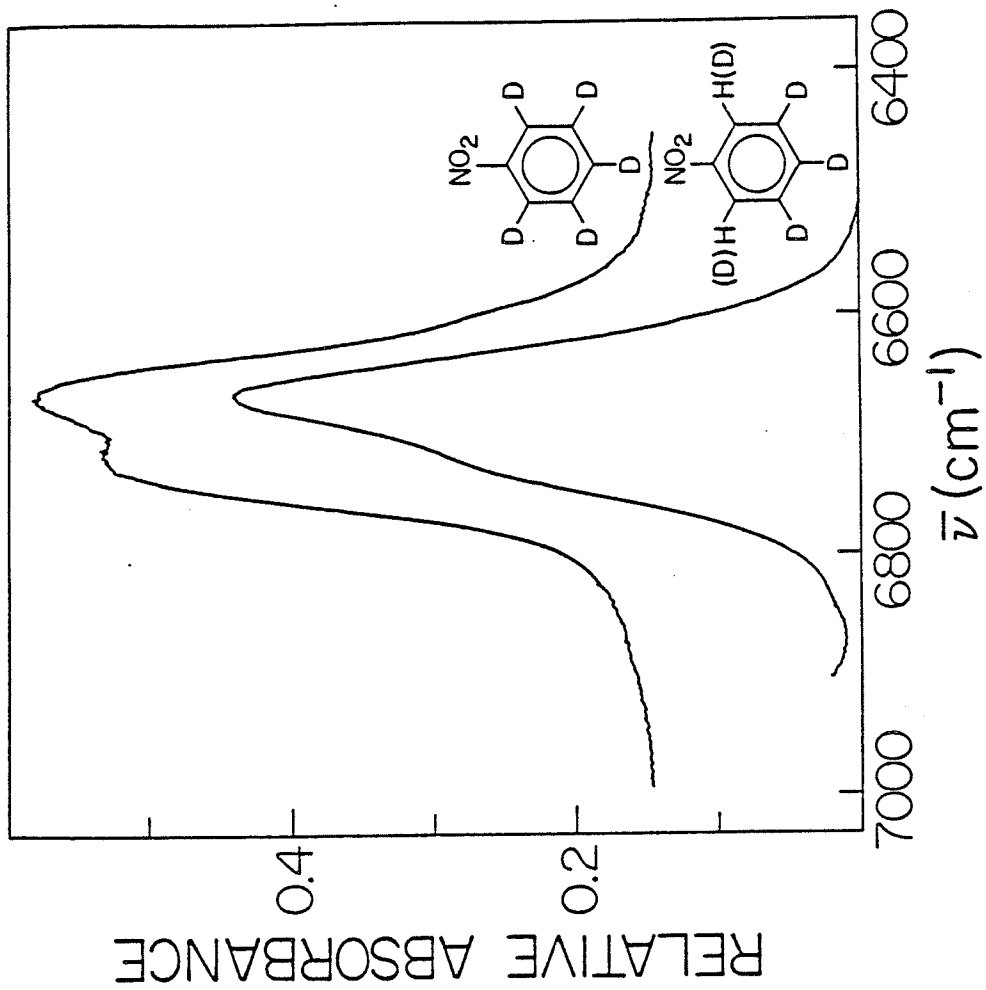
RELATIVE ABSORBANCE
0.4
0.2
7000
6800
6600
6400
$\bar{\nu}$ (cm^{-1})
NO2
D
D
D
D
D
NO2
H(D)
D
D
(D)H
D

Table IV. Parameters from the Curve Analysis of the $\Delta v = 3$ (CD) Spectra of Deuterated and Partially Deuterated Nitrobenzene

Molecules	Assignment	FWHM (cm^{-1})	$\bar{\nu}_{max}$ (cm^{-1})	Relative Area
3,4,5-tri-, 2,3-4,5-tetra-	ortho	77	6733	1.0
and pentadeuteronitrobenzene	meta, para	86	6664	2.9
pentadeuternitrobenzene	ortho	74	6732	2.0
	meta, para	83	6662	2.9

Figure 4

The liquid phase overtone spectra of nitrobenzene (upper spectrum), a 1:2:1 mixture of 3,4,5-tri-, 2,3,4,5-tetra- and pentadeuteronitrobenzene (middle spectrum) and pentadeuteronitrobenzene (lower spectrum) at room temperature in the region of $\Delta v = 3$ (CH), and $\Delta v = 4$ (CD). Left ordinate refers to the two upper spectra, right ordinate to the lower spectrum. Absorbance units are not exactly comparable between the two upper spectra. Recorded with the Beckman 5270.

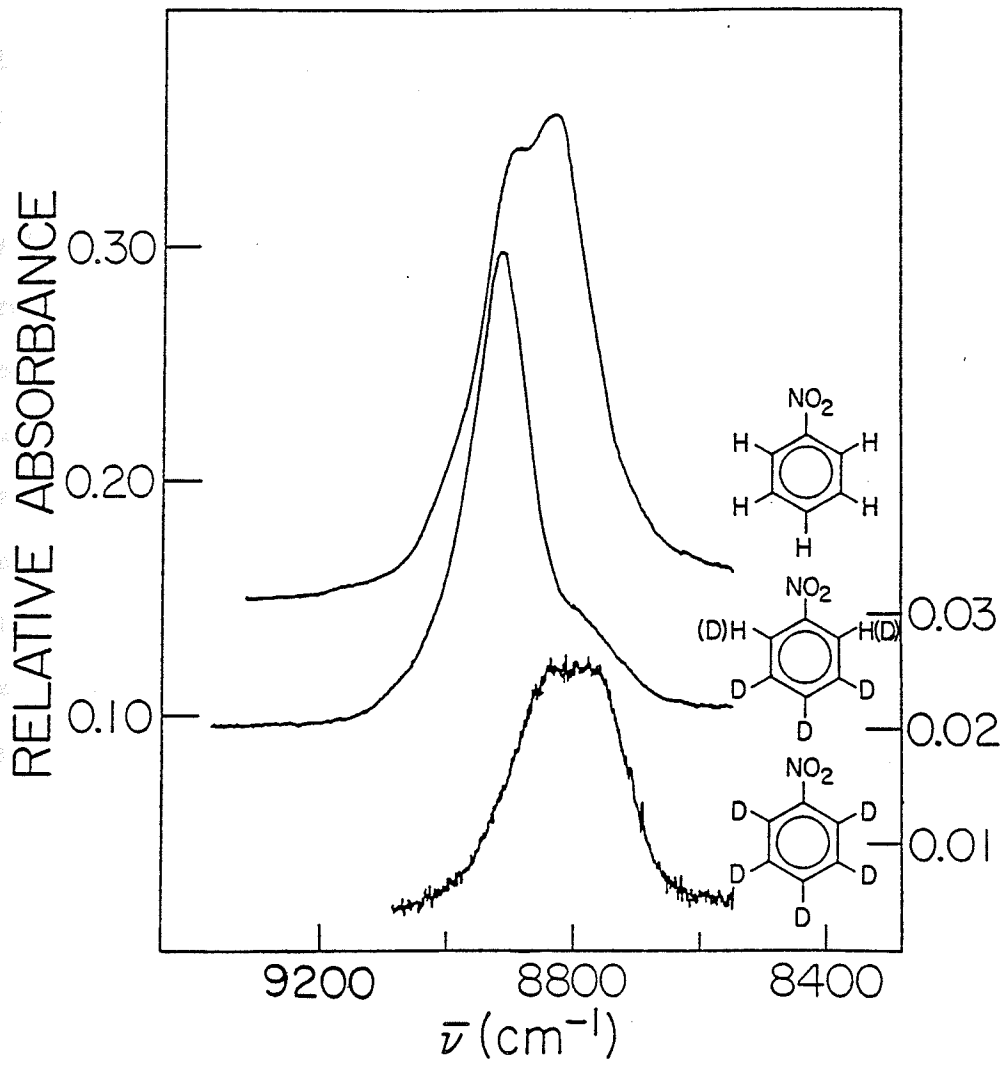
RELATIVE ABSORBANCE
0.30
0.20
0.10
0.03
0.02
0.01
9200
8800
8400
$\bar{\nu}$ (cm^{-1})
NO2
H
H
H
H
H
NO2
(D)H
H(D)
D
D
D
NO2
D
D
D
D
D

Table V. The single major peak in the spectrum of the mixture corresponds to the high frequency peak in the nitrobenzene doublet. The difference in the frequency match of 8 cm^{-1} is very small and is accounted for in part by the presence of the unresolved absorbance due to $\Delta v = 4$ (CD) of the remaining ortho CD oscillators. The low frequency shoulder in the mixture is due to $\Delta v = 4$ (CD) of the meta and para CD oscillators, as verified by comparison of this spectrum with that of pentadeuteronitrobenzene.

The assignment of the nitrobenzene spectra in section (ii) is thus fully confirmed. It is known that the intensity of peaks corresponding to inequivalent CH bonds does not necessarily reflect the number of hydrogen atoms of each particular type. Because of the results at $\Delta v = 3$ for both CH and CD oscillators it appears that in the case of nitrobenzene the ratio of peak areas does reflect the number of CH oscillators of a given type. The change in the ratio of the areas at the higher overtones is probably due to the fact that these spectra were taken in the liquid phase, as discussed in section (ii) of this Chapter.

Table V. Parameters from the Curve Analysis of the $\Delta v = 3$ (CH), $\Delta v = 4$ (CD) Spectra of Deuterated and Partially Deuterated Nitrobenzene

Molecule(s)	Assignment	FWHM (cm^{-1})	$\bar{\nu}_{max}$ (cm^{-1})	Relative Area
Nitrobenzene	ortho (H)	106	8904[a]	2.0
	meta, para (H)	108	8821[a]	2.7
3,4,5-tri-, 2,3,4,5-tetra	ortho (H)	101	8912	7.8
and pentadeuteronitro-	ortho (D)	not observable		
benzene	meta, para (D)	102	8771[b]	1.0
Pentadeuteronitrobenzene	ortho (D)	111	8854	2.0
	meta, para (D)	126	8760[b]	2.6

[a] All the spectra here were recorded on the Beckman 5270 and analyzed directly with the Nicolet 1280 data system. Discrepancies between these values and those in Table II arise from the different methods of data collection and treatment.

[b] The difference of 11 cm^{-1} is the result of the difficulty of accurately determining the peak maxima of small partially resolved peaks with the band fit procedure.

iv) Halogenated Benzenes

The overtone spectra of nineteen halogenated benzenes, ranging from mono- to penta-substitution, were obtained in the regions corresponding to $\Delta v = 2$ to 7. Some representative spectra are shown in Figures 5-12. The details of the analysis of all the spectra are presented in the subsequent parts of this section.

Figure 5

The CH-stretching overtone spectra of the four monohalobenzenes in the liquid phase, at room temperature, in the region of $\Delta v = 3$. Recorded on the Beckman 5270; 1 cm pathlength. The bromo-, chloro- and fluorobenzene spectra have been offset by 0.2, 0.4 and 0.6 absorbance units respectively.

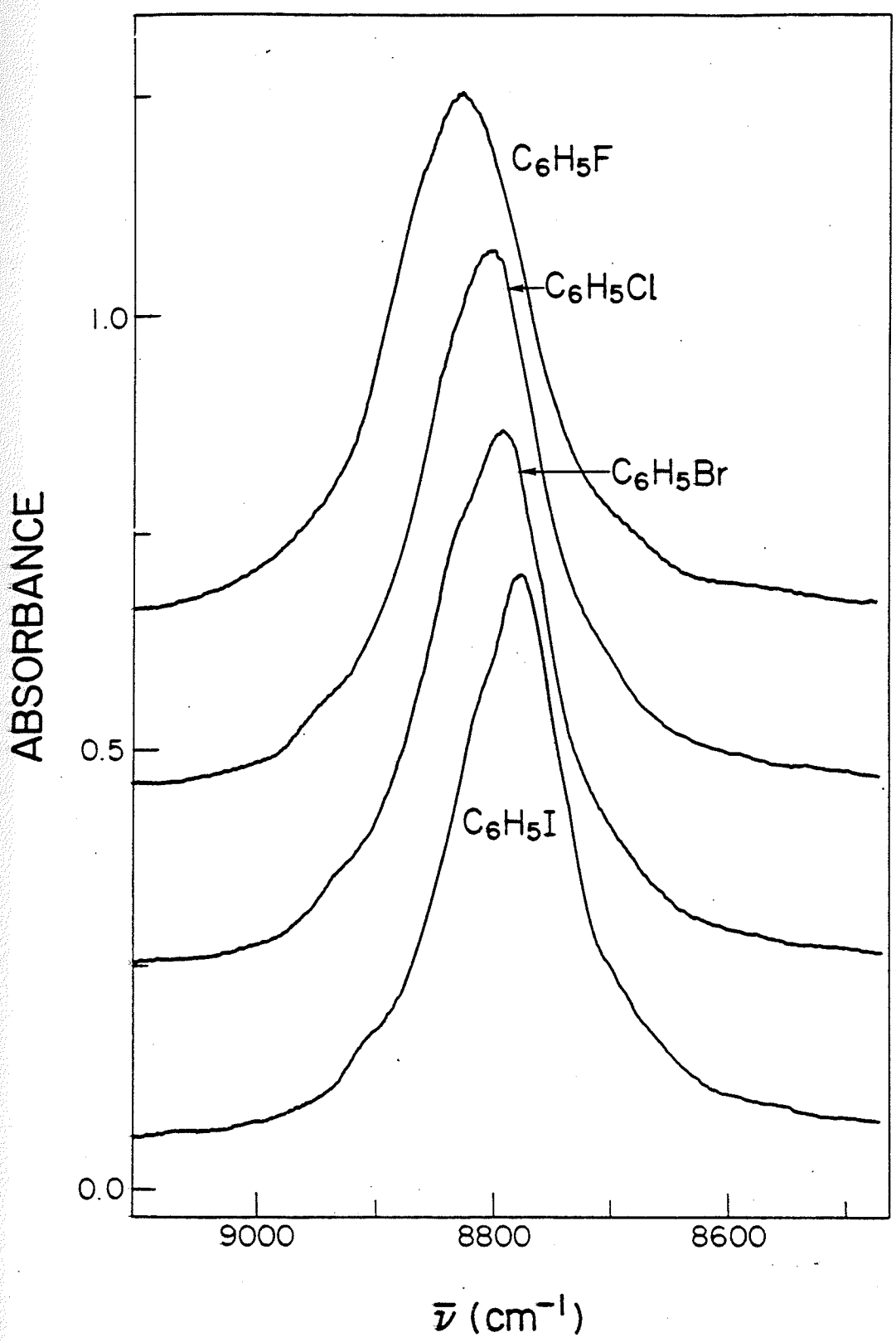
C6H5F
C6H5Cl
C6H5Br
C6H5I
ABSORBANCE
1.0
0.5
0.0
9000
8800
8600
ν̄ (cm⁻¹)

Figure 6

The CH-stretching overtone spectra of 1,3-dichlorobenzene in the liqui phase, 1 cm pathlength, (upper spectrum) and of a solution of 1,3-dibromobenzene in $CC\ell_4$, 2 cm pathlength (lower spectrum), at room temperature in the region of $\Delta v = 3$. Recorded on the Cary 14. The upper spectrum has been offset by 1.2 absorbance units.

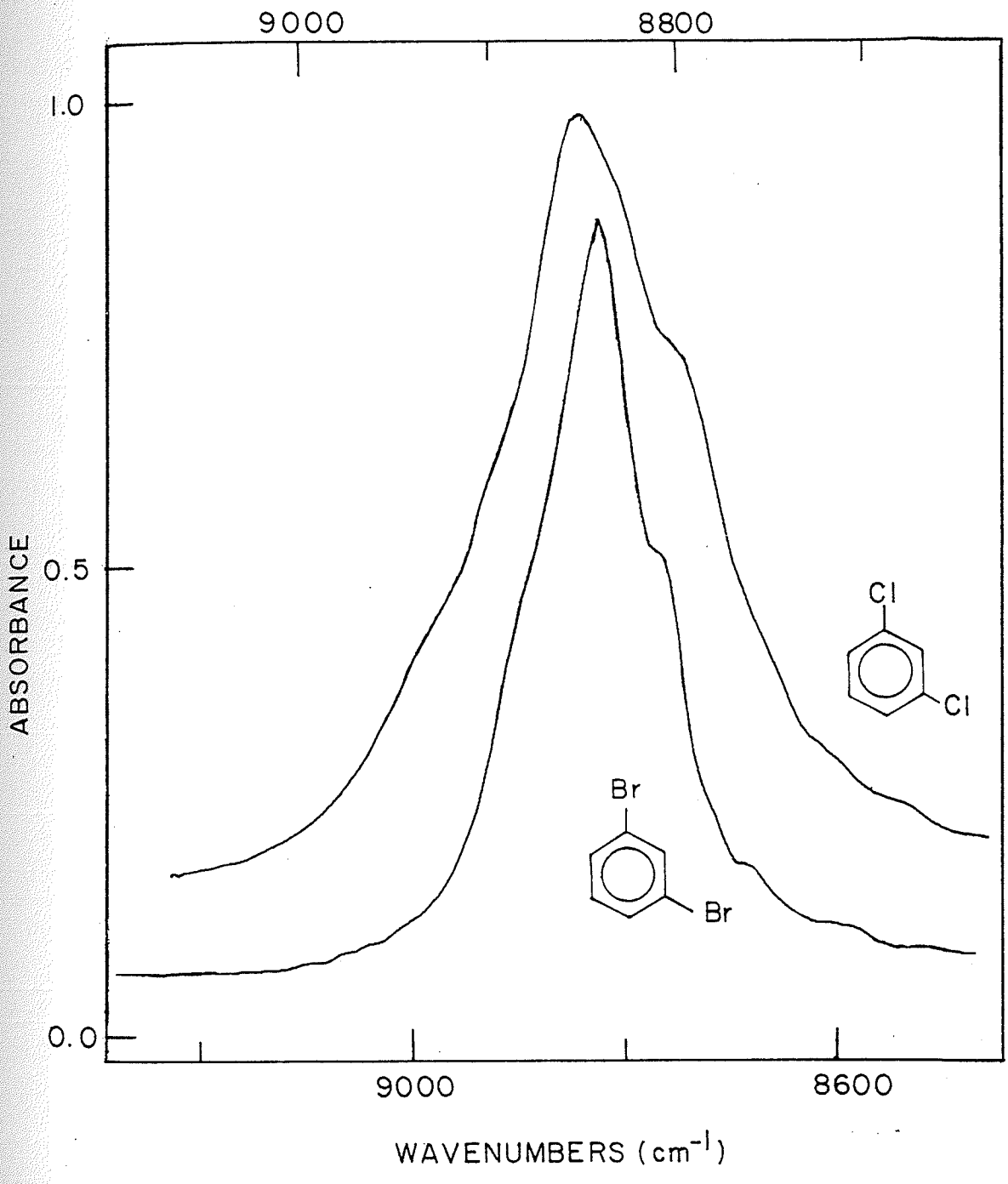
9000
8800
1.0
0.5
0.0
ABSORBANCE
Cl
Cl
Br
Br
9000
8600
WAVENUMBERS (cm⁻¹)

Figure 7

The CH-stretching overtone spectra of 1,4-difluorobenzene in the liquid phase, 0.5 cm pathlength, (lower spectrum) and of 1,4-dichlorobenzene in $CC\ell_4$, 4 cm pathlength (upper spectrum), at room temperature in the region of $\Delta v = 3$. Recorded on the Cary 14. Ordinate on LHS refers to lower spectrum and ordinate on RHS refers to upper spectrum.

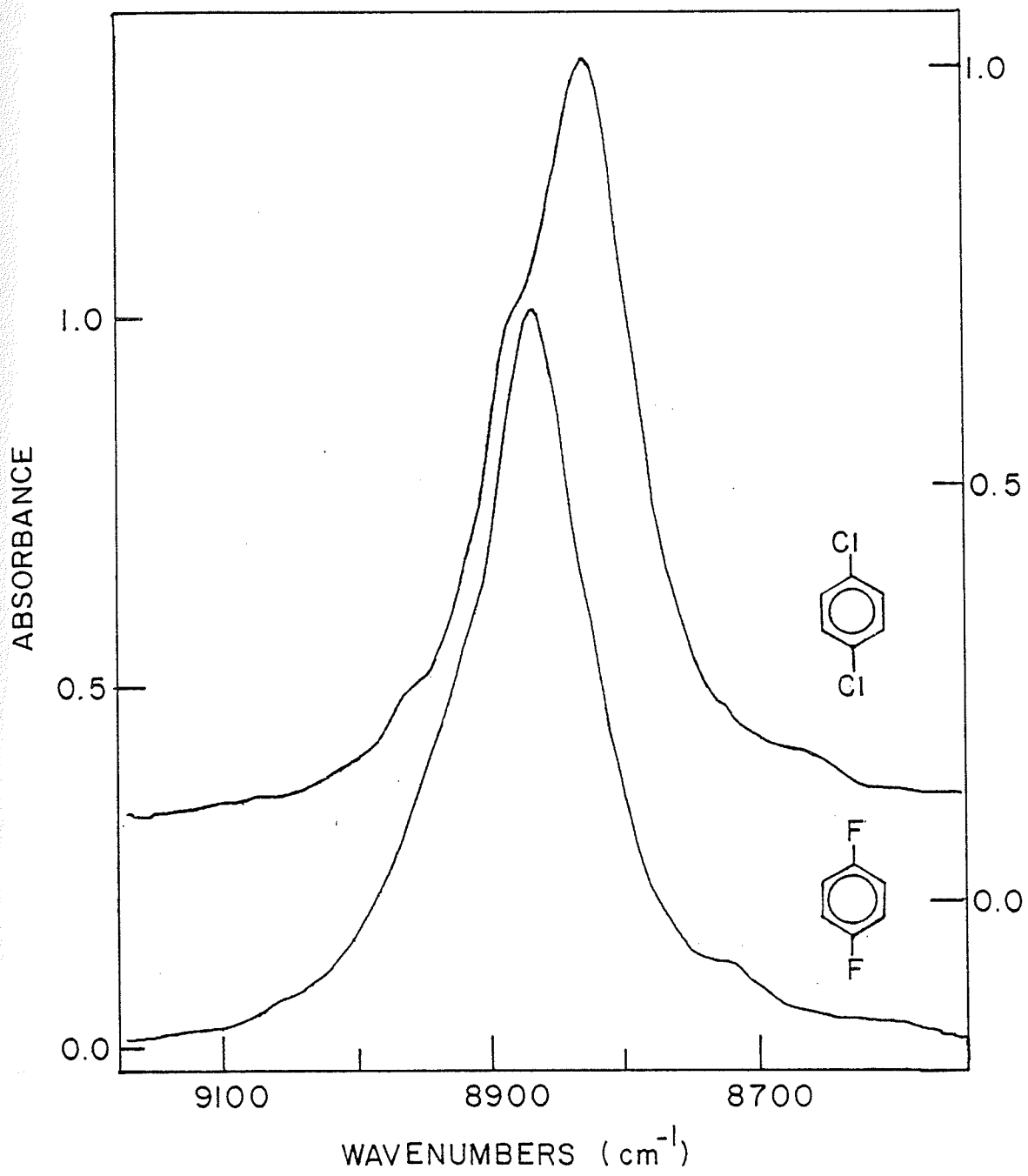
1.0
0.5
0.0
ABSORBANCE
1.0
0.5
0.0
Cl
Cl
F
F
9100
8900
8700
WAVENUMBERS (cm⁻¹)

Figure 8

The CH-stretching overtone spectra of 1,3,5-trifluorobenzene in the liquid phase, 2 cm pathlength, (lower spectrum) and of 1,3,5-trichlorobenzene in $CC\ell_4$, 10 cm pathlength (upper spectrum), at room temperature in the region of $\Delta v = 3$. Recorded on the Cary 14. Ordinate on LHS refers to lower spectrum, on RHS to upper spectrum

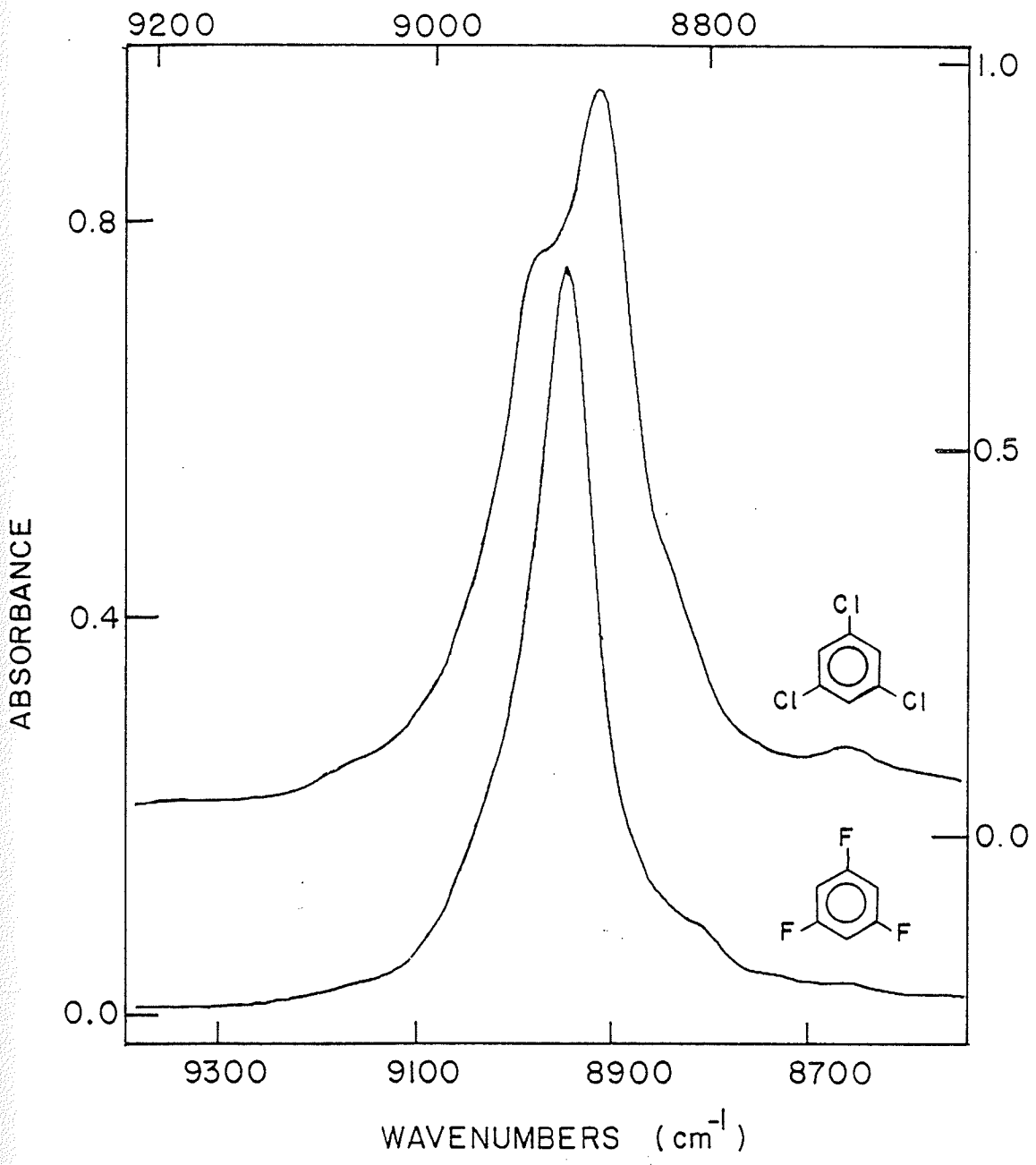
9200
9000
8800
1.0
0.8
0.5
0.4
0.0
ABSORBANCE
Cl
Cl
Cl
F
F
F
9300
9100
8900
8700
WAVENUMBERS (cm-1)

Figure 9

The CH-stretching overtone spectrum of pentafluorobenzene in the liquid phase at room temperature in the region of $\Delta\nu = 3$. 1 cm pathlength; recorded on the Cary 14.

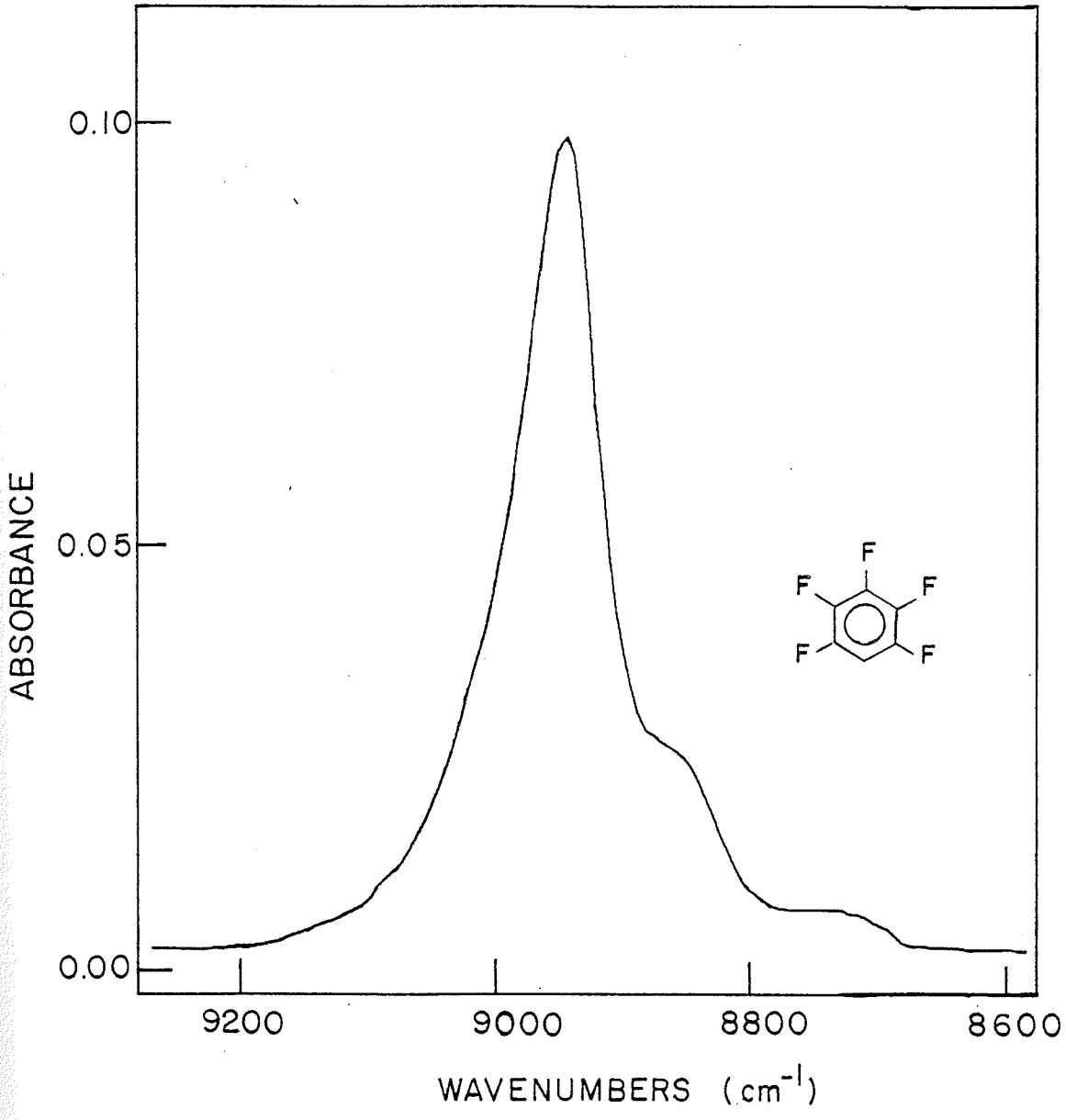
0.10
0.05
0.00
ABSORBANCE
9200
9000
8800
8600
WAVENUMBERS (cm⁻¹)
F
F
F
F
F

Figure 10

The CH-stretching overtone spectra of 1,4-dichlorobenzene, 4 cm pathlength (upper spectrum) and 1,4-dibromobenzene, 10 cm pathlength (lower spectrum) in $CC\ell_4$, at room temperature in the region of $\Delta v = 4$. Recorded on the Cary 14. Ordinate on LHS refers to lower spectrum; on RHS, to upper spectrum.

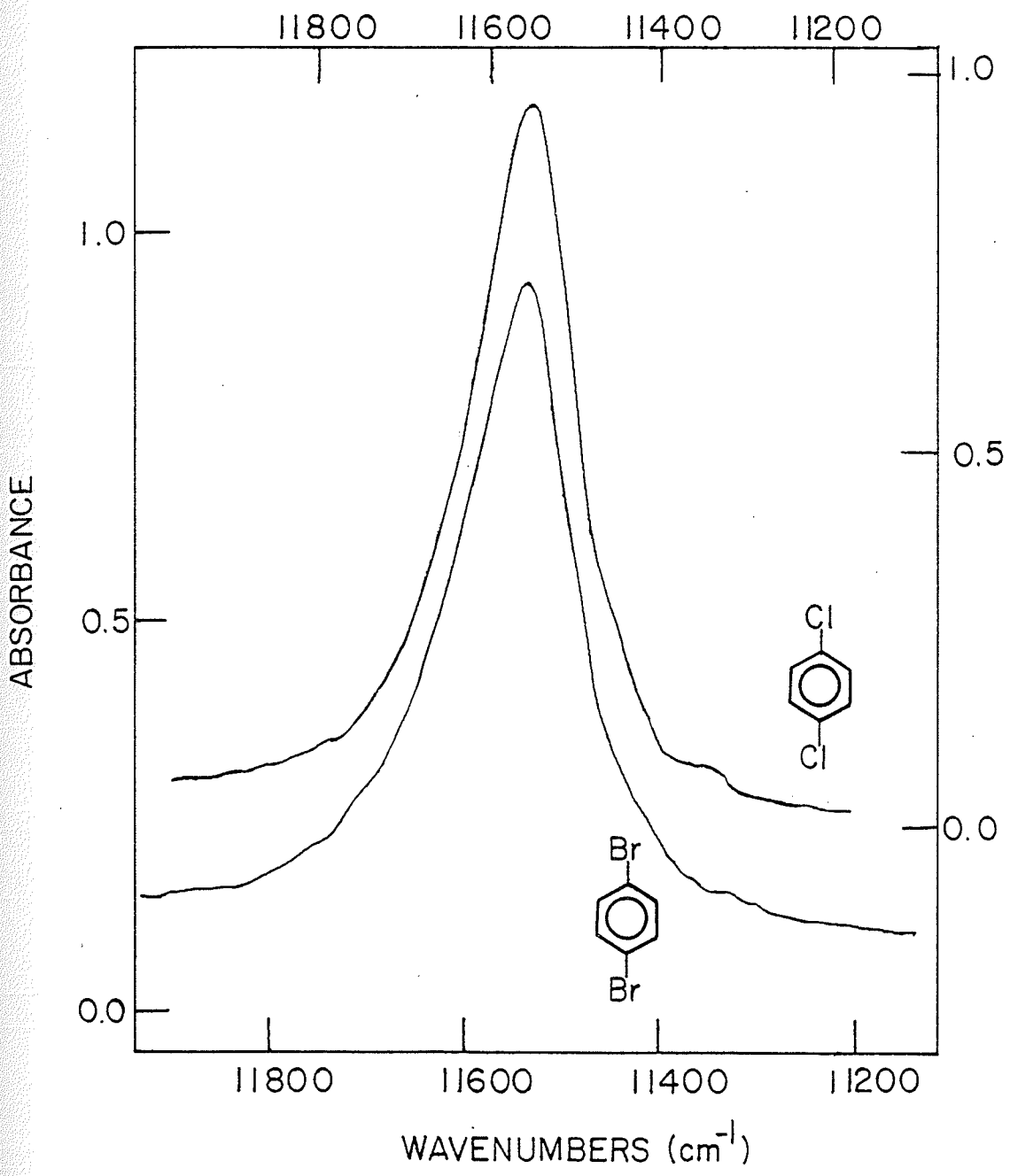
11800
11600
11400
11200
1.0
0.5
0.0
ABSORBANCE
Cl
Cl
Br
Br
WAVENUMBERS (cm⁻¹)

Figure 11

The CH-stretching overtone spectrum of 1,3-difluorobenzene in the liquid phase, at room temperature, in the region of $\Delta v = 5$. 10 cm pathlength; recorded on the Cary 219.

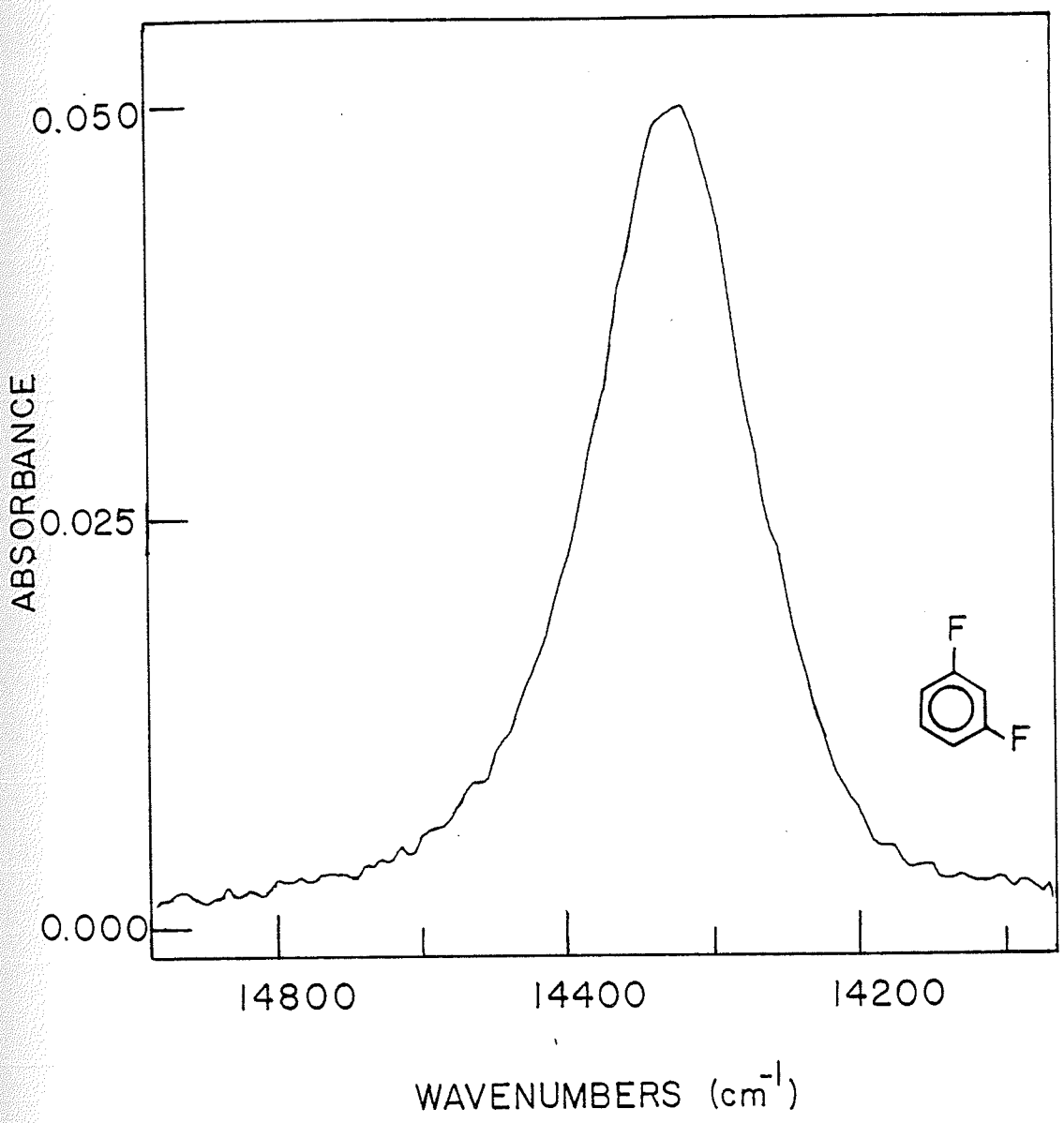
0.050
0.025
0.000
ABSORBANCE
14800
14400
14200
WAVENUMBERS (cm⁻¹)
F
F

Figure 12

The CH-stretching overtone spectra of 1,3-dichlorobenzene in $CC\ell_4$, 10 cm pathlength, recorded on the Cary 14 (lower spectrum) and 1,3-dibromo-benzene in $CC\ell_4$, 4 cm pathlength, recorded on the Cary 219 (upper spectrum) at room temperature in the region of $\Delta v = 5$. Ordinat on LHS refers to lower spectrum; on RHS, to upper spectrum.

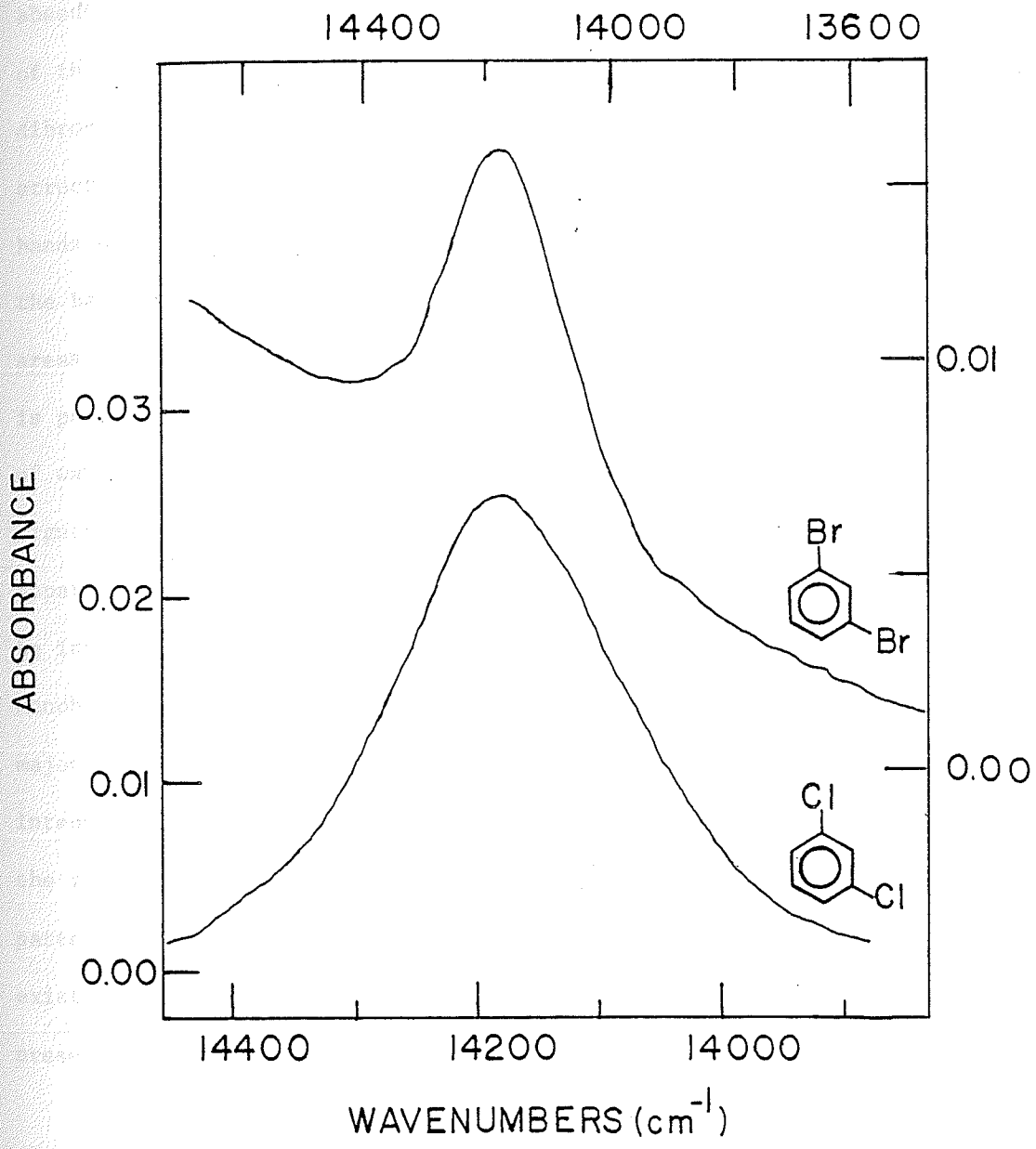
14400
14000
13600
0.01
0.03
0.02
0.01
0.00
0.00
Br
Br
Cl
Cl
ABSORBANCE
14400
14200
14000
WAVENUMBERS (cm-1)

a) Lineshape and Band Fit Results

On inspection of the experimental data it is immediately evident that the pattern of partial resolution of peaks due to inequivalent CH oscillators, apparent in the nitrobenzene spectra, is absent in the spectra of the halogenated benzenes. The $\Delta v = 3$ spectra of the four monohalobenzenes (Fig. 5) and of 1,3-dichloro- and 1,3-dibromobenzene (Fig. 6) are asymmetric, and contain partially resolved structure. However, it was not possible to decompose the overtone bands unambiguously. When up to seven calculated peaks are included in the band envelope, the accuracy of the peak positions and relative areas is questionable, particularly for poorly resolved shoulders. It is possible to obtain a reasonable fit (low RMS deviation) in a variety of ways. The results of the curve analysis of the six spectra in Figures 5 and 6 appear in Table VI. The problems discussed above are apparent. Furthermore, even the "best fit" results of Table VI cannot be interpreted in the manner of the nitrobenzene spectra. For the monohalobenzenes, the spectra are composed chiefly of two peaks, a major absorption (75-80% of the total intensity) and a second of lesser intensity (10-20%) shifted by about 50 cm^{-1} to the high energy side of the first peak. For these four molecules, it is expected that the same pattern of separation as in nitrobenzene (ortho; meta + para) will exist, though less pronounced. It is possible that such structure is present, but these data do not provide clear confirmation.

There should be three types of CH bond in the 1,3-disubstituted molecules, as follows

Table VI. Parameters from the Curve Analysis of Mono- and Dihalobenzenes in the Liquid Phase at $\Delta\nu = 3$

Molecule	Peak	FWHM (cm^{-1})	$\bar{\nu}_{max}$ (cm^{-1})	Percentage Area
Fluorobenzene	A	69	8872	10.2
	B	128	8818	89.8
Chlorobenzene	A	45	8939	2.0
	B	29	8887	1.3
	C	68	8844	14.5
	D	105	8791	80.2
	E	42	8684	1.6
Bromobenzene	A	35	8921	1.4
	B	75	8838	19.6
	C	106	8787	75.5
	D	63	8689	2.0
	E	49	8579	0.8
	F	29	8528	0.4
Iodobenzene	A	37	9056	0.1
	B	42	8905	2.0
	C	65	8823	14.3
	D	90	8772	75.0
	E	95	8676	5.6
	F	51	8558	1.2
	G	59	8481	1.4

Table VI. (Cont'd)

Molecule	Peak	FWHM (cm^{-1})	$\bar{\nu}_{max}$ (cm^{-1})	Percentage Area
1,3-Dichlorobenzene	A	53	8934	6.6
	B	34	8901	2.8
	C	78	8852	67.1
	D	64	8795	23.2
1,3-Dibromobenzene	A	78	8899	16.8
	B	87	8831	74.0
	C	37	8763	8.1
	D	26	8685	0.9

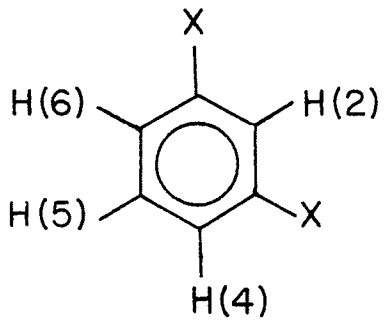

X=halogen

H(2) ≡ ortho + ortho

H(4),(6) ≡ ortho + para

H(5) ≡ meta + meta

From Figure 6, and Table VI it is clear that there are many small peaks in these two bands, but the CAP analysis does not produce three major peaks in the ratio 1:2:1. It might be argued that the relative areas of the peaks labelled C and D in 1,3-dichlorobenzene, and those labelled A and B in 1,3-dibromobenzene are about 1:3 and 3:1 respectively. Thus assuming that there was little difference between H(2) and H(4) in 1,3-dichlorobenzene, the peak at 8852 cm^{-1} might correspond to H(2), H(4) and H(6), while the peak at 8795 cm^{-1} corresponded to H(5). A similar argument would apply to the 1,3-dibromobenzene spectrum, by which the low frequency peak would correspond to H(4), H(5) and H(6), and the high frequency peak to H(2). Such assumptions and arguments are unwarranted for three reasons: ambiguity of line fit, Fermi resonance, and sample purity. The first reason has already been discussed.

The occurrence of Fermi resonance in overtone spectra is not uncommon[58,59]. In the dihalomethane spectra[28], there are significant

absorptions due to (v-1) quanta of CH stretch plus 2 quanta of CH bend, at each overtone. The frequency match between the (local + normal) combination and the pure local mode changes at each overtone because of the different anharmonicities involved. Thus the combination peaks "tune in" and "tune out" of resonance with the overtone peak throughout the overtone series, and the intensity falls off as the resonance interaction decreases. This interpretation is applied to the large, partially-resolved shoulders appearing in the $\Delta v = 3$ spectra of 1,4-dichlorobenzene (Fig. 7), 1,3,5-trichlorobenzene (Fig. 8), pentafluorobenzene (Fig. 9) and 1,2-dichlorobenzene (not shown). These peaks typically disappear at higher overtones; $\Delta v = 4$ of 1,4-dichlorobenzene (Fig. 10) can be fit with a single Lorentzian. The absence of structure in the higher overtones of the 1,3-disubstituted benzenes (Figs. 11,12) lends further credence to the assignment of the peaks at $\Delta v = 3$ to such combinations.

Finally, the purity of some compounds is sufficiently low (97-98%) that some of the smaller peaks could be due to impurities.

b) Full Width at Half Maximum (FWHM)

The FWHM for some of the halobenzenes studied are listed in Table VII. A strong argument for the existence of inequivalent CH bonds can be derived from these data. The FWHM at each overtone consistently follow the pattern mono-, 1,3-di-> 1,2-di->> 1,4-di-, 1,3,5-tri- and pentasubstituted. This ordering matches the number of inequivalent CH oscillator types: three for mono- and 1,3-disubstituted, two for 1,2-disubstituted, and one for the remainder. The differences are more pronounced at higher overtones, where the peaks would be expected to spread out because of the differences in ω and X.

Where the same number and type of inequivalent CH oscillators are present, the inequivalence would be expected to be greatest for fluorine and least for iodine, according to the results of Mizugai and Katayama[53] (σ_I) and Freymann[48] (electronegativity and dipole moment). This is found to be the case for the mono-, 1,2-di- and 1,3-disubstituted molecules, that is the FWHM are significantly larger where the halogen is fluorine. The FWHM of the 1,4-difluorobenzene overtones are also marginally larger, at Δv = 4,6, than those of the other two 1,4-dihalobenzenes, but the difference is not as large as the others, nor is it consistent. Presumably some broadening due to combinations is involved in all of the spectra, but the overall consistency of the results is striking.

Confirmation of the existence of partially resolved peaks directly ascribable to inequivalent CH oscillators was later found in the gas phase overtone spectra of the fluorinated benzenes (Chapter 4,

Table VII. FWHM (cm^{-1}) for Some Halogenated Benzenes

Substituent	FWHM at given Δv				
	2	3	4	5	6
F		140 ± 2	199 ± 2	256 ± 3	310 ± 5
Cℓ		122 ± 1	183 ± 1	228 ± 3	280 ± 13
Br		127 ± 2	187 ± 1	230 ± 3	273 ± 6
I		115 ± 2	169 ± 2	203 ± 10	
1,2-diF		130 ± 2	174 ± 1	225 ± 5	284 ± 8
1,2-diCℓ		125 ± 1	164 ± 1	214 ± 2	250 ± 4
1,2-diBr		123 ± 2	163 ± 2	210 ± 2	
1,3-diF	63 ± 1	137 ± 1	205 ± 3	258 ± 2	309 ± 8
1,3-diCℓ	58 ± 1	126 ± 1	178 ± 2	229 ± 3	
1,3-diBr	73 ± 1	139 ± 1	181 ± 2	227 ± 8	
1,4-diF	47 ± 1	108 ± 2	158 ± 1	192 ± 2	243 ± 8
1,4-diCℓ	31[a]	116 ± 1	141 ± 2	180 ± 8	231 ± 8
1,4-diBr	26[a]	112 ± 1	141 ± 2	186 ± 8	
1,3,5-triF	49 ± 1	79 ± 2	151 ± 2	176 ± 2	245 ± 8
1,3,5-triCℓ	47[a]	101 ± 1[b]	115 ± 1	162 ± 6	
penta-F	46 ± 1	82 ± 2	154 ± 5		

[a] resolved doublet

[b] unresolved shoulder

section (i)). The vapor pressures of the chloro-, bromo- and iodobenzenes were much too low for their gas phase overtone spectra to be obtained, and thus the liquid phase spectra shown here represent the best available data for these molecules. It is concluded that there do exist small differences among the CH bonds in these molecules, on the basis of the FWHM, and of the pattern of the frequency shifts, discussed in part (d) of this section.

c) Peak Maxima and Local Mode Parameters

Because of the difficulties encountered with the results of the curve analysis program, the peak maxima were taken to be the experimental band maxima, for the purpose of calculating the local mode parameters (eq. 3). The frequencies of the band maximum at each overtone for all the halogenated benzenes studied in the liquid phase are given in Table VIII. The local mode parameters, ω and X, are listed in Table IX along with the uncertainties and correlation coefficients. For 1,2,4,5-tetrachlorobenzene and pentafluorobenzene, data from $\Delta v = 2$ were also used in order to make a meaningful determination of the local mode parameters.

The uncertainties and correlation coefficients indicate an excellent fit (confidence level better than 0.001) for all the molecules except 1,4-dibromo-, 1,3,5-trichloro-, 1,3,5-tribromo- and 1,2,4,5-tetrachlorobenzene. For those marked with superscript "a", the confidence level is better than 0.01, and close to 0.001. For the tetrachlorobenzene, it is between 0.02 and 0.01. All of these compounds are solids, and poorly soluble in carbon tetrachloride, thus the observed spectral bands were of low intensity.

There is a small amount of variation in the values for X, the diagonal local mode anharmonicity constant, calculated for these molecules. It has already been noted that the magnitude of X decreases with increasing steric hindrance. The small but significant decreases in the magnitude of X for 1,3- and 1,4-dibromobenzene, 1,3,5-trichloro- and 1,3,5-tribromobenzene are further examples of the phenomenon. The decrease in the magnitude of X for the 1,3-dibromobenzene must represent an average over the three CH bond types present, but two of

Table VIII. Frequency of Band Maxima (cm^{-1}) at Each Overtone.

Molecule	Δv					
	2	3	4	5	6	7
fluorobenzene		8824	11543	14136	16633	19004
chlorobenzene		8798	11515	14097	16582	
bromobenzene		8785	11501	14078	16559	
iodobenzene		8771	11477	14045	16507	
1,2-difluorobenzene		8854	11563	14174	16661	
1,3-difluorobenzene	6057	8891	11617	14249	16759	19139
1,4-difluorobenzene	6040	8875	11598	14217	16711	19106
1,2-dichlorobenzene		8817[a]	11528	14129	11606	18975
1,3-dichlorobenzene	6016	8855	11569	14184	16667	
1,4-dichlorobenzene		8839	11558	14164	16644	
1,2-dibromobenzene	5990	8815	11513	14100	16570	
1,3-dibromobenzene	6004	8830	11552	14163		
1,4-dibromobenzene	6023	8822	11546	14150		
1,3,5-trifluorobenzene	6091	8943	11708	14347	16880	
1,3,5-trichlorobenzene		8880	11631	14272		
1,2,4-trichlorobenzene		8850	11585	14186	16683	
1,3,5-tribromobenzene	6050	8887	11620	14248		
1,2,4,5-tetrachlorobenzene	6025	8900	11609			
pentafluorobenzene	6077	8949	11694	14338		
benzene[b]	5983	8760	11443	14015	16467	18810

[a] doublet, band centre is used

[b] from Ref. 55

Table IX. Diagonal Local Mode CH-Stretching Anharmonicity Constants and Local Mode CH-Stretching Frequencies Calculated from the Peak Maxima of Table III.

Molecule	Δv_{CH}	$\omega_{CH}(cm^{-1})$	$X_{CH}(cm^{-1})$	r
fluorobenzene	3-7	3112 ± 1	-56.6 ± .3	-.99997
chlorobenzene	3-6	3104 ± 3	-56.7 ± .7	-.99985
bromobenzene	3-6	3099 ± 3	-56.6 ± .7	-.99987
iodobenzene	3-6	3098 ± 3	-57.8 ± .7	-.99984
1,2-difluorobenzene	3-6	3124 ± 3	-57.8 ± .5	-.99991
1,2-dichlorobenzene	3-7	3111 ± 1	-57.1 ± .2	-.99999
1,2-dibromobenzene	3-6	3112 ± 1	-58.8 ± .3	-.99997
1,3-difluorobenzene	3-7	3135 ± 2	-57.1 ± .5	-.99990
1,3-dichlorobenzene	3-6	3124 ± 3	-57.6 ± .6	-.99990
1,3-dibromobenzene	3-5	3109.6 ± .5	-55.4 ± .1	-.99999
1,4-difluorobenzene	3-7	3129 ± 1	-57.3 ± .3	-.99996
1,4-dichlorobenzene	3-6	3119 ± 2	-57.4 ± .3	-.99997
1,4-dibromobenzene[a]	3-5	3107 ± 3	-55.4 ± .7	-.99993
1,3,4-trifluorobenzene	3-6	3151 ± 2	-56.3 ± .5	-.99993
1,3,5-trichlorobenzene[a]	3-5	3119 ± 1	-52.9 ± .3	-.99998
1,3,5-tribromobenzene[a]	3-5	3130 ± 2	-56.0 ± .6	-.99995
1,2,4-trichlorobenzene	3-6	3121 ± 3	-56.6 ± .7	-.99984
1,2,4,5-tetrachlorobenzene[b]	2-4	3126 ± 3	-55.0 ± 1	-.9953
pentafluorobenzene	2-5	3153 ± 4	-57.2 ± 1	-.99991
benzene[c]	4-9	3091	-57.6	

[a] Confidence level better than 0.01. (see text) Ref. 60

[b] Confidence level better than 0.02. Ref. 60

[c] From Ref. 55

the three types (H(2), H(4) and (6)) would experience the steric crowding of the bulky bromine subsitutents.

The value of ω ranges from a low of 3098 cm^{-1} for iodobenzene to a high of 3153 cm^{-1} for pentafluorobenzene. In general the changes parallel the number and type of substituents, the higher values corresponding to substituents with larger values of σ_I. This is discussed more fully in part (d), and in Chapter 4 (i)(d).

d) Correlation with σ_I

The sigma parameters are generally determined experimentally from ionization equilibria, but they are interpreted as a measure of the change in the charge distribution at the meta and para positions of the substituted molecule. The two chief mechanisms by which an alteration can be effected, resonance and induction, are parameterized as σ_R and σ_I respectively.

The data in this section have already been published[61]. At the time that this work was done, the gas phase overtone spectra of the fluorinated benzenes and the molecular orbital calculations had not yet been performed. The approach to the analysis of the frequency shifts taken in the published work relied on the distinction between "through-space" and "through-bond" effects on the sigma electron populations. Such distinctions are sometimes too artificial, and the evidence supporting the distinctions is not conclusive[62,63]. Topsom[64] has separated the effects according to seven distinct mechanisms which are useful in picturing the substituent effect, but are not useful in the quantitative sense required by this work. Furthermore, it has become apparent from the molecular orbital calculations that the change in the π electron density is also a significant factor in determining the variations among the CH bonds. There are insufficient data in this report to investigate the possiblity of a dual substituent parameter correlation (σ_I and σ_R) in the manner of Reynolds et al.[65] nor is it likely that such an investigation would be more useful than the molecular orbital calculations. The values of σ_I and σ_R are measured experimentally for the meta and para positions only. For CH bonds ortho to a substituent these parameters have no meaning[66], although

the changes may be in the same direction but of greater magnitude than at the meta or para positions. To the degree that this is true, and where σ_R values are similar, or small, the positions of the overtone band maxima should correlate with σ_I.

The shift in the position of the band maximum at each overtone, $\Delta\bar{\nu}$ (cm^{-1}), relative to that reported for benzene[55], and the value of σ_I for each molecule[29,63] are given in Table X. The data for nitrobenzene are included. For molecules with more than one substituent, σ_I was multiplied by the number of substituents on the ring. The shift in the local mode frequency $\Delta\omega$ is also given in Table X.

The correlations between the frequency shift, $\Delta\bar{\nu}$, or $\Delta\omega$ and σ_I are in Table XI. For the number of data points, the confidence level is better than 0.001[60] for all correlations except those at $\Delta v = 2$ and 7. At $\Delta v = 2$, the local mode behavior is not fully established. The few peaks at $\Delta v = 7$ were of low intensity, and it was difficult to ascertain the positions of the band maxima. More importantly, they included only benzene, fluorobenzene and the three difluorobenzenes (vide infra).

The correlation between σ_I and $\Delta\bar{\nu}$ at $\Delta v = 5$ is shown graphically in Fig. 13. The causes of the scatter in the data points are

(1) the assumption of simple additivity of σ_I with increasing subsitution and

(2) the assumption that the ortho, meta and para positions are equivalent.

Table X. Shift[a] in Position of Band Maximum (cm^{-1}) at Each Overtone and σ_I for Halo- and Nitro-Substituted Benzenes.

Molecule	$\bar{\Delta\nu}$ at given Δv							
	$\Delta\omega$	2	3	4	5	6	7	σ_I[b]
fluorobenzene	21		64	100	121	166	194	0.56
chlorobenzene	13		38	72	82	115		0.51
bromobenzene	9		25	58	63	92		0.50
iodobenzene	8		11	34	30	40		0.43
nitrobenzne (o)	41		139	192	259	328		0.64
(m,p)	18		55	71	97	128		0.64
1,2-difluorobenzene	33		94	120	159	194		1.12
1,3-difluorobenzene	44	74	131	174	234	292	329	1.12
1,4-difluorobenzene	38	57	115	155	202	244	296	1.12
1,2-dichlorobenzene	20		57	85	114	139	165	1.02
1,3-dichlorobenzene	33	33	95	126	169	200		1.02
1,4-dichlorobenzene	28		79	115	149	177		1.02
1,2-dibromobenzene	21	7	55	70	85	103		1.00
1,3-dibromobenzene	19	21	70	109	148			1.00
1,4-dibromobenzene	16	40	62	103	142			1.00
1,3,5-trifluorobenzene	60	108	183	265	332	413		1.68
1,3,5-trichlorobenzene	31		120	188	257			1.53
1,2,4-trichlorobenzene	30		90	142	171	216		1.53
1,3,5-tribromobenzene	39	67	127	177	233			1.50
1,2,4,5-tetrachlorobenzene	35	42	140	166				2.04
pentafluorobenzene	62	96	189	251	323			2.80

Table X (Cont'd)

[a]Shift relative to benzene as reported by Patel, Tam, and Kerl. Ref. 55.

[b]σ_I from Ref. 29, 63.

Table XI. Correlation[a] between Frequency Shift or $\Delta\omega$ (cm^{-1}) with σ_I at Each Overtone.

Δv	No. of data points	Slope	Intercept	r
2	9	60.7 ± 0.8	-17.8 ± 0.7	0.80268
3	19	91.4 ± 0.5	-10.6 ± 0.5	0.87932
4	19	125.5 ± 0.8	-7.0 ± 0.7	0.89288
5	19	167.5 ± 0.9	-15.0 ± 0.8	0.89429
6	14	222 ± 1	-21.7 ± 0.9	0.88768
7	5	238 ± 4	14.6 ± 0.9	0.89472
$\Delta\omega$	19	26.6 ± 0.5	-1.2 ± 0.5	0.84160

[a]Does not include data for 1,2,4,5-tetrachlorobenzene, pentafluorobenzene or the ortho H's from nitrobenzene.

Figure 13

The correlation between the frequency shift of the CH-stretching overtone band maxima at $\Delta v = 5$ and σ_I. The line represents a least mean squares fit of the data, with the exclusion of the points for the ortho CH (ortho-H) bonds of nitrobenzene, and pentafluorobenzene (PENTA-F).

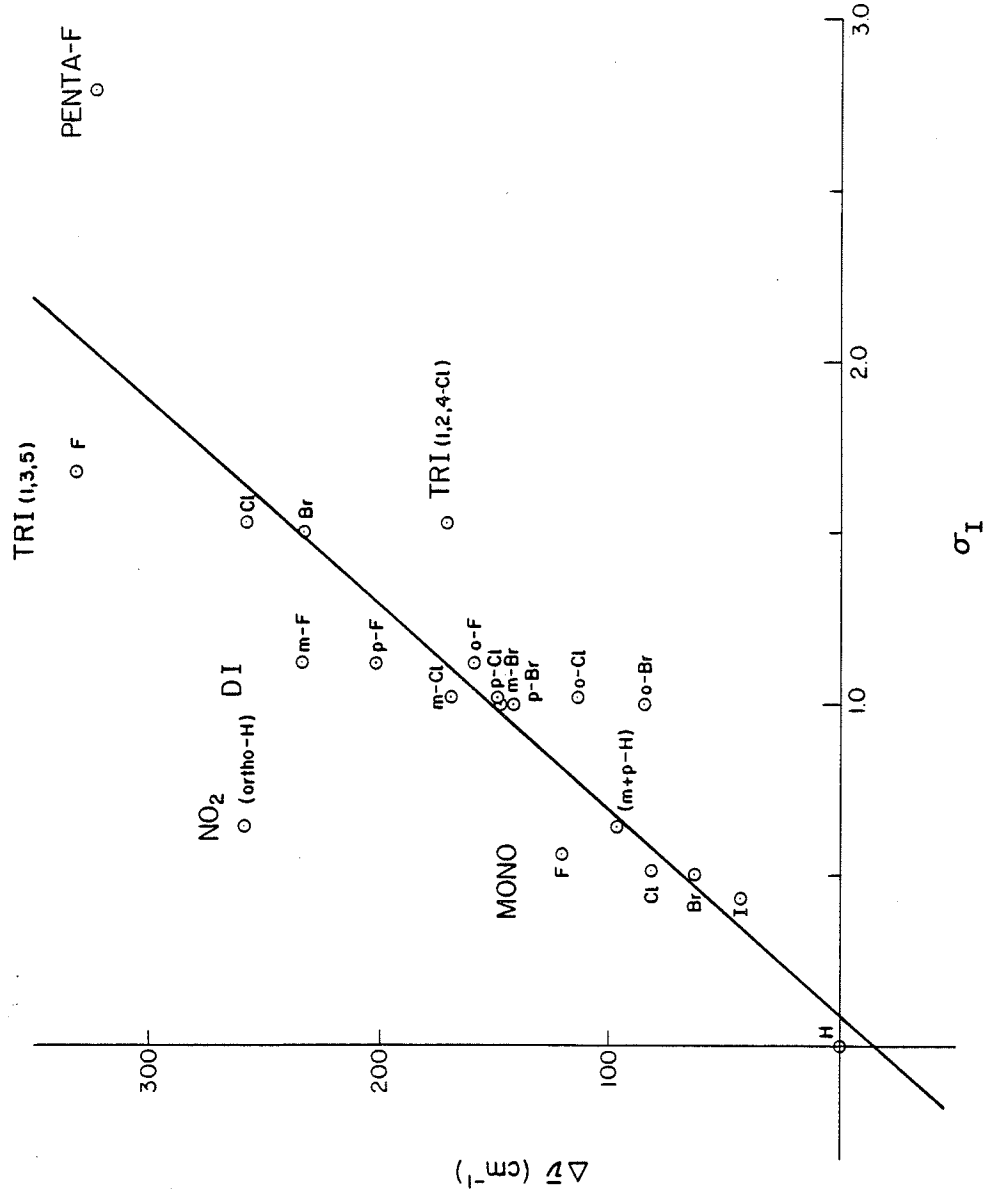
PENTA-F
TRI (1,3,5)
F
TRI (1,2,4-Cl)
Cl
Br
m-F
p-F
m-Cl
o-F
p-Cl
m-Br
p-Br
o-Cl
o-Br
NO2
(ortho-H)
DI
(m+p-H)
MONO
F
Cl
Br
I
H
300
200
100
1.0
2.0
3.0
Δν (cm⁻¹)
σI

Of the two points for nitrobenzene, the peak corresponding to the meta and para CH oscillators follows the overall correlation between $\Delta\bar{\nu}$ and σ_I, while the peak corresponding to the ortho CH oscillators is well above the line. This is in accord with the interpretation of σ_I as a measure of the changes at the meta and para positions, while the change at the ortho position is similar but more pronounced. The separation between the peak maxima of the monohalobenzenes is greater than might be anticipated on the basis of the variation in σ_I. This is the result of the averaging of different CH bond types within the overall bandshape.

For the disubstituted halogenated benzenes, the shifts occur consistently in the order 1,3-> 1,4->> 1,2-disubstituted. Here the band centres are averages for the 1,3- and 1,2-disubstituted benzenes. Contributions to the 1,3-band maxima are from ($\underline{o}$+$\underline{o}$), ($\underline{o}$+$\underline{p}$) and ($\underline{m}$+$\underline{m}$) influenced CH oscillators. The ($\underline{o}$+$\underline{o}$) peak should appear at the highest frequency. By similar assignments the band maxima for the three substitution types can be expressed as

$$\begin{aligned} \Delta\bar{\nu}\ (1,3) &\propto (\underline{o}+\underline{o}) + 2(\underline{o}+\underline{p}) + (\underline{m}+\underline{m}) = 4\underline{o} + 2\underline{m} + 2\underline{p} \\ \Delta\bar{\nu}\ (1,4) &\propto 4(\underline{o}+\underline{m}) = 4\underline{o} + 4\underline{m} \\ \Delta\bar{\nu}\ (1,2) &\propto 2(\underline{o}+\underline{m}) + 2(\underline{m}+\underline{p}) = 2\underline{o} + 4\underline{m} + 2\underline{p} \end{aligned} \qquad (5)$$

There are three unknowns and three frequency shifts for each halogen, but the data do not yield consistent values for the ortho, meta and para effects. This result suggests that

(1) σ_R may also be involved, since σ_R is much greater for F than for Cℓ or Br and

(2) there may be a non-linear response to increased subsitution.

With regard to point (2), Reynolds[67] and co-workers have observed such a non-linear response in the substituent chemical shift of disubstituted molecules. This arises because of competition among the subsitutents for the available electron population, for withdrawal, or the reverse, for electron donation.

The variations in X will also contribute to the observed shift, especially at higher overtones, because of the Xv^2 term in eq. 3. The correlation between $\Delta\omega$ and σ_I would be free of this contribution, but it is no better than the frequency shift correlations (Table XI).

e) Dissociation Energies

If the local CH-stretching potential is taken to be a Morse potential[68], then the energy for dissociation along the CH stretching coordinate can be obtained from

$$D_e^M\ (cm^{-1}) = -\omega^2/4X \qquad (6)$$

where ω and X are the local mode parameters. An alternative representation of the potential is that of Lippincott-Schroeder[69]

$$D_e^{LS}\ (cm^{-1}) = -\omega^2/[5.33X-(36.3/r^2)] \qquad (7)$$

where r is the equilibrium CH bond length. These values were determined from the LM parameters in Tables III and IX, and are listed in Table XII. For comparison, the experimental dissociation of benzene has been reported[110] as 110.5 kcal/mole, or 3.87×10^4 cm^{-1}. Since the σ_I values should be related to bond strength, the correlation between σ_I and D_e^M or D_e^{LS} was also calculated. There was no correlation of any significance (confidence level poorer than 0.02).

From Table XII, it is apparent that the uncertainties in D_e are of the same order of magnitude as the differences in D_e relative to benzene. Also, the value of X varies with steric hindrance, and not necessarily with intrinsic bond strength. While the Lippincott-Schroeder potential may lead to more accurate values of D_e, it does not correspond exactly to the local mode equation (eq. 3). This leads to a further estimated error of about 5%. The extra term in the Lippincott-Schroeder equation introduces a bond length dependence, but at this point no estimates of the variation in r had been made, and the differences of a few thousandths of an Angstrom proved negligible in eq. 7. Thus, while D_e^{LS} may be useful for diatomic molecules, they do not prove to be informative here.

Table XII. Dissociation Energies along the Local CH-Stretching Coordinate from the Morse and Lippincott-Schroeder Potentials.

Molecule	D_e^M($cm^{-1} \times 10^{-4}$)	D_e^{LS}($cm^{-1} \times 10^{-4}$)
fluorobenzene	4.27 ± 0.09	2.91 ± 0.08
chlorobenzene	4.2 ± 0.2	2.9 ± 0.2
bromobenzene	4.3 ± 0.2	2.9 ± 0.2
iodobenzene	4.2 ± 0.2	2.8 ± 0.2
nitrobenzene (o)	4.4 ± 0.2	3.0 ± 0.1
(m,p)	4.2 ± 0.1	2.9 ± 0.1
1,2-difluorobenzene	4.2 ± 0.1	2.9 ± 0.1
1,2-dichlorobenzene	4.23 ± 0.06	2.88 ± 0.05
1,2-dibromobenzene	4.11 ± 0.08	2.81 ± 0.07
1,3-difluorobenzene	4.3 ± 0.2	2.9 ± 0.1
1,3-dichlorobenzene	4.2 ± 0.2	2.9 ± 0.2
1,3-dibromobenzene	4.36 ± 0.03	2.96 ± 0.03
1,4-difluorobenzene	4.27 ± 0.09	2.91 ± 0.08
1,4-dichlorobenzene	4.23 ± 0.09	2.89 ± 0.08
1,4-dibromobenzene	4.3 ± 0.2	2.9 ± 0.2
1,3,5-trifluorobenzene	4.4 ± 0.2	3.0 ± 0.1
1,3,5-trichlorobenzene	4.6 ± 0.1	3.10 ± 0.09
1,2,4-trichlorobenzene	4.3 ± 0.2	2.9 ± 0.2
1,3,5-tribromobenzene	4.4 ± 0.2	3.0 ± 0.2
pentafluorobenzene	4.4 ± 0.3	3.0 ± 0.3
benzene[a]	4.14 ± 0.06	2.8 ± 0.1

[a]Data from Ref. 55.

v) Summary

The study of the overtone spectra of substituted benzenes in the liquid phase provided information concerning the nature of the effect of substituents on the aryl CH bonds. The partially resolved doublets in the nitrobenzene overtone spectra were shown to arise from differences in ω and X for the CH oscillators ortho, or meta and para to the substituent. The correlation of the frequency shifts with σ_I was found to apply for the CH bonds in the meta and para positions on nitrobenzene. It was not completely adequate as an explanation of the variation in the positions of the band maxima, even for the monosubstituted compounds. At higher levels of substitution, the majority of the CH bonds are ortho to at least one substituent. While the overall correlation with σ_I was good there was considerable scatter of the data.

Evidence for the presence of inequivalent CH oscillators was found in the FWHM of the overtone bands, and in the ordering of the frequency shift of the band maxima ($\Delta\bar{\nu}$) relative to those of benzene. It was not possible to confirm the presence of inequivalent CH bonds from deconvolution of the overtone bands.

The magnitude of X, the diagonal local mode anharmonicity constant, decreased when bulky substituents were present. This was interpreted as a decrease in anharmonicity due to steric crowding.

CHAPTER 4

CH-STRETCHING OVERTONE SPECTRA OF MOLECULES IN THE GAS PHASE

There are a variety of mechanisms which contribute to line width in the liquid phase, for example, a Franck-Condon progression in the librational subspace could account both for line broadening and the typical asymmetry to the high energy side of the absorption[156]. The theory of gas phase overtone line shapes has received considerable attention[70,157]. It has been shown[158] that the line broadening is dominated by homogeneous processes which yield a narrow, near-Lorentzian band. Partially resolved peaks due to inequivalent CH oscillators should be more readily discerned in gas phase spectra. The boiling points of the fluorinated benzenes are all below 100°C, those of toluene and the xylenes are slightly higher, at 110°C and around 140°C, respectively. Those of 1,3- and 1,4-cyclohexadiene, and of α,α,α- trifluorotoluene are also low. The gas phase overtone spectra of all these compounds were thus accessible with the equipment described in Ch.2iii(b).

At the same time, molecular orbital calculations on molecules of this size, with extended basis sets, have begun to appear in the literature. These provide a much more detailed and accurate picture of the changes in the electron distribution in the molecule upon substitution than was heretofore possible. These calculations are also far more sensitive than the σ_I or σ_R parameters, and enable one to examine the different positions on the ring individually. They are also expected to be superior to the substituent parameters because they describe the molecule from an ab initio standpoint, and are devoid of the experimental complications of the empirical parameters.

The results of the study of gas phase overtone spectra and ab initio molecular orbital calculations are presented in this chapter.

i) Fluorinated Benzenes

a) Peak Positions and Assignments

The gas phase overtone spectra of fluorobenzene at $\Delta v = 3$ and 4 are shown in Figure 14. The dashed line represents the band envelope calculated from the Nicolet 1280 band fit program. The spectrum in the $\Delta v = 5$ region for fluorobenzene is shown in Figure 15. The spectra of the three difluorobenzenes at $\Delta v = 3$, 4 and 5 are shown in Figures 16-18. The spectrum of 1,3,5-trifluorobenzene at $\Delta v = 3$ is shown in Figure 19. The spectra of the three tetrafluorobenzenes at $\Delta v = 2$, 3 and 4 are shown in Figures 20-22.

The positions of the peak maxima were determined with the band fitting procedure and are listed in Table XIII, along with the local mode parameters calculated from eq. 3. Where inequivalent CH bonds were present, the ratio of the calculated peak areas was determined, and the results appear in Table XIV.

The assignment of the peaks follows from the interpretation of the effects of a substituent on a CH bond ortho, meta or para to it, as described in Chapter 3(iv)(a) and (d). The assignments are further corroborated by molecular orbital calculations with full geometry optimization, discussed in part (c) of this section.

As with the NO_2 group, fluorine has a large value of σ_I, that is, it withdraws sigma electrons from the ring. This is manifested in the CH-stretching overtone spectra as a shift to higher frequencies, which is a maximum for the CH bond ortho to the substituent. The gas phase overtone spectra of fluorobenzene, (Figs. 14, 15) are similar to those of nitrobenzene (Figs. 1, 2) in that they are partially resolved doublets. The ratio of the peak areas from the deconvolution

Figure 14

The calculated (dashed) and experimentally observed CH-stretching overtone spectra of gas phase fluorobenzene, 86°C, in the region of $\Delta v = 3$, single scan (lower spectrum) and $\Delta v = 4$, sum of 4 scans (upper spectrum). Recorded on the Beckman 5270; 12.75 m pathlength.

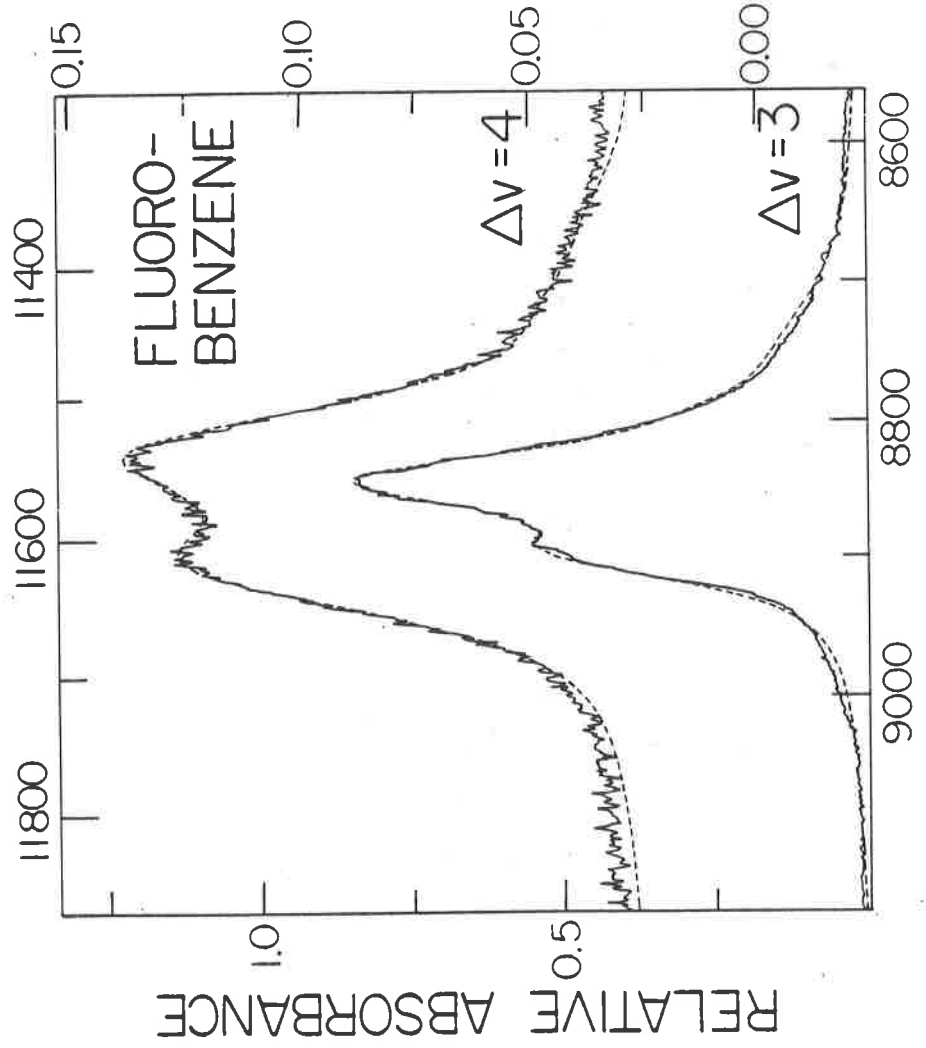
RELATIVE ABSORBANCE
1.0
0.5
11800
11600
11400
9000
8800
8600
$\bar{\nu}$ (cm^{-1})
FLUORO-
BENZENE
Δv=4
Δv=3
0.15
0.10
0.05
0.00

Figure 15

The CH-stretching overtone spectrum of gas phase fluorobenzene, 87°C, in the region of $\Delta v = 5$. Recorded on the Beckman 5270; 3.75 m pathlength, sum of 4 scans.

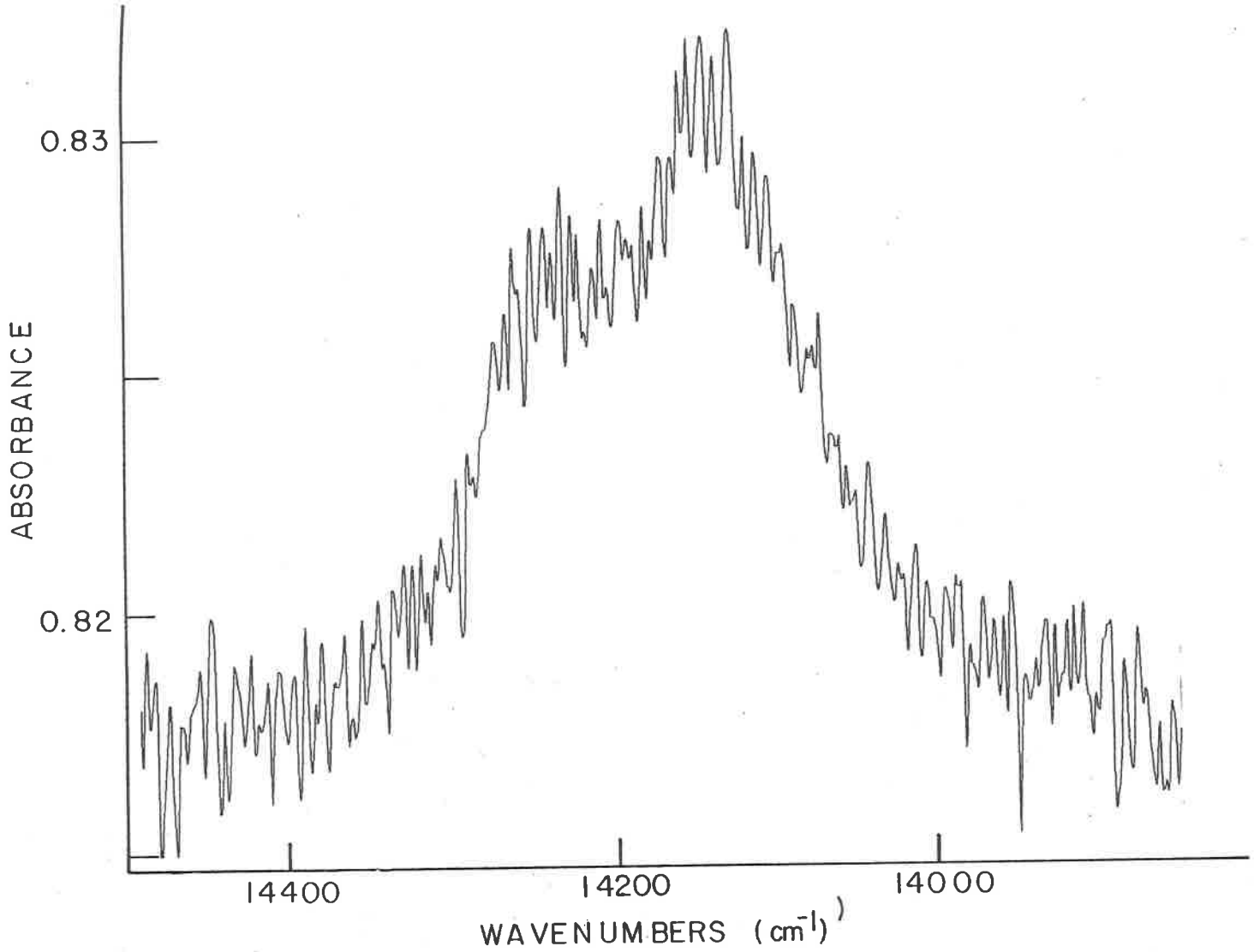
0.83
0.82
ABSORBANCE
14400
14200
14000
WAVENUMBERS (cm⁻¹)

Figure 16

The CH-stretching overtone spectra of 1,2-difluorobenzene, 12.75 m pathlength (lower spectrum); 1,3-difluorobenzene, 14.25 m pathlength (middle spectrum); and 1,4-difluorobenzene, 9.75 m pathlength (upper spectrum), in the gas phase, 86°C, in the region of $\Delta v = 3$. Recorded on the Beckman 5270, single scan of each spectrum.

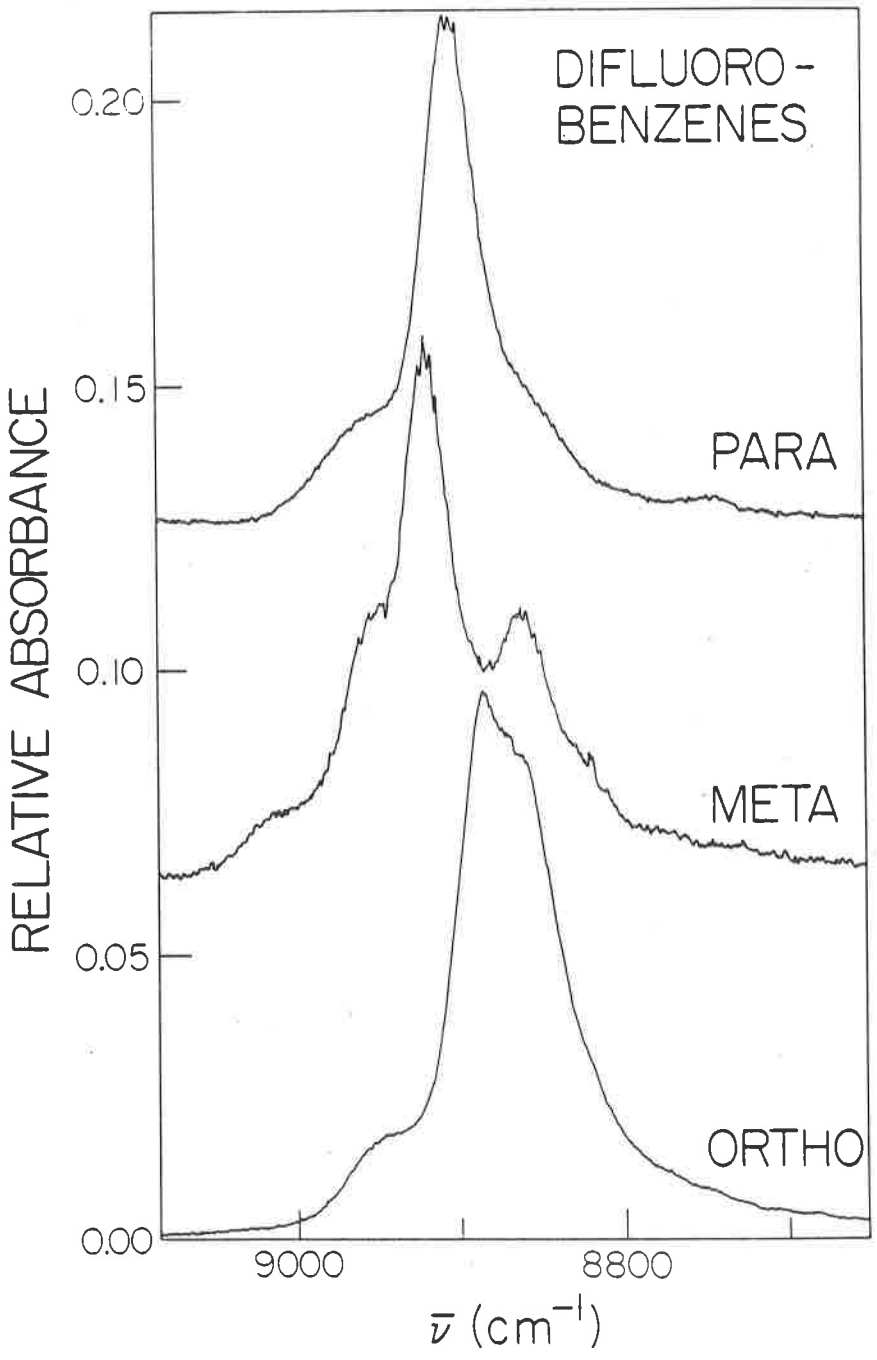
DIFLUORO-
BENZENES
PARA
META
ORTHO
RELATIVE ABSORBANCE
0.20
0.15
0.10
0.05
0.00
9000
8800
$\bar{\nu}$ (cm^{-1})

Figure 17

The CH-stretching overtone spectra of 1,2-difluorobenzene, 12.75 m pathlength, sum of 5 scans (lower spectrum); 1,3-difluorobenzene, 14.25 m pathlength, sum of 6 scans (middle spectrum); and 1,4-difluorobenzene, 9.75 m pathlength, sum of 2 scans (upper spectrum), in the gas phase, 86°C, in the region of $\Delta v = 4$. Recorded on the Beckman 5270.

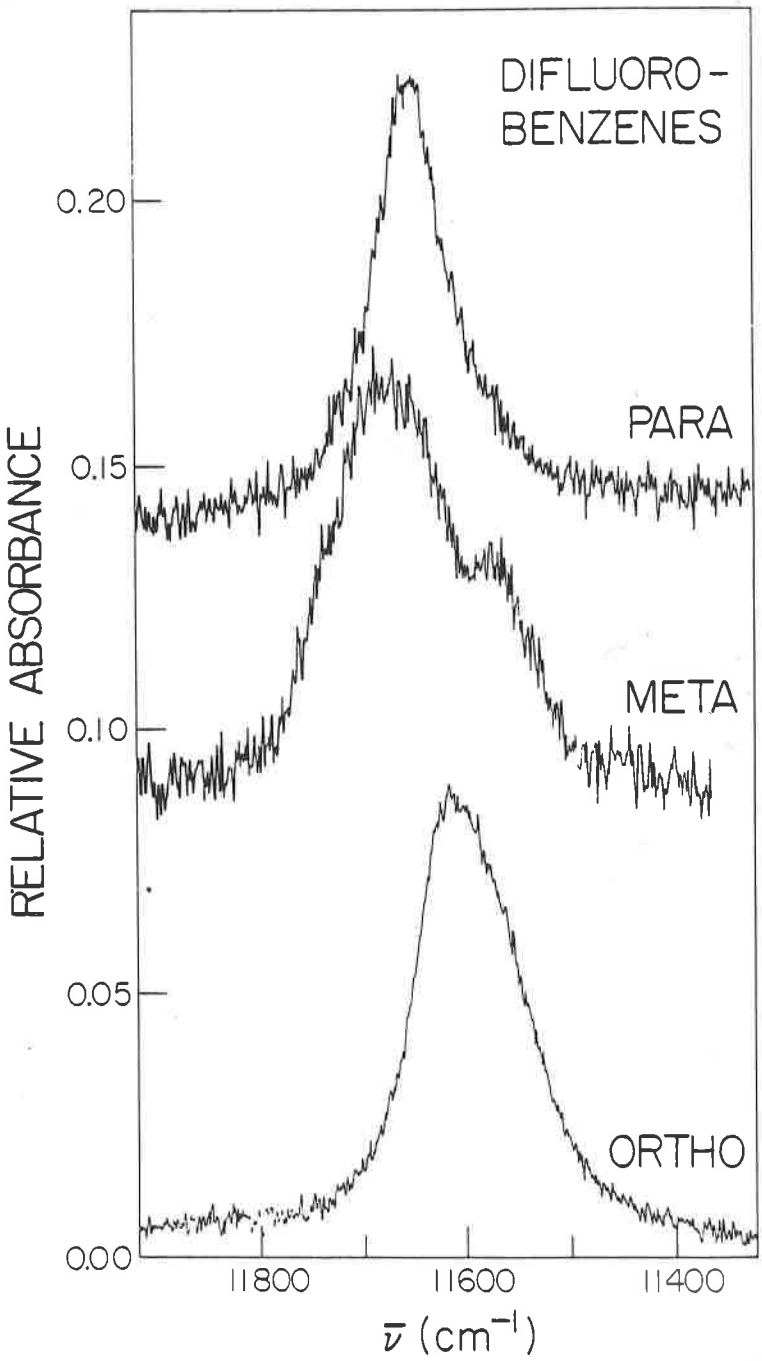
DIFLUORO-
BENZENES
PARA
META
ORTHO
RELATIVE ABSORBANCE
0.20
0.15
0.10
0.05
0.00
11800
11600
11400
$\bar{\nu}$ (cm^{-1})

Figure 18

The CH-stretching overtone spectra of 1,2-difluorobenzene, 8.25 m pathlength, single scan (lower spectrum); 1,3-difluorobenzene, 9.75 m pathlength, sum of 7 scans (middle spectrum); and 1,4-difluorobenzene, 9.75 m pathlength, sum of 2 scans (upper spectrum), in the gas phase, 86°C, in the region of $\Delta v = 5$. Recorded on the Beckman 5270.

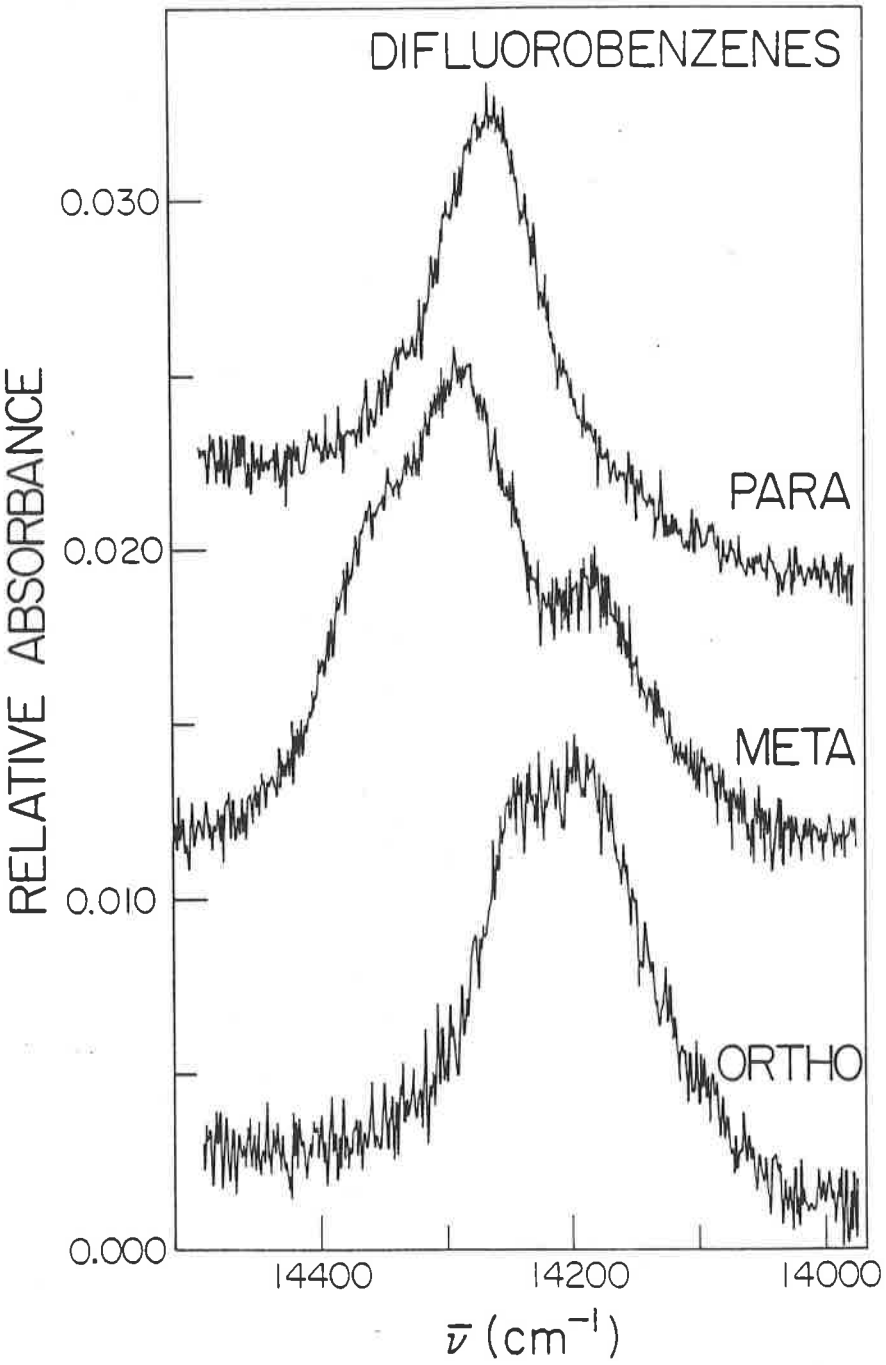
DIFLUOROBENZENES
PARA
META
ORTHO
RELATIVE ABSORBANCE
0.030
0.020
0.010
0.000
14400
14200
14000
$\bar{\nu}$ (cm^{-1})

Figure 19

The CH-stretching overtone spectrum of 1,3,5-trifluorobenzene in the gas phase, 86°C, in the region of $\Delta v = 3$. 12.75 m pathlength; recorded on the Beckman 5270, single scan.

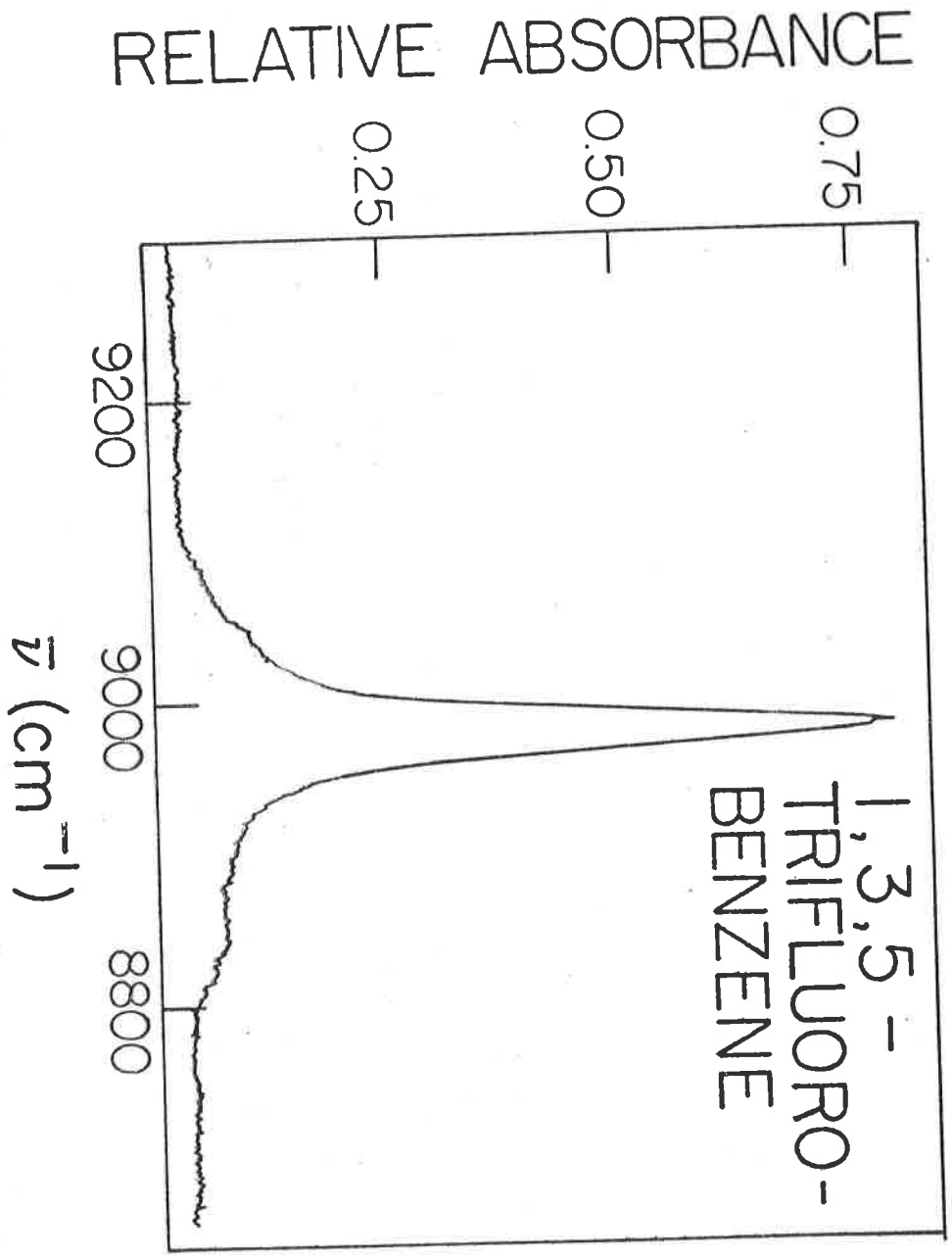
RELATIVE ABSORBANCE
0.25
0.50
0.75
9200
9000
8800
ν̄ (cm⁻¹)
1,3,5 - TRIFLUORO-BENZENE

Figure 20

The CH-stretching overtone spectra of gas phase 1,2,3,4-tetrafluorobenzene (lower spectrum), 1,2,4,5-tetrafluorobenzene (middle spectrum), and 1,2,3,5-tetrafluorobenzene (upper spectrum), 86°C, in the region of $\Delta v = 2$. 9.75 m pathlength; recorded on the Beckman 5270; single scan of each spectrum.

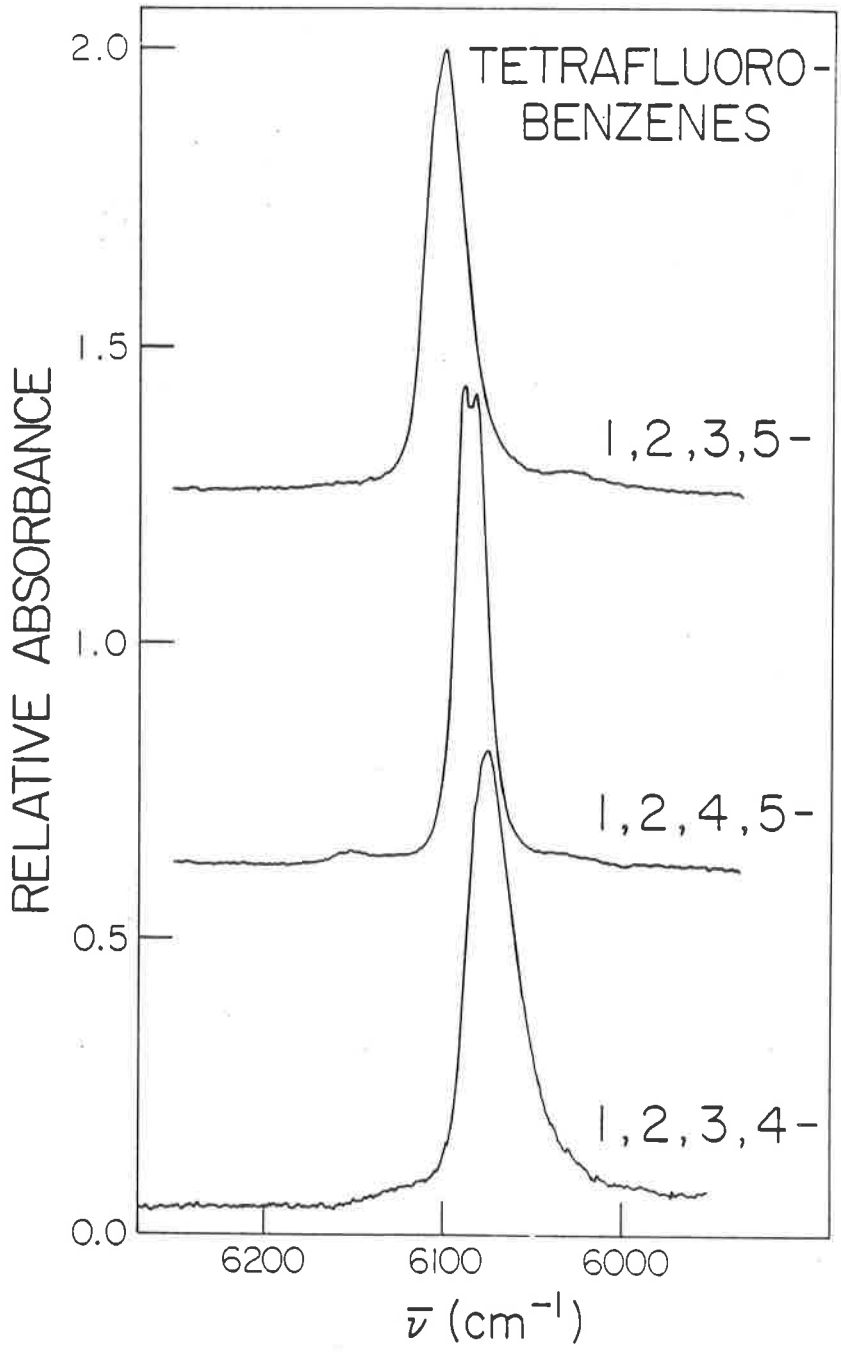
TETRAFLUORO-
BENZENES
1,2,3,5-
1,2,4,5-
1,2,3,4-
RELATIVE ABSORBANCE
2.0
1.5
1.0
0.5
0.0
6200
6100
6000
$\bar{\nu}$ (cm^{-1})

Figure 21

The CH-stretching overtone spectra of gas phase 1,2,3,4-tetrafluorobenzene (lower spectrum), 1,2,4,5-tetrafluorobenzene (middle spectrum), and 1,2,3,5-tetrafluorobenzene (upper spectrum), 86°C, in the region of $\Delta v = 3$. 9.75 m pathlength; recorded on the Beckman 5270; single scan of each spectrum.

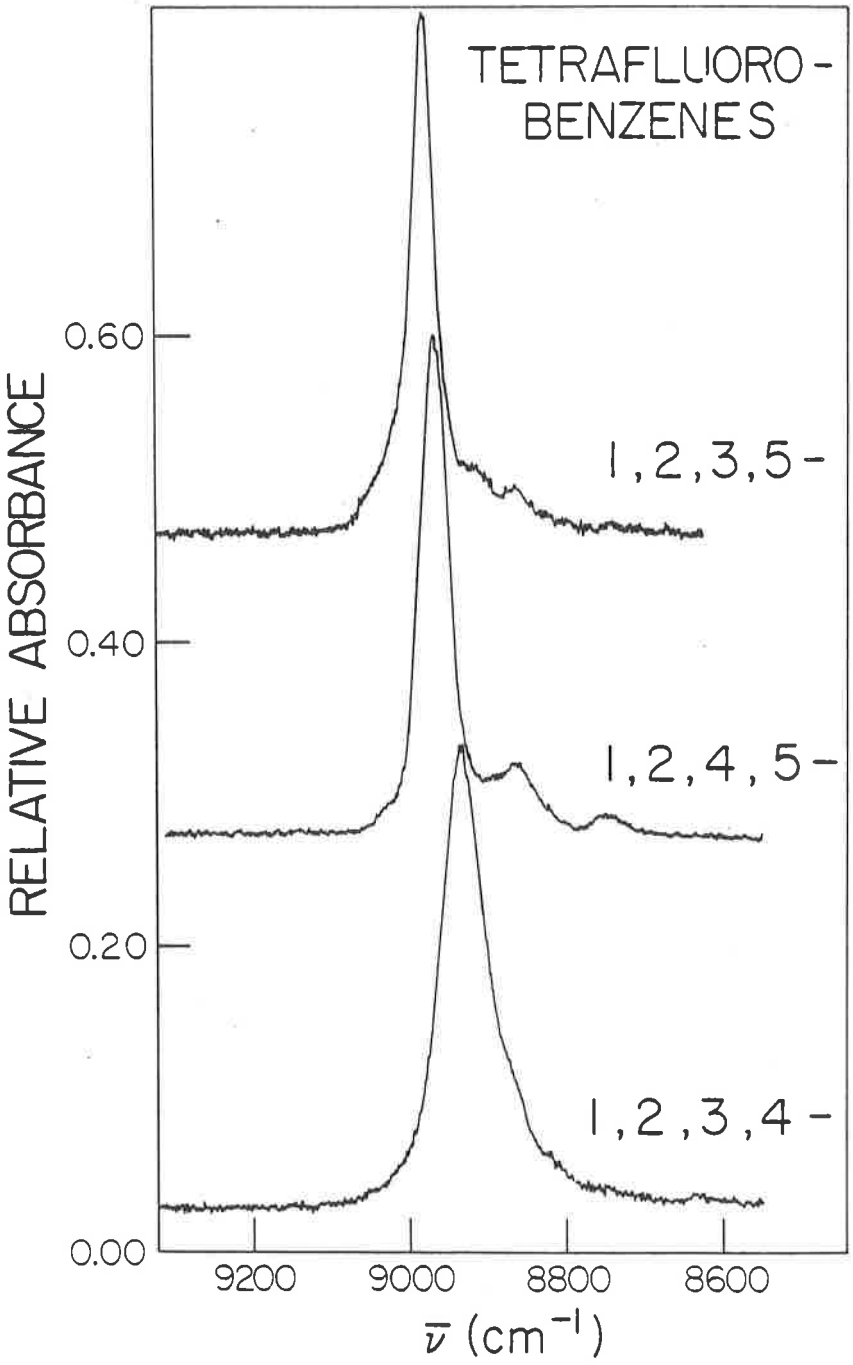
TETRAFLUORO-
BENZENES
1,2,3,5-
1,2,4,5-
1,2,3,4-
RELATIVE ABSORBANCE
0.60
0.40
0.20
0.00
9200
9000
8800
8600
$\bar{\nu}$ (cm^{-1})

Figure 22

The CH-stretching overtone spectra of 1,2,3,4-tetrafluorobenzene, sum of 7 scans (lower spectrum), 1,2,4,5-tetrafluorobenzene, sum of 9 scans (middle spectrum) and 1,2,3,5-tetrafluorobenzene, sum of 5 scans (upper spectrum), in the gas phase, 86°C, in the region of $\Delta v = 4$. 9.75 m pathlength; recorded on the Beckman 5270.

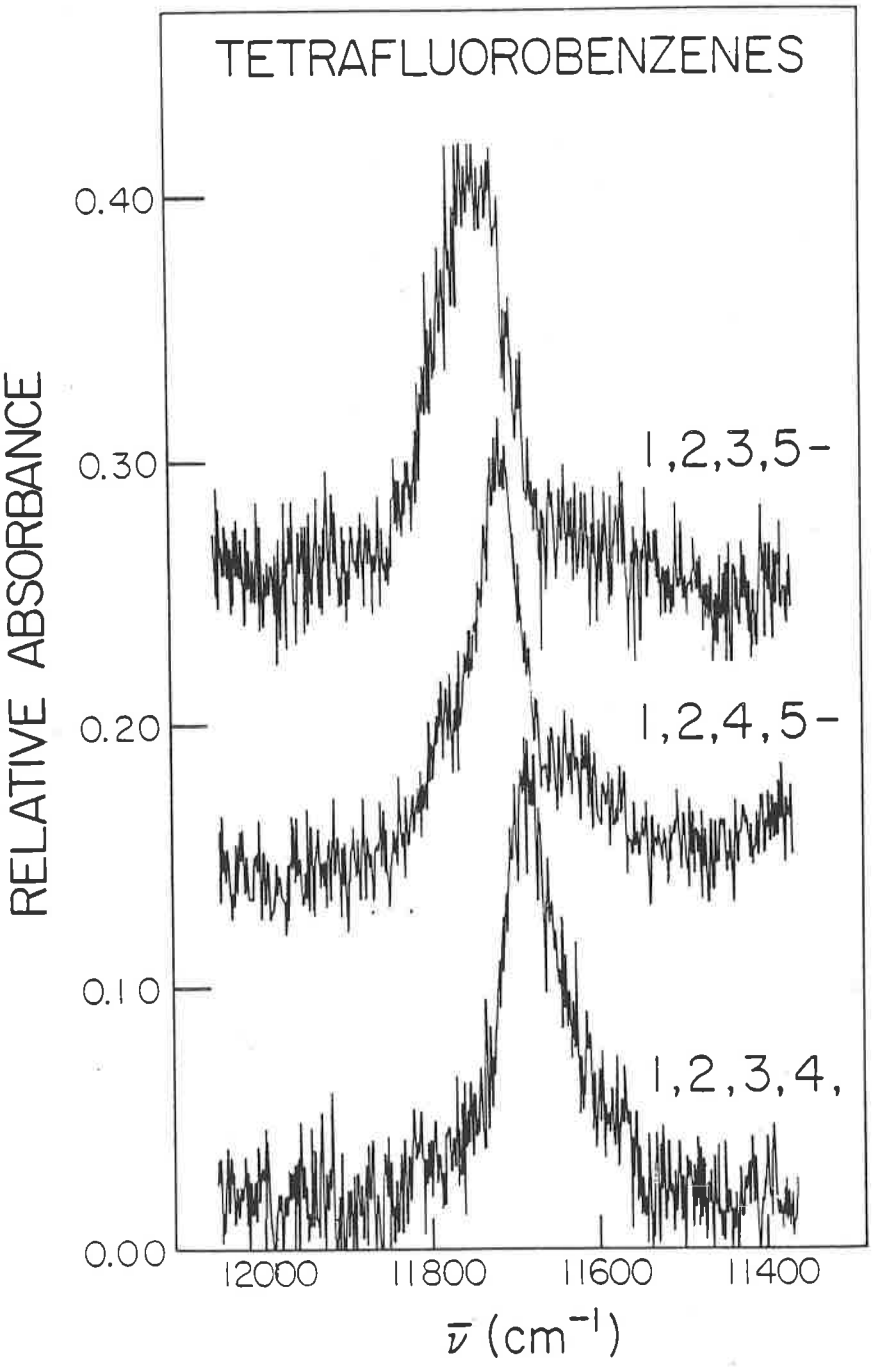
TETRAFLUOROBENZENES
RELATIVE ABSORBANCE
0.40
0.30
0.20
0.10
0.00
1,2,3,5-
1,2,4,5-
1,2,3,4,
12000
11800
11600
11400
$\bar{\nu}$ (cm^{-1})

Table XIII. Calculated Peak Positions and Local Mode Parameters from the Gas Phase Overtone Spectra of Fluorinated Benzenes

Molecule	Assignment	Δv	$\bar{\nu}_{max}$ (cm^{-1})	ω (cm^{-1})	X (cm^{-1})
fluorobenzene	H(2)	3	8892	3140±3	-58.6±0.7
		4	11617		
		5	14234		
	H(3),H(4)	3	8840	3127±6	-60.3±1.4
		4	11535		
		5	14130		
1,2-difluorobenzene	H(3)	3	8889	3134.4±0.7	-57.2±0.2
		4	11621		
		5	14242		
	H(4)	3	8859	3128±4	-58.7±1.0
		4	11570		
		5	14178		
1,3-difluorobenzene	H(2)	3	8958	3160±8	-57.5±1.8
		4	11727		
		5	14355		
	H(4)	3	8920	3150±2	-58.8±0.4
		4	11661		
		5	14279		

Table XIII (cont'd)

Molecule	Assignment	Δv	$\bar{\nu}_{max}$ (cm^{-1})	ω (cm^{-1})	X (cm^{-1})
1,3-difluorobenzene	H(5)	3	8863	3133±8	-59.8±2.0
		4	11564		
		5	14173		
1,4-difluorobenzene		3	8904	3143±6	-58.0±1.3
		4	11650		
		5	14261		
1,3,5-trifluorobenzene		3	8980	3164±8	-56.5±2.0
		4	11761		
		5	14401		
1,2,3,4-tetrafluorobenzene		2	6076	3155±3	-58.9±1.0
		3	8932		
		4	11681		
1,2,3,5-tetrafluorobenzene		2	6108	3171±2	-59.0±0.8
		3	8980		
		4	11743		
1,2,4,5-tetrafluorobenzene		2	6089	3159±6	-57.6±1.8
			6081[a]		
		3	8964		
		4	11709		

[a]Line fit uses the centre of the doublet at Δv = 2.

Table XIV. Relative Peak Areas from Curve Analysis of Gas Phase Spectra of Fluorinated Benzenes

Molecule	Assignment	Relative areas at given Δν		
		3	4	5
fluorobenzene	H(2)	2.0	2.0	2.0
	H(3),H(4)	3.5	2.2	4.0
1,2-difluorobenzene	H(3)	1.0	1.0	1.0
	H(4)	1.4	1.2	1.2
1,3-difluorobenzene	H(2)	1.2	1.0	1.0
	H(4)	2.0	2.3	2.1
	H(5)	1.3	1.0	1.1

(Table XIV) is about 3:2, low to high frequency. This ratio is roughly the same at each overtone; the reversal in the ratios, observed with the nitrobenzene liquid phase spectra at higher overtones, does not occur.

The spectra of the three difluorobenzenes at Δv = 3, 4 and 5 (Figs. 16-18) display precisely the characteristics predicted earlier. The 1,2-difluorobenzene spectra consist of partially resolved doublets at each overtone. The higher frequency peak is assigned to the overtone vibrations of the CH bonds in the (3) and (6) positions. The ratio of the peak areas is about 1:1 throughout the overtone series, although there is more uncertainty with these peaks since they are only separated by 30 to 50 cm^{-1}, at Δv = 3-5. The 1,3-difluorobenzene spectra all exhibit triplet structure. The ratio of the calculated peak areas is about 1:2:1 at each overtone, and the peaks are assigned as the overtone vibrations of CH(2), CH(4) and CH(6), CH(5), from highest to lowest frequency. The 1,4-difluorobenzene spectra are essentially single peaks at each overtone, as are those of the tri- and tetrafluorobenzenes, corresponding to the single CH bond type in each molecule.

b) Local Mode Parameters

The calculated peak maxima were used in eq. 3 to obtain the local mode parameters for each resolved CH oscillator type (Table XIII). The correlation coefficients ranged from -0.9994 to -0.99999, which indicate an excellent linear fit[60].

The values of the anharmonicity constant, X, for all the molecules, are close to the value reported[70] for gas phase benzene, -57.1 ± 0.2 cm^{-1}, within the uncertainty limits. The small size of the fluorine substituent renders unlikely the possibility of its producing steric crowding. There is also no evidence of a relationship between X and the shift in the position of the overtone maxima, though grounds for such a relationship have been postulated[58]. This problem is addressed further in part (c) of this section. A more reliable calculation of X, based on better spectra and more overtones, would be required in order to investigate these possibilities.

The value of ω varied with the number of substituents on the ring, and their position relative to the CH bond. This had been anticipated from the liquid phase study, and could also be foreseen from the actual peak positions. The reasons for these variations are discussed in detail in parts (c), (d) and (e) of this section.

c) Frequency Shift and Bond Length

The existence of a relationship between the equilibrium length of a bond and its stretching frequency has been proposed many times in the literature. The common factor is always presumed to be the bond strength. In his paper on the overtone spectra of benzene in 1929, Ellis[3] concluded that the differences in the frequencies of the CH overtone peak maxima of benzene, methane, hexane, cyclohexane and chloroform arose from the difference in the bond energies. He observed a doubling in the overtone spectra of cyclohexane[3,31] which he attributed to the presence of different types of CH bonds associated with the same carbon atom. The assignment of these peaks to the axial and equatorial CH bonds in cyclohexane was confirmed a few years ago[32].

In 1934, Badger[71] proposed an empirical relationship between k_o, the bond force constant, and r_e, the equilibrium bond length, for a series of diatomics from all rows of the periodic table. The generalizations of the rules which he and others[68,72,73] developed were found to be applicable only in a crude sense, since many factors are involved in determining bond length. However, it has been shown that for a given type of bond, some correlation does exist. In 1962, Bernstein[74] showed that the average of the fundamental XH stretching frequencies (X = C, N or O) accurately represented the XH bond force constant, and could be related to the equilibrium XH bond length. Over the last decade, McKean[20,75] has refined this approach by studying the fundamental CH stretching frequency of molecules in which all but one proton have been replaced by deuterium. He correlated the fundamental frequency of this isolated CH oscillator, $\bar{\nu}_{CH}^{iso}$, with the dissociation energy and with the equilibrium CH bond length as determined by a

variety of other techniques. The correlation is remarkably good and an empirical relationship between the CH bond length, r_{CH}^{iso}, and $\bar{\nu}_{CH}^{iso}$ has been established[20,76]

$$r_{CH}^{iso}(\text{Å}) = 1.3982 - 0.0001023\ \bar{\nu}_{CH}^{iso} \qquad (8)$$

which holds over a range of 0.040 Å. Hayward and Henry[13b] reported a very good correlation between $\bar{\nu}_{CH}^{iso}$ and overtone CH stretching frequencies at $\Delta v = 5$ for seven hydrocarbons including ethane, chloroform and benzene. Mizugai and Katayama[22] found a linear relationship between the liquid phase fifth overtone frequency and r_{CH} for four heterocyclics, benzene and fluorobenzene (all CH assumed to be equivalent) rewritten here as

$$r_{CH}\ (\text{Å}) = 1.304 - 0.00001333\ \bar{\nu}_{\Delta v = 6} \qquad (9)$$

where 16467 cm^{-1} has been taken as the $\Delta v = 6$ transition energy for benzene. Uncertainty was not determined. Strauss et al.[77] showed that the fundamental frequencies extrapolated from the gas phase overtones of four cycloalkanes were close to the $\bar{\nu}_{CH}^{iso}$ values, for both the axial and equatorial bonds. Wong and Moore[21] correlated the gas phase fifth overtone frequencies of a series of small alkanes and alkenes with CH bond lengths from IR or microwave spectroscopy, and from 4-31G molecular orbital geometry optimizations. The latter correlation was excellent

$$r_{CH}^{o}\ (4\text{-}31G)(\text{Å}) = (1.319 \pm 0.022) - (1.426 \pm 0.134) \times 10^{-5}\ \bar{\nu}_{\Delta v = 6} \qquad (10)$$

with a correlation coefficient of -0.966 for twelve data points (confidence level better than 0.001)[60]. They again demonstrated the correlation between $\Delta\nu_{\Delta v = 6}$ and $\bar{\nu}_{CH}^{iso}$.

One of the most useful developments in this area has been that which is expressed in eq. 10. Since the extended, split-valence

basis sets are more sensitive to the valence interactions[41,43,45], the optimized geometries model even very small differences in bond length very well. Several groups, Boggs, Pulay and coworkers[41,44-46], and Schäfer, Van Alsenoy, Scarsdale and coworkers[43,78], among others, have demonstrated the usefulness of such calculations for small polyatomic molecules, particularly when the usual methods of experimental analysis such as microwave or gas electron diffraction yield ambiguous or conflicting results.

In this report, the two approaches, experimental and quantum mechanical, are pursued and compared. From McKean's work[20], a shift in the fundamental CH stretching frequency of 10 cm^{-1} corresponds to a change in CH bond length of 0.001 Å. Wong and Moore[21] found that at $\Delta v = 6$, a shift of 69 cm^{-1} corresponded to the same bond length change, 0.001 Å. With fewer data points, in the liquid phase at $\Delta v = 6$, Mizugai and Katayama[22] got a value of 75 cm^{-1} for a 0.001 Å change in bond length. Provided that the magnitudes of X are comparable, it is clear that a shift in the position of an overtone peak relative to benzene will be due to the variation in the local mode frequency. By averaging the results of McKean, Wong and Moore, and Mizugai and Katayama, it is found that a frequency shift of 11v cm^{-1} corresponds to a bond length change of 0.001 Å for a given Δv. The equation

$$r_{CH}^{LM}(\text{Å}) = 1.084 - \left(\frac{\Delta\bar{\nu}}{11v}\right) \times (0.001) \qquad (11)$$

was used to calculate the CH bond length from the shift in the position of the peak maximum relative to benzene at each overtone. The shifts of the calculated peak maxima ($\Delta\bar{\nu}$) for the gas phase overtone spectra of the fluorinated benzenes at $\Delta v = 2$-5 appear in Table XV. Bond

Table XV. Frequency Shifts (cm^{-1}) Relative to Benzene[a] at Δv = 2 to 5 for Fluorinated Benzenes in the Gas Phase

Molecule	Assignment	Δv			
		2	3	4	5
fluorobenzene	H(2)		94	119	128
	H(3),H(4)		42	37	48
1,2-difluorobenzene	H(3)		91	123	170
	H(4)		61	72	106
1,3-difluorobenzene	H(2)		160	229	282
	H(4)		122	163	207
	H(5)		65	66	101
1,4-difluorobenzene			106	152	188
1,3,5-trifluorobenzene			182	263	329
1,2,3,4-tetrafluorobenzene		104	134	183	
1,2,3,5-tetrafluorobenzene		135	182	245	
1,2,4,5-tetrafluorobenzene		117	166	211	

[a] from Ref. 70

Table XVI. Experimental and Ab Initio CH Bond Lengths in Benzene and Fluorinated Benzenes, in Å

Molecule	Assignment	r_{CH}^{LM}	r_{CH}^{STO-3G}	r_{CH}^{4-21G}[a]
benzene		1.084[b]	1.08258[c]	1.084[d]
fluorobenzene	H(2)	1.081_4	1.081_9	1.081_3
	H(3)	1.083_0	1.082_5	1.083_4
	H(4)	1.083_0	1.082_1	1.083_1
1,2-difluorobenzene	H(3)	1.081_1	1.082_3	1.081_6[f]
	H(4)	1.082_2	1.082_2	1.082_6[f]
1,3-difluorobenzene	H(2)	1.079_0	1.080_9	1.079
	H(4)	1.080_3	1.081_0	1.081
	H(5)	1.082_2	1.083_5	1.083
1,4-difluorobenzene		1.080_7	1.082_3	1.081_2[f]
1,3,5-trifluorobenzene		1.078_2	1.080_2	1.078
1,2,3,4-tetrafluorobenzene		1.079_7	1.082_0	
1,2,3,5-tetrafluorobenzene		1.078_2	1.080_8	
1,2,4,5-tetrafluorobenzene		1.079_0	1.082_1	
pentafluorobenzene		1.078_9[e]		1.079

[a] From Ref. 45, except for benzene, 1,2- and 1,4-difluorobenzene

[b] Assigned

[c] From Ref. 79

[d] From Ref. 44

[e] From the liquid phase frequency shift, Table X

[f] This work

lengths were calculated from the data in Table XV, with eq. 11, and averaged over the three overtones. The results appear in Table XVI, denoted r_{CH}^{LM}.

The fully optimized geometries of all eight fluorinated benzenes were determined with the STO-3G basis set. Because of size limitations discussed in Chapter 2, the 4-21G geometry optimizations were not performed on the tetrafluorobenzenes. The fully optimized geometries of some of these molecules have been published by Boggs et al.[45] Geometry optimizations on 1,2- and 1,4-difluorobenzene were performed with the MONSTERGAUSS[36-38] program, with the Pople 4-21G basis set[42]. The bond lengths calculated with the 4-21G basis set are shorter than experimental r_e and r_o values. In practice, a correction term is added to the calculated values for purposes of easier comparison. The important parameter is the difference between the calculated CH bond lengths. The ab initio bond lengths from the STO-3G and 4-21G geometry optimizations, denoted r_{CH}^{STO-3G} and r_{CH}^{4-21G}, are also listed in Table XVI.

The values of the r_{CH}^{STO-3G} bond lengths are about the same as the experimental r_{CH}^{LM} values, but they do not mirror the small variations predicted from the spectra. There are less data at the 4-21G level, but there is a marked improvement in the correlation.

Although this section deals only with the gas phase spectra of the fluorinated benzenes, r_{CH}^{LM} has been calculated for liquid phase anisole, nitrobenzene and pentafluorobenzene, and for gas phase toluene, ortho-fluorotoluene and the 1,3- and 1,4-cyclohexadienes. The STO-3G geometry optimizations on some of these molecules were also

performed, and the 4-21G optimized geometries of some have been published. The details are documented in later sections of this chapter, but for the purpose of understanding the correlations, the data are included here. In Figure 23, the correlation between r_{CH}^{LM} and r_{CH}^{STO-3G} is displayed. This basis set does reproduce CH bond lengths reasonably well, but there is considerable scatter in the data. The 4-21G calculations are markedly superior (Fig. 24). The relationship between r_{CH}^{LM} and r_{CH}^{4-21G} is

$$r_{CH}^{4-21G}\ (\text{Å}) = (0.9679 \pm 0.0118)\ r_{CH}^{LM} + (.0349 \pm .0129) \qquad (12)$$

with a correlation coefficient of 0.991 for twenty-two data points.

Three matters require some further consideration here: the variation in X, the determination of r_{CH} by other means and finally, the meaning of bond length at this level of precision. With regard to the first, according to eq. 3 a difference of 2 cm^{-1} in X would result in a separation of 18, 32, and 50 cm^{-1} at Δv = 3, 4 and 5, respectively, for two oscillators with the same local mode frequency. This would be manifested as a gradual increase in the value of r_{CH}^{LM} calculated at successively higher overtones. The errors would be 0.0005, 0.0007 and 0.0010 Å respectively, for the example given above. For the fluorobenzenes, X does not reflect steric hindrance (Chapter 4i(b)). Most of the data in Table X show that the magnitude of X is the same as that of benzene, within uncertainty limits. It has been observed that the magnitude of X can be significantly larger for the longer, weaker alkyl CH bonds[57]. This was found to affect the calculation of r_{CH}^{LM} for the cyclohexadienes (Chapter 4iii).

As for the second factor, the measurement of CH bond lengths by other techniques to within a few thousandths of an Angstrom is

Figure 23

The relationship between CH bond lengths, determined from eq. 11 and the shift in the position of the overtone maxima, (r_{CH}^{LM}), and CH bond lengths determined by ab initio geometry optimization at the STO-3G level, (r_{CH}^{STO-3G}), for benzene, the fluorinated benzenes (Table XVI), ortho-xylene and ortho-fluorotoluene, gas phase spectra; and nitrobenzene and anisole liquid phase spectra.

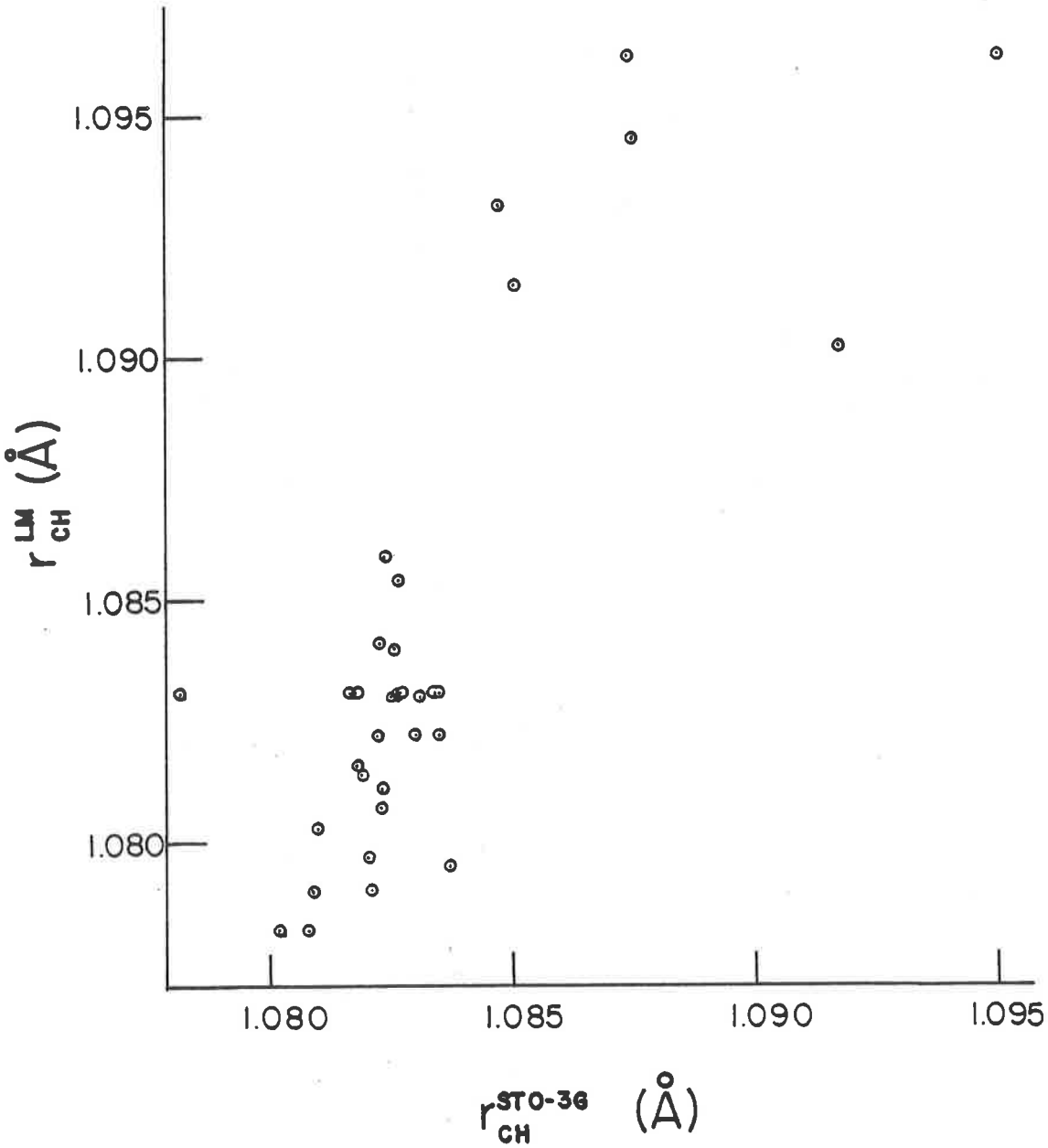
1.095
1.090
1.085
1.080
r_{CH}^{LM} (Å)
1.080
1.085
1.090
1.095
r_{CH}^{STO-3G} (Å)

Figure 24

The correlation between CH bond lengths, determined from eq. 11 and the shift in the position of the overtone maxima, (r_{CH}^{LM}), and CH bond lengths determined by ab initio geometry optimization at the 4-21G level, (r_{CH}^{4-21G}), for benzene, mono-; 1,2-, 1,3-, 1,4-di-; and 1,3,5-trifluorobenzene, toluene (planar), gas phase spectra, nitrobenzene and pentafluorobenzene, liquid phase spectra.

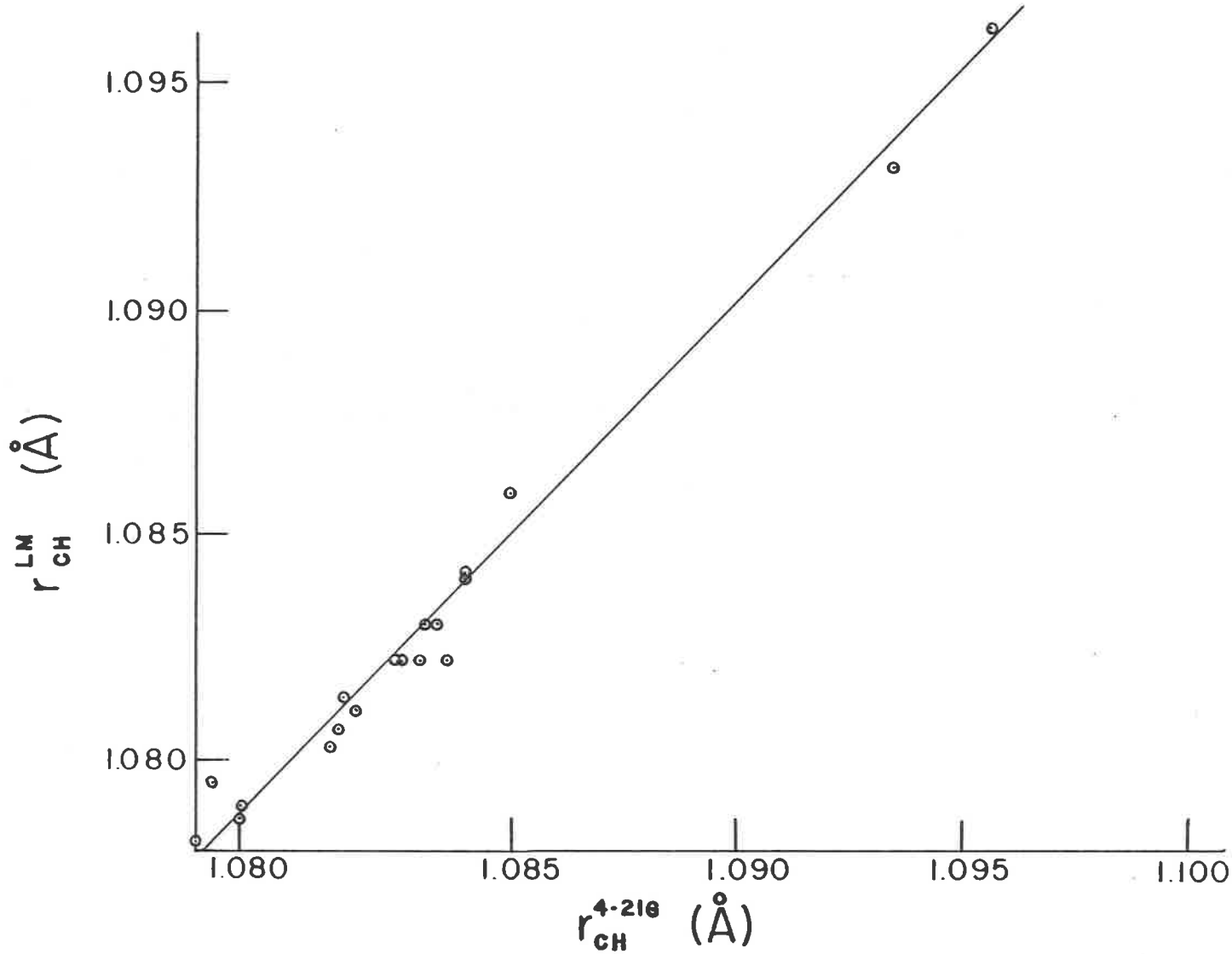
1.095
1.090
1.085
1.080
r_{CH}^{LM} (Å)
1.080
1.085
1.090
1.095
1.100
$r_{CH}^{4\text{-}21G}$ (Å)

virtually impossible for molecules of this size. Microwave data with full substitution structures are almost non-existent, and the results from partial substitution can be ambiguous. The structure of toluene (Chapter 4(ii)) is a case in point. Gas electron diffraction uncertainties are usually on the order of hundredths of an Angstrom. In the last five years, the carbon-13 satellite peaks in the proton NMR spectra of partially oriented molecules in liquid crystals have been used to predict bond lengths to a very high degree of precision, often to ten thousandths of an Angstrom. The structure of fluorobenzene has been determined in this way[80], as well as by microwave[81]. The CH bond lengths from these studies are compared to the r_{CH}^{LM} and $r_{CH}^{4\text{-}21G}$ values in Table XVII. The carbon-carbon bond lengths are also included. Both the NMR and microwave studies find the shortest CH bond will be in the para position, in contrast to the local mode and ab initio results.

Despite the precision of the NMR technique it is subject to various sources of error for the purposes of these comparisons. First, the technique only produces distance ratios. In order to convert these to actual bond lengths it is necessary to assume the length of some bond. The C(4)-C(5) bond length of 1.3976 was taken from the microwave results. Any error would appear in all other bond lengths. The NMR carbon-carbon distances are close to those from the microwave and ab initio calculations. However, the NMR carbon-hydrogen distances determined in different liquid crystal media do not agree with each other or with those from the other techniques. Since the r_{CH} values depend on the choice of liquid crystal, they cannot be determined as reliably as the uncertainties seem to indicate. A second problem could

Table XVII. Bond Lengths in Fluorobenzene from Experimental and Ab Initio Studies. References in brackets.

Bond	r_{CH}^{LM}	4-21G (44)	Liquid crystal* (80) (a)	(b)	Microwave (81)
C(2)H(2)	1.081_4	1.081_3	1.0782±0.0009	1.0790±0.0001	1.081±0.005
C(3)H(3)	1.083_0	1.083_4	1.0773±0.0007	1.0788±0.0003	1.083±0.004
C(4)H(4)	1.083_0	1.083_1	1.0760±0.0013	1.0789±0.0007	1.080±0.004
C(1)C(2)		1.3876	1.3767±0.0038	1.3852±0.0017	1.383±0.003
C(2)C(3)		1.3963	1.3920±0.0031	1.4011±0.0015	1.395±0.001
C(3)C(4)		1.3978	1.3976	1.3976	1.397±0.001

*(a) and (b) refer to determinations in two different liquid crystal media.

lie in the need to correct the NMR results for vibrational effects[82]. The direct dipole couplings are functions of the internal coordinates, thus they are dependent on the magnitude of the vibrational motion and temperature. Correction for this dependence has required the use of empirical force field calculations. These corrections were performed for the fluorobenzene study, and resulted in changes of up to 0.04 Å for the CH bond lengths.

Another example of the determination of structure from carbon-13 satellite proton NMR which should be mentioned here is that done for chlorobenzene[84]. Here the ortho, meta and para CH bonds were predicted to be 1.0775, 1.0712, and 1.0794 ± 0.0008 Å, respectively, after correction for harmonic vibration. The partially resolved doublet observed in the nitrobenzene spectra corresponded to a difference in bond length of about 0.003 Å. The difference in bond lengths of up to 0.008 Å predicted for chlorobenzene was not apparent in the liquid phase spectra (Fig. 5) or in the gas phase spectra (not shown) which were recorded for $\Delta v = 3$ and 4.

The microwave uncertainties are much larger for the CH than the CC bonds, thus all the CH bonds are equivalent within the reported uncertainties. McKean[83] has recently observed that substitution structures in microwave cannot, by their nature, be used to determine CH bond lengths, because of the isotopic dependence.

In conclusion, the determination of CH bond lengths from changes in overtone frequency, in conjunction with the optimized geometries from split-valence basis set molecular orbital calculations, is the method of choice for molecules of this size.

Finally, the question of the meaning of CH bond lengths measured to this precision should be addressed. There are many ways of

determining bond lengths experimentally, each of which involves inherent uncertainties (see Ref. 159 for a discussion of measurement techniques and associated uncertainties). The r_{CH}^{LM} values are the result of spectroscopic measurements which include both the fundamental frequency and the anharmonicity. As stated above, since the X values are virtually identical for the fluorobenzenes, anharmonicity does not present a problem. The fact that the observed overtone frequencies correlate closely with the ab initio calculated bond lengths indicates the validity of the long-held assumption that in the ground electronic state the Born-Oppenheimer approximation is valid and the "true" structure of the molecule is the Born-Oppenheimer equilibrium structure[160]. The experimental evidence from the $\bar{\nu}_{CH}^{iso}$ studies has shown that the frequency-bond length correlation holds over a very large range of bond lengths and types[20]. Recently[161], the isotropic Raman spectra of $\bar{\nu}_{CH}^{iso}$ of gas phase alkanes have been related to r_{CH}^{4-31G}, with a precision of ± 0.0001 Å. Again, the question of the validity of such precision arises, but it is the tenet of this thesis that the experimentally observable differences in the CH-stretching frequency do reflect differences in the equilibrium CH bond strength and length, as predicted from geometry optimized ab initio calculations.

d) Bond Lengths and Changes in Electron Population Distribution

The effect of the substituents on CH bond lengths is electronic in nature. The correlation with σ_I demonstrated the dependence of the frequency shift on the electron withdrawing or donating power of the substituent, within the sigma electron framework. Ellis[3] referred to a "tightening" of the CH bond in $CHC\ell_3$ due to the electronegativity of the chlorine atoms. Freymann[48] correlated the overtone frequency shift of substituted benzenes with the electric dipole moment and the electronegativity of the substituent. Mizugai and Katayama[53] concluded that the withdrawal of sigma electrons somehow resulted in increased bond strength and decreased bond length.

The variation in CH bond lengths from alkane to alkene to alkyne has been interpreted as a hybridization effect, in valence bond terms, since the work of Pauling[85,86], Coulson[87,88], Stoicheff and Herzberg[89], and Mulliken[90]. Within this picture, the CH bond length is found to decrease with increasing s character in the carbon hybridization. Smaller changes in hybridization resulting from substitution, for example, would produce further small changes in bond length[91].

The simple valence bond picture should have a counterpart within molecular orbital theory. CH bond length differences as small as 0.001 to 0.002 Å have been experimentally unverifiable, prior to the work of McKean[20]. The molecular orbital calculations[45] at the 4-21G level, with full geometry optimization, predicted CH bond lengths which were in very good agreement with those determined from the overtone frequency shift. It was reasonable to assume that the changes in

electron population in these calculations would also model the bond length/strength changes. It was necessary to determine which factors changed most upon substitution, and correlated with the bond length variation. Molecular orbitals do not describe a molecule as possessing distinct chemical bonds. Localized bond-like orbitals can be produced by various techniques[92,93], but this method was not chosen. Instead, the change in the electron population, as determined from the Mulliken population analysis matrix[94], was examined. The gross orbital population assigned to an atom contains many contributions which involve the overlap between the atomic orbitals on that atom and atomic orbitals on all other atoms in the molecule. The "non-bonded" contribution, i.e., overlap between atomic orbitals on atoms which are not formally bonded, is generally small, and varies only slightly upon substitution (vide infra). These terms are omitted as a first approximation.

The CH bond strength is considered to arise from both "ionic" and "covalent" contributions[90]. A basis-set dependent population parameter is defined

$$P^{Basis} = \underbrace{\left[\sum_{\mu,\nu}^{C} P_{\mu\nu}S_{\mu\nu} - \sum_{\mu,\nu}^{H} P_{\mu\nu}S_{\mu\nu} \right]}_{\text{IONIC}} + \underbrace{\left[2 \sum_{\mu}^{C} \sum_{\nu}^{H} P_{\mu\nu}S_{\mu\nu} \right]}_{\text{COVALENT}} \quad (13)$$

The covalent contribution to bonding is contained in the last term, which is just a bond order term and corresponds to the total electron population shared between the carbon and hydrogen atomic orbitals, i.e., twice the off-diagonal terms between bonded carbon and hydrogen from the Mulliken population matrix condensed to atoms. Here, μ and ν refer to atomic orbitals on carbon and hydrogen respectively, and $P_{\mu\nu}$

and $S_{\mu\nu}$ have the usual significance of density matrix element and overlap integral.

The ionic contribution is measured as the difference in the electron population parameters residing on the carbon and hydrogen. These are the first two terms, each of which is the sum of the electron populations in the atomic orbitals of the given atom summed over all molecular orbitals, i.e., the diagonal term in the Mulliken population matrix of charges condensed to atoms. Here, μ and ν refer to atomic orbitals either on carbon or on hydrogen, as indicated by the superscript. The unequal sharing of the electron density in the bond order term would add a small amount to the ionic term, but this is not included here.

The literature values[45] for the 4-21G optimized geometries of mono-, 1,3-di-, and 1,3,5-trifluorobenzene were used in single calculations at the 4-21G level, to obtain the associated Mulliken population matrices. The values of P^{STO-3G} and P^{4-21G} calculated from eq. 13 and the Mulliken population matrices for the fully optimized geometries are given in Tables XVIII and XIX respectively. An analogous parameter, denoted P^{Basis}_{Gross} can be obtained if the gross atomic electron populations are used in evaluating the ionic contribution, instead of the diagonal terms in the population matrix. The gross population contains the diagonal term plus one half of the population shared between the atom and each of the other atoms in the molecule. The values of P^{Basis}_{Gross} are also listed in Tables XVIII and XIX.

Molecular orbital calculations with geometry optimization, and in some cases the CH-overtone spectra, of various molecules other than fluorinated benzenes were also obtained. Details are discussed

Table XVIII. Local Mode and Ab Initio CH Bond Lengths, and Electron Population Parameters at STO-3G Level

Molecule	Assignment	r_{CH}^{LM} (Å)	r_{CH}^{STO-3G} (Å)	p^{STO-3G} (e^-)	p_{Gross}^{STO-3G} (e^-)
benzene		1.0840	1.08258	4.9627	5.9163
fluorobenzene	CH(2)	1.081_4	1.081_9	5.0072	5.9472
	CH(3)	1.083_0	1.083_1	4.9543	5.9118
	CH(4)	1.083_0	1.082_5	4.9741	5.9272
1,2-difluorobenzene	CH(3)	1.081_1	1.082_3	5.0009	5.9435
	CH(4)	1.082_2	1.082_2	4.9656	5.9225
1,3-difluorobenzene	CH(2)	1.079_0	1.080_9	5.0544	5.9803
	CH(4)	1.080_3	1.081_0	5.0201	5.9590
	CH(5)	1.082_2	1.083_5	4.9457	5.9076
1,4-difluorobenzene		1.080_7	1.082_3	4.9731	5.9430
1,3,5-trifluorobenzene		1.078_2	1.080_2	5.0663	5.9906
1,2,3,4-tetrafluorobenzene		1.079_7	1.082_0	5.0034	5.9495
1,2,3,5-tetrafluorobenzene		1.078_2	1.080_8	5.0583	5.9854
1,2,4,5-tetrafluorobenzene		1.079_0	1.082_1	5.0390	5.9706
nitrobenzene	CH(2)	1.079_5	1.083_7	4.9878	5.9368
	CH(3)	1.082_2	1.083_0	4.9696	5.9247
	CH(4)	1.082_2	1.083_5	4.9651	5.9150
2-fluorotoluene	CH(3)	1.081_6	1.081_8	5.0049	5.9466
(staggered)[a]	CH(4)	1.083_1	1.082_7	4.9573	5.9146
	CH(5)	1.083_1	1.081_8	4.9719	5.9257
	CH(6)	1.085_4	1.082_7	4.9632	5.9141

Table XVIII (cont'd)

Molecule	Assignment	r_{CH}^{LM} (Å)	r_{CH}^{STO-3G} (Å)	p^{STO-3G} (e^-)	p_{Gross}^{STO-3G} (e^-)
	Methyl CH(0°)	1.091_5	1.085_1	4.8690	6.0204
	Methyl CH(60°)	1.094_5	1.087_6	4.8659	6.0193
o-xylene[b]	CH(3)	1.085_9	1.082_4	4.9684	5.9161
	CH(4)	1.084_1	1.082_3	4.9637	5.9182
	Methyl CH(0°)	1.093_1	1.084_8	4.8738	6.0142
	Methyl CH(60°)	1.096_2	1.087_5	4.8647	6.0206
anisole	CH(2)	1.083_1	1.078_3	5.0095	5.9557
(cis-staggered)[c]	CH(3)	1.083_1	1.083_4	4.9490	5.9068
	CH(4)	1.083_1	1.081_7	4.9766	5.9304
	CH(5)	1.083_1	1.083_5	4.9507	5.9087
	CH(6)	1.083_1	1.081_6	4.9993	5.9436
	Methyl CH(0°)	1.090_2	1.091_8	4.8653	5.8985
	Methyl CH(60°)	1.096_2	1.094_1	4.8359	5.8790
methanol[d,e]	Methyl CH (trans)		1.091_5	4.8661	5.8998
	Methyl CH (gauche)		1.095_1	4.8431	5.8779
2-methoxypyridine[e]	CH(3)		1.080_6	5.0234	5.9690
(cis-staggered)[c]	CH(4)		1.083_8	4.9744	5.9048
	CH(5)		1.087_2	4.9365	5.8193
	CH(6)		1.080_4	5.0096	5.9513

Table XVIII (cont'd)

Molecule	Assignment	r_{CH}^{LM} (Å)	r_{CH}^{STO-3G} (Å)	p^{STO-3G} (e^-)	p_{Gross}^{STO-3G} (e^-)
	Methyl CH(0°)		1.091_7	4.8559	
	Methyl CH(60°)		1.0930	4.8421	

[a]Staggered conformation of methyl group with respect to fluorine substituent. The unique methyl CH lies in the ring plane trans to C(2)-F

[b]Ref. 124

[c]$O-C_{methyl}$ bond is <u>cis</u> with respect to C(1)-C(2) anisole, or C(2)-C(3), pyridine. Methyl group is staggered with respect to CH(2), anisole, or CH(3), 2-methoxypyridine

[d]<u>trans</u> and <u>gauche</u> refer to orientation with respect to OH bond

[e]from Ref. 95

Table XIX. Local Mode and Ab Initio Bond Lengths and Electron Population Parameters at the 4-21G Level

Molecule	Assignment	r_{CH}^{LM} (Å)	r_{CH}^{4-21G} (Å)	P^{4-21G} (e^-)	P_{Gross}^{4-21G} (e^-)
benzene[a]		1.084	1.084	5.5474	6.2740
fluorobenzene[b]	CH(2)	1.081_4	1.081_3	5.8550	6.3437
	CH(3)	1.083_0	1.083_4	5.6156	6.2772
	CH(4)	1.083_0	1.083_1	5.5758	6.2908
1,2-difluorobenzene	CH(3)	1.081_1	1.081_6	5.9165	6.3426
	CH(4)	1.082_2	1.082_6	5.6323	6.2931
1,3-difluorobenzene[b]	CH(2)	1.079_0	1.079	6.1705	6.4151
	CH(4)	1.080_3	1.081	5.8783	6.3607
	CH(5)	1.082_2	1.083	5.6845	6.2815
1,4-difluorobenzene		1.080_7	1.081_2	5.9307	6.3468
1,3,5-trifluorobenzene[b]		1.078_2	1.078	6.1895	6.4264
Toluene (planar)[c]	CH(2)	1.085_9	1.085	5.5315	6.2654
	CH(3)	1.084_1	1.084	5.5314	6.2622
	CH(4)	1.084_1	1.084	5.5499	6.2807
	CH(5)	1.084_1	1.084	5.5266	6.2627
	CH(6)	1.085_9	1.085	5.5536	6.2676
Methyl	CH(0°)	1.093_1	1.093_5	5.5622	6.5686
Methyl	CH(60°)	1.096_2	1.095_6	5.5439	6.5650
(orthogonal)	CH(2)		1.085	5.5426	6.2667
	CH(3)		1.084	5.5279	6.2621
	CH(4)		1.084	5.5504	6.2810

Table XIX (cont'd)

Molecule	Assignment	r_{CH}^{LM} (Å)	r_{CH}^{4-21G} (Å)	P^{4-21G} (e^-)	P_{Gross}^{4-21G} (e^-)
	Methyl CH(30°)		1.094_4	5.5590	6.5687
	Methyl CH(90°)		1.097_0	5.5340	6.5615
Pentafluorobenzene[b]		1.0787	1.079		
Nitrobenzene[d]	CH(2)	1.079_5	1.078_4		
	CH(3)	1.082_2	1.082_5		
	CH(4)	1.082_2	1.083_6		

[a]Ab initio optimized bond lengths from Ref. 44

[b]Ab initio optimized bond lengths from Ref. 45

[c]Ab initio optimized bond lengths from Ref. 46

[d]Ab initio optimized bond lengths from Ref. 96

in later sections but the bond lengths and parameters are listed here for completeness. The r_{CH}^{LM}, r_{CH}^{STO-3G} and r_{CH}^{4-21G} values are listed for comparison. Correlations between the bond lengths and parameters were calculated by a standard least squares fit. The results appear in Table XX and are discussed below.

r_{CH}^{LM} with r_{CH}^{STO-3G} or r_{CH}^{4-21G}

The correlation between experimental and ab initio bond lengths has already been mentioned in part (c) of this section, and is discussed in more detail here. The correlation between r_{CH}^{LM} and r_{CH}^{STO-3G} is significant at the 0.001 confidence level for the fourteen data points involving benzene and the fluorinated benzenes. However, the correlation is markedly worse when all 28 aryl CH data points are included (confidence poorer than 0.1)[60]. This reflects the insensitivity of the basis set to small CH bond length changes. The correlation appears to be very good when the methyl CH bond lengths are included but the slope and intercept of the "best fit" is changed considerably, the slope by a factor of three, and the intercept by 0.34 Å. In other words, the best result that can be achieved with geometry optimization at the STO-3G level is a distinction between aryl and alkyl CH bonds, which generally differ in length by about 0.01 Å (see also Fig. 23).

The correlation between experimental and calculated CH bond lengths improves significantly with the split-valence basis set. The correlation for the benzene plus fluorinated benzenes is excellent, and retains its high level of significance when all available data are included. For nitrobenzene, there is very good agreement between r_{CH}^{LM} and r_{CH}^{4-21G}, in contrast to the r_{CH}^{STO-3G} data which disagreed completely.

Table XX. Correlations between Experimental and Calculated r_{CH} and Electron Population Parameters for Various Data Sets

X	Y	Slope	Intercept	r[a]	No. of Points	Data Set[b]
r_{CH}^{LM}	r_{CH}^{STO-3G}	0.3914±0.0461	0.6589±0.0498	0.7925	14	benzene, fluorinated benzenes
		0.2121±0.0271	0.8527±0.0293	0.5133[c]	23	all aryl except anisole[d]
		0.1689±0.0245	0.8994±0.0266	0.2942[e]	28	all aryl
		0.4839±0.0095	0.5587±0.0104	0.7095	34	all aryl plus methyl
r_{CH}^{LM}	P^{STO-3G}	-19.711±0.046	26.307±0.050	-0.9046	14	benzene, fluorinated benzenes
		-13.563±0.027	19.661±0.029	-0.8160	23	all aryl except anisole[d]
		-13.265±0.025	19.340±0.025	-0.7787	28	all aryl
		-10.802±0.009	16.675±0.010	-0.9260	34	aryl plus methyl
r_{CH}^{STO-3G}	P^{STO-3G}	-40.000±0.081	48.278±0.088	-0.9065	14	benzene, fluorinated benzenes

Table XX (cont'd)

X	Y	Slope	Intercept	r	No. of Points	Data Set[a]
		-18.981±0.027	25.534±0.030	-0.7430	27	all aryl except anisole[d]
		-16.171±0.020	22.489±0.022	-0.7066	32	all aryl
		-13.970±0.009	20.102±0.010	-0.8871	42	all aryl plus methyl
r_{CH}^{LM}	r_{CH}^{4-21G}	1.0312±0.051	-0.0335±0.0555	0.9865	12	benzene, fluorinated benzenes
		0.9328±0.0310	0.0728±0.0293	0.9638	20	aryl
		0.9679±0.0122	0.0349±0.0125	0.9905	22	aryl plus methyl
r_{CH}^{LM}	P^{4-21G}	-125.39±0.05	141.41±0.06	-0.9721	11	benzene, fluorinated benzenes
		-94.801±0.032	108.35±0.035	-0.9318	16	all aryl
r_{CH}^{4-21G}	P^{4-21G}	-118.69±0.05	134.20±0.05	-0.9717	11	benzene, fluorinated benzenes
		-109.11±0.04	123.84±0.04	-0.9676	16	all aryl
		-107.50±0.03	122.10±0.04	-0.9660	19	aryl plus methyl

Table XX (cont'd)

---

[a]Confidence level <0.001, unless otherwise noted. Ref. 60.

[b]All data for the calculations are listed in Table XVIII (STO-3G) or Table XIX (4-21G). Here the names of the molecules and the type of CH bond (aryl or methyl) are given for each calculation.

[c]Confidence level <0.02. Ref. 60

[d]Anisole was considered to be a special case, since gas phase spectra for $\Delta v > 3$ were not obtained, and the results were unsatisfactory.

[e]Confidence level <0.1. Ref. 60

The slope and intercept of the "best fit" is changed little upon inclusion of the two alkyl CH bond lengths, the slope by 3% and the intercept by 0.04 Å.

r_{CH}^{LM} or r_{CH}^{STO-3G} with P^{STO-3G}

The parameter correlates fairly well with both the experimental and the ab initio bond lengths at the STO-3G level. The correlation between r_{CH}^{LM} and P^{STO-3G} for benzene and the fluorinated benzenes only is shown in Figure 25. The complete set of data on r_{CH}^{LM} and P^{STO-3G} is shown in Figure 26.

It is interesting to note that the correlation remains significant at the 0.001 confidence level for r_{CH}^{LM} (aryl) and P^{STO-3G} (aryl) even though the correlation between r_{CH}^{LM} and r_{CH}^{STO-3G} is very poor for the aryl data set. The potential is nearly flat with respect to CH bond length changes at the STO-3G level. Optimization of fluorobenzene was done sequentially: the ring and C-F bond lengths were optimized serially, first, and then the CH bond lengths and angles were optimized. The total energy of the molecule was lowered by only 0.15 kJ/mole on the final step. It appears from the correlation results, however, that the electron population distribution still contains information about the bond strength.

r_{CH}^{LM} or r_{CH}^{4-21G} with P^{4-21G}

At the 4-21G level, the correlation between the population parameter and r_{CH}, experimental or ab initio, is excellent for the aryl CH bonds. For benzene and the fluorinated benzenes, r_{CH}^{LM} and P^{4-21G} appear graphically in Figure 25 also. The parameters for the aryl and alkyl CH bonds are not comparable, although for a given bond type, the

Figure 25

The correlation between CH bond lengths in benzene and the fluorinated benzenes, obtained from eq. 11, r_{CH}^{LM}, and the frequency shifts in the overtone spectra, and a bond strength parameter derived from ab initio electron population analysis at the STO-3G level (lower) and 4-21G (upper) (see also Tables XVIII, XIX and XX).

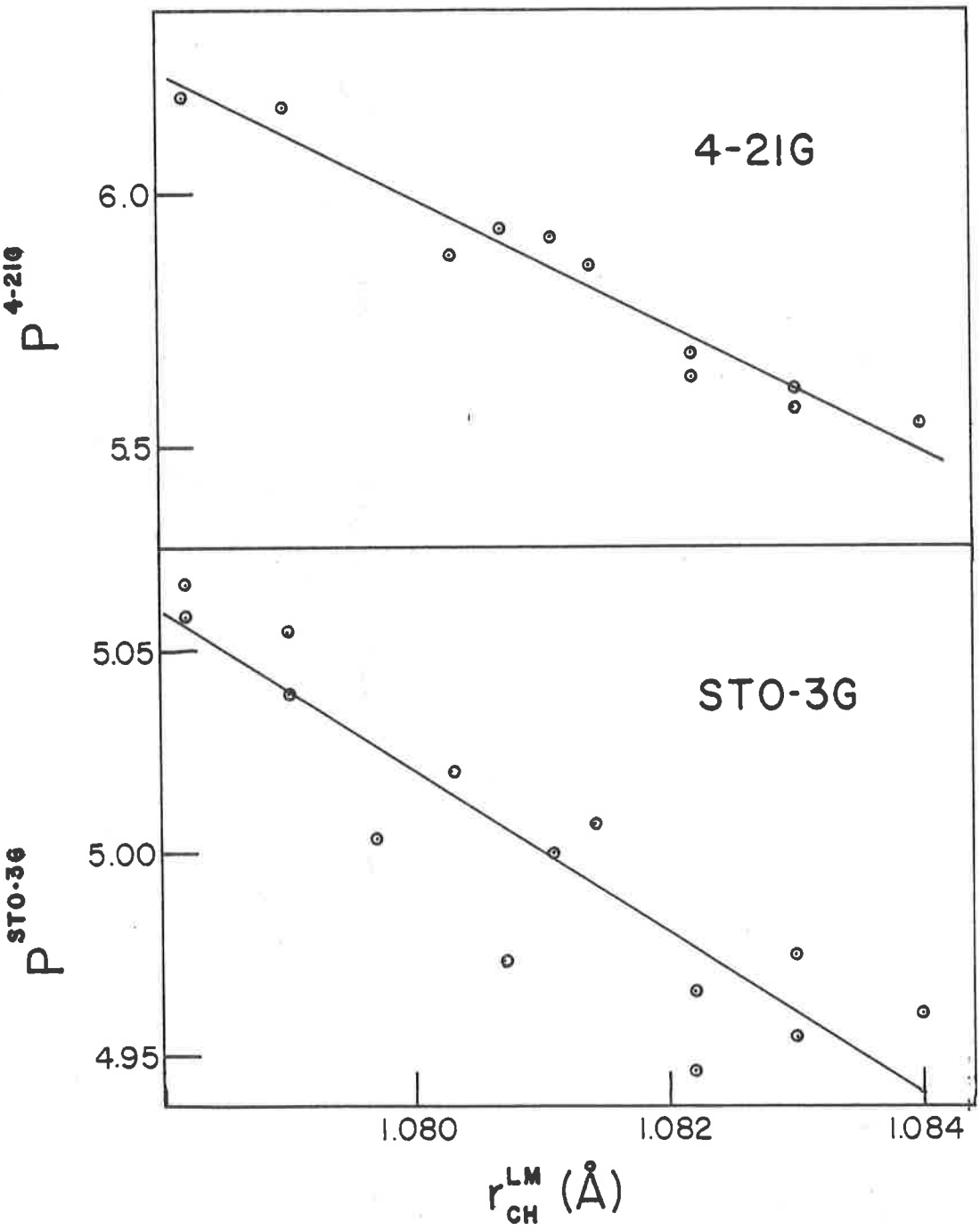
4-21G
6.0
5.5
$P^{4\text{-}21G}$
STO-3G
5.05
5.00
4.95
$P^{STO\text{-}3G}$
1.080
1.082
1.084
r_{CH}^{LM} (Å)

Figure 26

The relationship between CH bond lengths obtained from geometry optimization at the STO-3G level, and a bond strength parameter derived from the corresponding electron population analysis (see also Table XVIII).

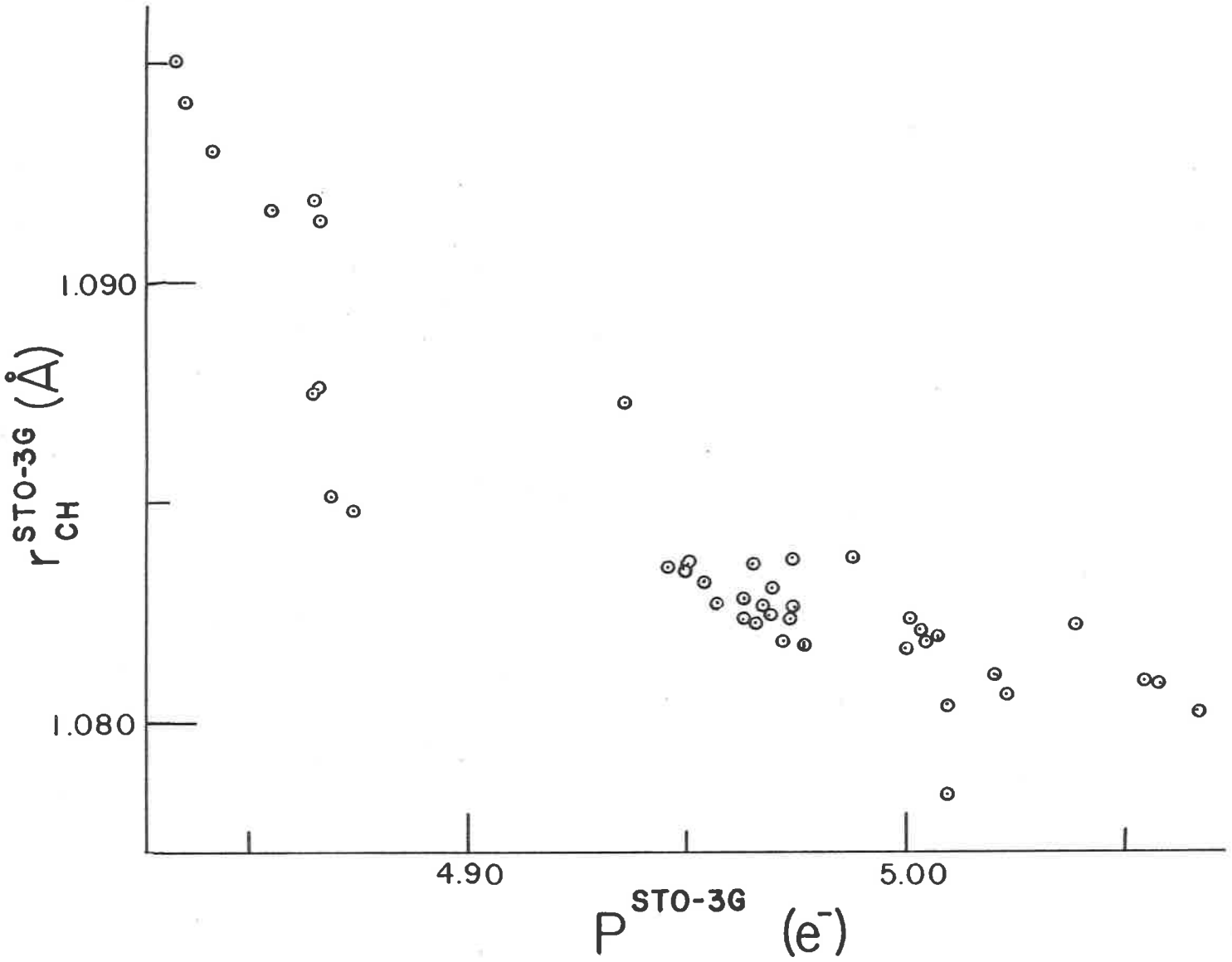
1.090
1.080
r_{CH}^{STO-3G} (Å)
4.90
5.00
P^{STO-3G} (e^-)

bond length changes can still be interpreted in terms of the changes in the electron populations. At the 4-21G level, the non-bonded interactions are larger than at the STO-3G level, and play a significant part in the bond length variation.

For many of the correlations in Table XX the confidence level is better than 0.001 [60]. More precise data on confidence levels were not obtained, but it can reasonably be argued that the correlations of r_{CH}^{LM} with data from the 4-21G basis set are better than those with data from the STO-3G basis set. For example the correlation coefficient for the fourteen r_{CH}^{LM}, r_{CH}^{STO-3G} (benzene, fluorinated benzenes) data points is 0.7925 compared to a value of 0.9865 for the twelve r_{CH}^{LM}, r_{CH}^{4-21G} data points. Similar comparisons can be made for the remaining data in Table XX.

At the 4-21G level, the ab initio bond lengths model the small variations in CH bond lengths predicted from the frequency shifts of the overtone band maxima. The changes in the electron population parameter defined by eq. 13 also model these variations. The interpretation of the causes of the bond length variation is implicit in the original definition of the parameter, which purports to measure changes in the ionic and covalent contributions to the bond strength. These contributions are now examined in detail for the fluorobenzene molecule. Then, the additivity of electron redistribution for higher levels of substitution is demonstrated.

Detailed analysis of electron distribution in fluorobenzene

The electron population residing on a carbon atom, $\sum_{\mu,\nu}^{C} P_{\mu\nu}S_{\mu\nu}$, can be divided into sigma and pi terms, as can that of

fluorine, denoted q_σ, q_π, etc. These terms are listed in Tables XXI and XXII, for benzene and fluorobenzene, at the STO-3G and 4-21G levels, respectively. The populations on the hydrogen atoms, and the bond order terms are also included. It can be seen, on comparison with benzene, that pi electrons are donated to the carbon atoms ortho and para to the fluorine substituent, and withdrawn from the carbon atoms at the meta position. This well-known phenomenon was first documented in detail for a series of substituted benzenes, in calculations at the STO-3G level, by Pople et al.[97] The carbon sigma electron population also varies significantly, and the two effects result in an increase in electron population at the ortho carbon. At the same time, the sigma electron population on the hydrogen atoms decreases as sigma electrons are withdrawn by the fluorine, particularly from the ortho hydrogens. The overall result is an increase in the ionic contribution to the bond strength at the ortho position, as the carbon atom becomes more negative, and the hydrogen atom more positive. The existence of a small positive charge on the hydrogen atom in 1,4-difluorobenzene and 1,2,4,5-tetrafluorobenzene was shown by Steele and Whiffen[98] from IR studies of the out-of-plane CH bending vibrations.

The covalent contribution to the bond strength, the bond order term, actually decreases from para to meta to ortho, but only by a total of 0.007 electrons (4-21G). Presumably sigma electron density is being withdrawn from the sigma bond framework also.

The gross orbital populations for fluorobenzene and benzene are listed in Tables XXIII and XXIV, at the STO-3G and 4-21G levels respectively. Although the electron distribution varies with the basis

Table XXI. Electron Population Distribution on Benzene and Fluorobenzene at the STO-3G Level, from the Mulliken Population Matrix

Molecule	Atom	Position	q_σ (e^-)	q_π (e^-)	q_{Total} (e^-)	Bond Order (e^-)
Benzene	C		3.9839	0.7867	4.7706	
	H		0.5983			0.7904
Fluorobenzene	C	1	3.9752	0.7826	4.7578	
		2	3.9739	0.8309	4.8048	
		3	3.9872	0.7700	4.7572	
		4	3.9688	0.8085	4.7773	
	H	2	0.5856			0.7877
		3	0.5932			0.7901
		4	0.5950			0.7918

Table XXII. Electron Population Distribution on Benzene and Fluorobenzene, at the 4-21G Level, from the Mulliken Population Matrix

Molecule	Atom	Position	q_σ (e^-)	q_π (e^-)	q_{Total} (e^-)	Bond Order (e^-)
Benzene	C		4.4425	0.7327	5.1752	
	H		0.4251			0.7972
Fluorobenzene	C	1	4.1320	0.7218	4.8538	
		2	4.6656	0.7989	5.4648	
		3	4.5219	0.7075	5.2294	
		4	4.4365	0.7573	5.1938	
	H	2	0.4004			0.7906
		3	0.4091			0.7954
		4	0.4153			0.7972

set, and the magnitude of the parameter changes with either the basis set or the use of atom only or gross orbital populations, the same trends in the terms always appear, see for example Figure 25. The difference between P^{Basis} and P^{Basis}_{Gross} is just the inclusion of "non-bonded" electron populations. It is shown later that these terms are small and remain fairly constant, so that the correlation with P^{Basis}_{Gross} is really just reflecting the correlation with P^{Basis}. A significant increase in the sigma electron density on the ortho carbon atom is calculated at the 4-21G level (charges on atoms only) Table XXII. This increase is not as great in the other three data sets, though it is still present. The 4-21G basis set is known to overemphasize the ionic terms[99] (e.g. overestimation of the dipole moment) so that the increase at the 4-21G level may be related to this inadequacy.

From the gross orbital populations it is possible to determine the quantity of sigma and pi electrons donated to or withdrawn from the ring. From the STO-3G calculations the fluorine atom gains 0.204 sigma electrons (Table XXIII), and donates 0.070 pi electrons to the ring. At the 4-21G level (Table XXIV) the quantities are 0.474 sigma electrons withdrawn and 0.069 pi electrons donated. The results are summarized in Figure 27.

Additivity at higher levels of substitution

The results for fluorobenzene are typical of the results for all the fluorinated benzenes, with either basis set. There is a remarkably good degree of additivity, evident at the STO-3G level, up to tetrasubstitution. The total number of electrons donated or withdrawn as determined from the fluorine atom gross orbital

Table XXIII. Gross Electron Populations on Benzene and Fluorobenzene at STO-3G

Molecule	Atom	Position	q_σ (e^-)	q_π (e^-)	Total (e^-)
Benzene	C		5.0629	1.0000	6.0629
	H		0.9371		
Fluorobenzene	C	1	4.8552	1.0042	5.8594
		2	5.0484	1.0386	6.0870
		3	5.0691	0.9844	6.0535
		4	5.0504	1.0200	6.0704
	H	2	0.9279		
		3	0.9320		
		4	0.9350		
	F		7.2045	1.9294	9.1339

Table XXIV. Gross Electron Populations on Benzene and Fluorobenzene at 4-21G

Molecule	Atom	Position	q_σ (e^-)	q_π (e^-)	Total (e^-)
Benzene	C		5.2384	1.0000	6.2384
	H		0.7616		
Fluorobenzene	C	1	4.6150	0.9967	5.6117
		2	5.2352	1.0495	6.2847
		3	5.2548	0.9749	6.2297
		4	5.2243	1.0230	6.2473
	H	2	0.7286		
		3	0.7478		
		4	0.7538		
	F		7.4742	1.9315	9.4057

Figure 27

Electron donation to and withdrawal from the ring, in fluorobenzene, and concomitant variations at the ring positions at the STO-3G level.

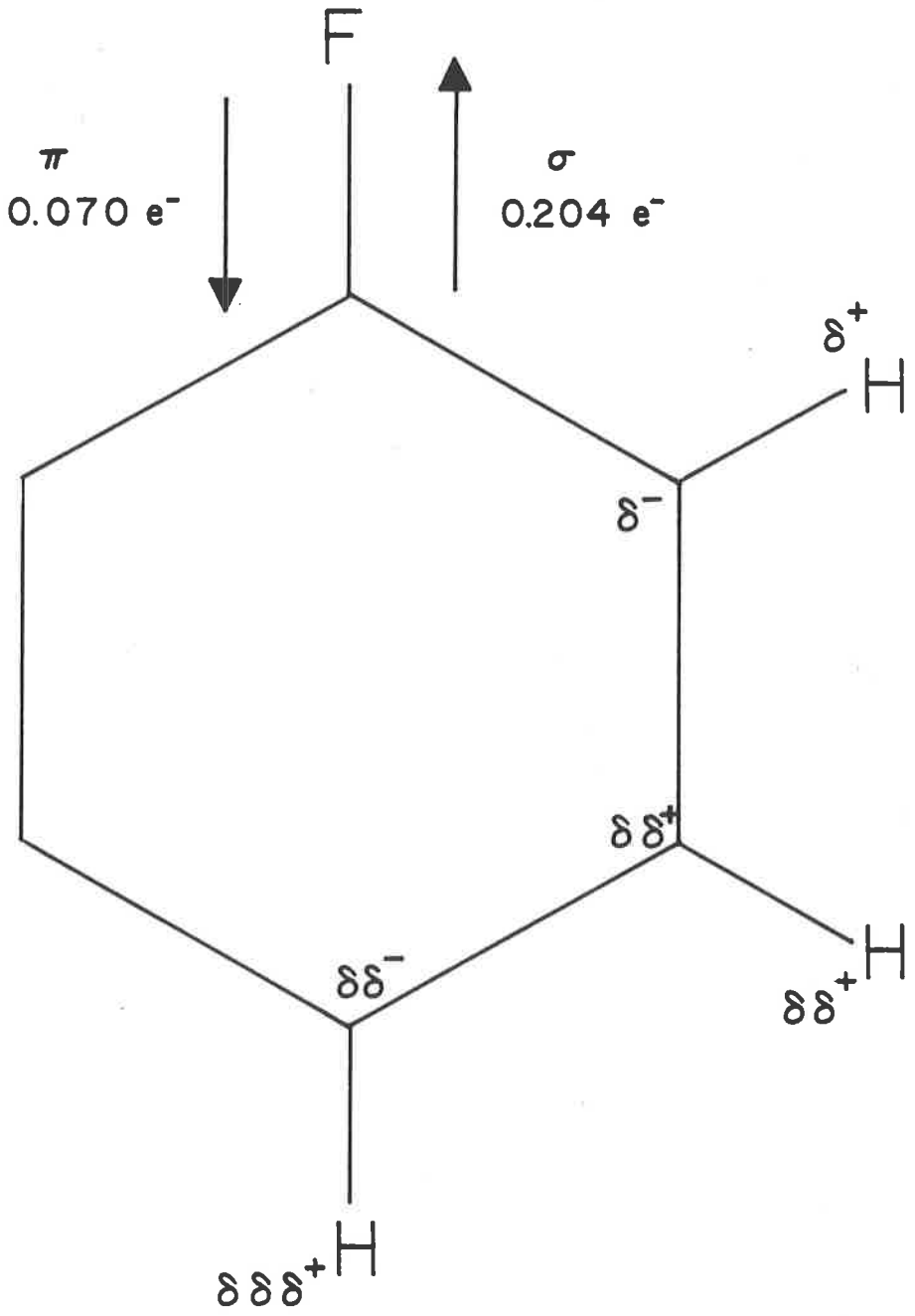
F
π
0.070 e⁻
σ
0.204 e⁻
δ⁺
H
δ⁻
δδ⁺
H
δδ⁺
δδ⁻
δδδ⁺
H

populations, is given in Table XXV for all fluorinated benzenes, at the STO-3G and 4-21G levels. The results are almost exactly additive for all but 1,2-difluorobenzene and the tetrafluorobenzenes. Here the quantities of pi electrons donated and sigma electrons withdrawn are slightly less than two or four times the fluorobenzene values. This is probably an example of non-linear response with increased levels of substitution, similar to that observed in NMR studies[67]. Although the differences are small among the three tetrafluorobenzenes it may be significant that the decreased response is greatest for the 1,2,3,4-tetrafluorobenzene in which all four fluorine atoms are adjacent. The total amount of electron population donated or withdrawn is also less for 1,2-difluorobenzene, where once again the substituents are adjacent. This appears at both the STO-3G and 4-21G levels of calculation.

The additivity of the results is consistent in even smaller details, such as the amount of change in the sigma and pi populations at each of the carbon atoms, the population on each hydrogen atom, and the bond order with either basis. The changes in these quantities relative to benzene were calculated for fluorobenzene. The expected changes in molecules with two or more fluorine atoms attached were then predicted by assuming that the changes would accumulate by simple addition. Thus the change at C(1) in 1,2-difluorobenzene would be the sum of the changes at C(1) and C(2) in fluorobenzene, etc. The predicted results are compared with those actually found from the ab initio geometry optimized calculations in Tables XXVI and XXVII for the STO-3G and 4-21G basis sets, respectively. In most cases, the agreement between predicted and ab initiovalues is excellent, within a few millielectrons or better.

Table XXV. Total Donation (+) or Withdrawal (-) of Electrons by Fluorines in Fluorinated Benzenes at STO-3G and 4-21G Levels

Basis Set	Molecule	Δq_σ (e^-)	Δq_π (e^-)	Total (e^-)
STO-3G	fluorobenzene	-0.2044	0.0705	-0.1339
	1,2-difluorobenzene	-0.3875	0.1355	-0.2520
	1,3-difluorobenzene	-0.4050	0.1452	-0.2598
	1,4-difluorobenzene	-0.4033	0.1373	-0.2660
	1,3,5-trifluorobenzene	-0.5998	0.2335	-0.3763
	1,2,3,4-tetrafluorobenzene	-0.7373	0.2687	-0.4684
	1,2,3,5-tetrafluorobenzene	-0.7543	0.2787	-0.4758
	1,2,4,5-tetrafluorobenzene	-0.7530	0.2718	-0.4812
4-21G	fluorobenzene	-0.4742	0.0685	-0.4057
	1,2-difluorobenzene	-0.9142	0.1381	-0.7761
	1,3-difluorobenzene	-0.9400	0.1424	-0.7976
	1,4-difluorobenzene	-0.9452	0.1413	-0.8039
	1,3,5-trifluorobenzene	-1.3995	0.2222	-1.1773

Table XXVI. Comparison of Predicted[a] and Calculated (Ab Initio) Changes in Electron Populations in Fluorinated Benzenes at the STO-3G Level

Molecule	Position	Calculated (Predicted) millielectrons			
		Δq^{C}_{σ}	Δq^{C}_{π}	Δq^{H}_{σ}	$\Delta q^{Bond\ Order}_{\sigma}$
fluorobenzene	1	-8.7	-4.1		
	2	-10.0	44.2	-12.6	-2.7
	3	3.2	-16.6	-5.1	-0.3
	4	-15.2	21.8	-3.3	+1.5
1,2-difluorobenzene	1	-17.5 (-18.7)	38.6 (40.1)		
	3	-4.4 (-6.8)	27.8 (27.6)	-17.8 (-17.7)	-3.0 (-3.0)
	4	-11.7 (-12.0)	5.0 (5.2)	-8.3 (-8.4)	1.3 (1.2)
1,3-difluorobenzene	1	-7.8 (-5.4)	-19.6 (-20.7)		
	2	-20.0 (-19.8)	90.1 (88.6)	-26.7 (-25.4)	-5.1 (-5.4)
	4	-25.1 (-25.2)	67.0 (66.1)	-16.3 (-15.9)	-0.8 (-1.2)
	5	6.2 (6.4)	-33.1 (-33.2)	-10.5 (-10.2)	-0.5 (-0.6)

Table XXVI (cont'd)

Molecule	Position	Calculated (Predicted) millielectrons			
		Δq_{σ}^{C}	Δq_{π}^{C}	Δq_{σ}^{H}	$\Delta q_{\sigma}^{\text{Bond Order}}$
1,4-difluorobenzene	1	-22.7 (-23.9)	-17.6 (-17.7)		
	2	-6.5 (-6.8)	27.2 (27.6)	-18.5 (-17.7)	-3.0 (-3.0)
1,3,5-trifluorobenzene	1	-7.9 (-2.2)	-34.3 (-37.3)		
	2	-3.5 (-3.5)	112.4(110.2)	-29.4 (-28.5)	-3.7 (-3.9)
1,2,3,4-tetrafluoro-	1	-27.6 (-30.7)	43.7 (45.3)		
	2	-22.7 (-25.5)	67.0 (67.7)		
	5	-15.6 (-18.8)	32.4 (32.8)	-25.7 (-26.1)	-1.9 (-1.8)
1,2,3,5-tetrafluoro-	1	-21.3 (-12.1)	9.3 (6.9)		
	2	-44.1 (-43.7)	99.8(106.1)		
	4	-23.1 (-31.8)	89.7 (93.6)	-31.6 (-29.0)	-4.5 (-4.2)
	5	-25.6 (-17.4)	-13.7 (-15.5)		

Table XXVI (cont'd)

Molecule	Position	Calculated (Predicted) millielectrons			
		Δq_{σ}^{C}	Δq_{π}^{C}	Δq_{σ}^{H}	$\Delta q_{\sigma}^{\text{Bond Order}}$
1,2,4,5-tetrafluoro-	1	-30.3 (-30.7)	44.2 (45.3)		
	3	-8.5 (-13.6)	55.7 (55.2)	-35.5 (-35.4)	-6.4 (-6.0)

[a]The calculated values only are reported for fluorobenzene. For the remaining molecules the predicted values, in brackets were obtained by taking the appropriate combination of terms from fluorobenzene.

Table XXVII. Comparison of Predicted[a] and Calculated (Ab Initio) Changes in Electron Populations in Fluorinated Benzenes at the 4-21G Level

Molecule	Position	Calculated (Predicted) Millielectrons			
		Δq_{σ}^{C}	Δq_{π}^{C}	Δq_{σ}^{H}	$\Delta q_{\sigma}^{\text{Bond Order}}$
fluorobenzene	1	-310.5	-10.9		
	2	223.4	66.2	-24.7	-6.6
	3	79.4	-25.2	-16.0	-1.9
	4	-6.0	24.6	-9.9	0.0
1,2-difluorobenzene	1	- 62.1 (-87.1)	-55.7 (55.3)		
	3	302.5 (302.8)	42.7 (41.0)	-36.7 (-40.7)	-12.4 (-8.5)
	4	63.5 (73.4)	-1.1 (-0.6)	-24.4 (-25.9)	-1.8 (-1.9)
1,3-difluorobenzene	1	-240.9 (-231.1)	-32.9 (-36.1)		
	2	462.7 (446.8)	122.1 (132.4)	-45.6 (-49.5)	-11.8 (-13.3)
	4	213.3 (217.4)	90.8 (90.8)	-33.3 (-34.6)	-7.5 (-6.6)
	5	160.1 (159.1)	-49.9 (-50.4)	-31.2 (-31.9)	-4.3 (-3.8)

Table XXVII (cont'd)

Molecule	Position	Calculated (Predicted) millielectrons			
		Δq_{σ}^{C}	Δq_{π}^{C}	Δq_{σ}^{H}	$\Delta q_{\sigma}^{\text{Bond Order}}$
1,4-difluorobenzene	1	313.6 (-316.5)	8.7 (13.7)		
	2	308.1 (302.8)	46.4 (41.0)	-37.3 (-40.7)	-8.4 (-8.5)
1,3,5-trifluorobenzene	1	-175.1 (-151.4)	-53.7 (-61.3)		
	2	446.1 (440.8)	156.3 (157.0)	-53.0 (-59.3)	-13.1 (-13.3)

[a]See footnote, Table XXVI.

While the data in Tables XXVI and XXVII are for the terms defined in eq. 13, the same additivity is also found for the gross orbital populations. The only condition on the additivity is that the population be taken from calculations at the optimized geometries. Prior to optimization, with only standard bond lengths, these correspondences do not occur, although the overall trend might still be visible.

Non-bonded terms

As a first approximation, the off-diagonal terms in the Mulliken population matrix of charges condensed to atoms were omitted if the two atoms were not formally bonded. Such terms must reflect upon the final optimized geometry and electron distribution. It was found that such terms were small, in general, and did not alter greatly upon substitution. The magnitudes of these non-bonded terms, and their variation upon increasing the number of substituents at the STO-3G level, are given in Table XXVIII. It was found that, except for the tetrafluorobenzenes, the only significant factor was the identity of the substituents ortho to the atom in question. The numbering used in the table corresponds to

X = H or F

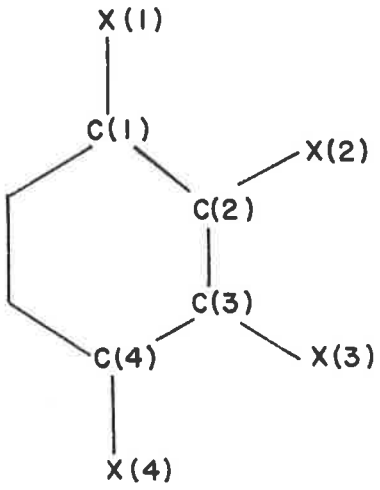

Table XXVIII. Off-diagonal Terms from the Mulliken Population Matrix for Fluorinated Benzenes at STO-3G

Atom A	Atom B	Shared population (electrons)[a]					
		X(1)=H X(2)=H	X(1)=H X(2)=F	X(1)=F X(2)=H	X(1)=F X(2)=F	X(1)=F X(2)=F X(3)=F	Maximum Variation
C(1)	C(2)	0.5099	0.4970		0.4825	0.4760	0.034
	C(3)	-0.0310	-0.0291	0.0274	-0.0283	-0.0322	0.003
	C(4)	-0.0120	-0.0119	-0.0119	-0.0109	-0.0095	0.002
C(1)	X(2)	-0.0258	-0.0263	-0.0239	-0.0240	-0.0160	0.008
	X(3)	0.0014	0.0014	0.0002	0.0002	0.0001	0.001
	X(4)	0.0	0.0	0.0	0.0	0.0	0.0
X(1)	X(2)	-0.0038	-0.0005	-0.0006	-0.0006	0.0	0.003
	X(3)	0.0	0.0	0.0	0.0	0.0	0.0
	X(4)	0.0	0.0	0.0	0.0	0.0	0.0

[a] X(1), X(2), X(3) and X(4) identify the substituent, H or F, attached to carbon (1), (2), (3), or (4). Where X(3) and X(4) are not identified, they may be H or F.

The table also includes the carbon-carbon bond order terms for bonded carbon pairs, which vary considerably.

The results were similar for the 4-21G calculations, but slightly more complex. It seems that the population depends on the identities of X(1), X(2) and X(3), at all levels of substitution. Again, the greatest variation occurs in the C-C bonded term, because of the drastic alteration in the sigma and pi electron population distribution, which is very pronounced in this basis set. The maximum change occurred in 1,3,5-trifluorobenzene, where the C(1)—C(2) term was 0.179 elecrons less than in benzene. The C—H interactions varied by only 0.013 electrons at most, and the H—X (X = H or F) interactions by 0.001 electrons. Thus the omission of these terms at either level of calculation appeared to be justified.

e) Correlation with σ_I

From their studies on $\Delta v = 6$ of mono- and di-substituted benzenes[53,54], Mizugai and Katayama concluded that the withdrawal of sigma electrons was responsible for the increase in CH bond strength. As the molecular orbital calculations and the interpretation of P^{Basis} have shown, this is one of the factors. There are several inadequacies in the σ_I correlation

- it cannot be measured at the ortho position
- it is an empirical parameter based on liquid phase acid equilibria, not individual bond strengths
- it is not additive even at disubstitution
- it does not reflect changes in the pi electron distribution

In Figure 28, the shift in frequency at $\Delta v = 4$ for gas phase toluene and the xylenes, and the fluorinated benzenes is plotted against σ_I, again with the assumption of simple additivity. In comparison with Figure 12, $\Delta\bar{\nu}$ with σ_I, liquid phase, it is clear that the presence of unresolved peaks due to inequivalent CH oscillators was responsible for the scatter in the liquid phase data. Since CH bonds ortho to the most number of fluorine or methyl substituents give the greatest frequency shift for a given level of substitution (i.e. H(2) for fluorobenzene, toluene, and 1,3-difluoro or 1,3-dimethylbenzene) the frequency shift ordering in the liquid phase was m > p >> o-disubstituted. The similar pattern of ordering for the dichloro- and dibromobenzene liquid phase overtone spectra is a good indication that inequivalent CH bonds are present in these molecules also.

Because the molecular orbital calculations show that the redistribution and donation of pi electrons is also a factor in the

Figure 28

Relationship between the frequency shift in the gas phase CH-stretching overtone maxima of fluorinated benzenes, toluene and the xylenes, and benzene; and σ_I. Aryl CH bonds only.

For mono- and di-substituted, the numbers refer to the position of the hydrogen on the ring. For di-substituted, the letters o, m and p refer to ortho, meta and para . For tri- and tetra-substituted, the numbers refer to the positions of the substituents on the ring.

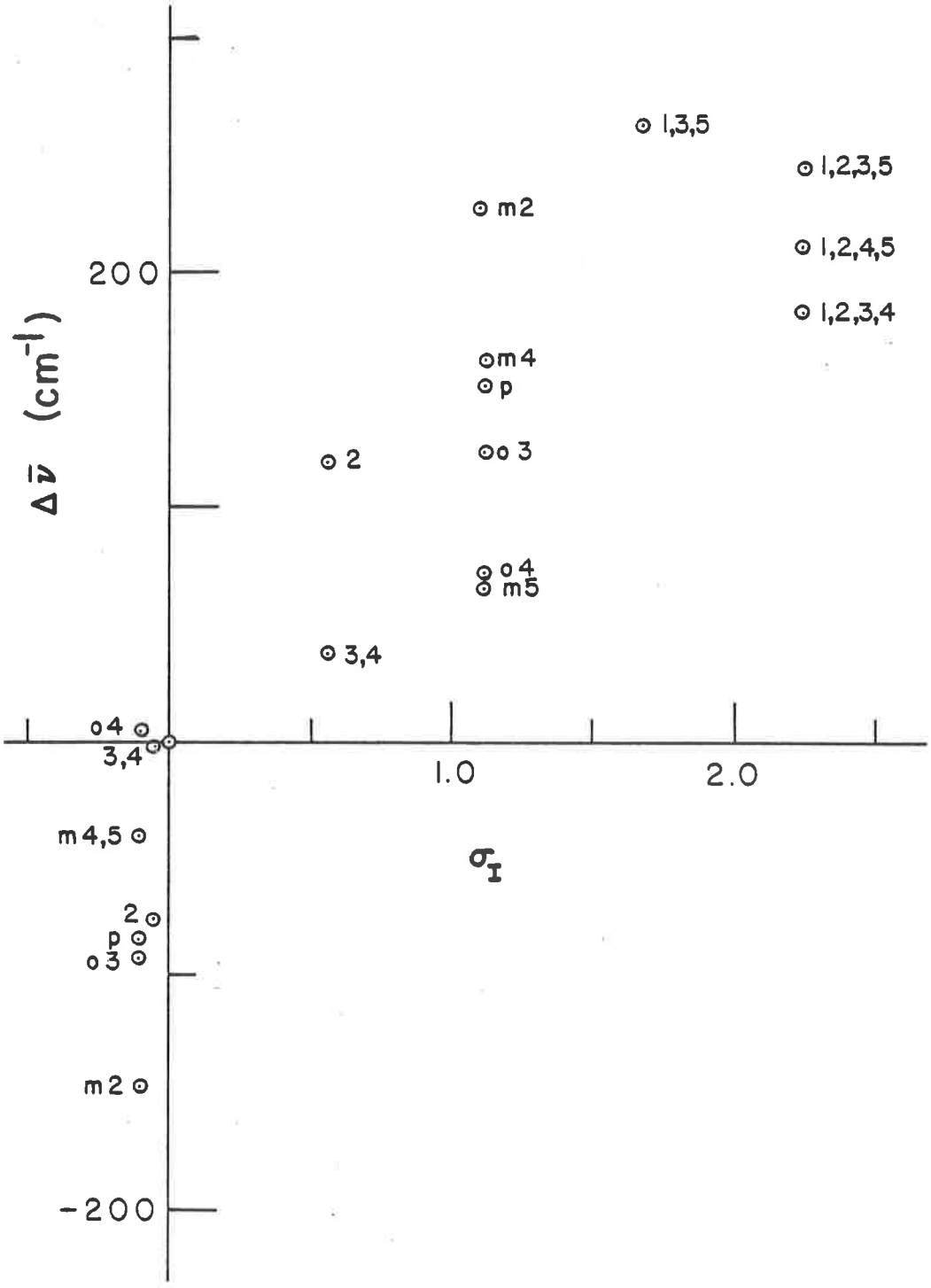
1,3,5
1,2,3,5
m2
1,2,4,5
1,2,3,4
200
m4
p
2
3
4
m5
3,4
4
3,4
1.0
2.0
m4,5
2
p
3
m2
-200
$\Delta\bar{\nu}$ (cm^{-1})
σ_I

bond length variation, it might be argued that some suitable dual substituent parameter[100] relationship, ($\sigma_I + f(\sigma_R)$), could account for the frequency shifts. However, it would then become necessary to compensate for the enhanced effect at the ortho position and this, plus the consideration that these parameters are empirically based, suggests the the correlation would not be very informative. While the correlation of substituent induced changes in molecular spectra with σ_I and σ_R is of great value[101], for the work described here the ab initio molecular orbital calculations are strongly preferred.

f) Linewidths

The full widths at half maximum were determined for all gas phase fluorinated benzene spectra by curve decomposition. The results are listed in Table XXIX. It is difficult to estimate uncertainties in some cases. The FWHM of overlapping peaks calculated in the band fit are less reliable than those of isolated peaks, especially for the less intense peaks. Small variations in the calculated linewidths among peaks in a band can result in the same apparent quality of fit. As noted in the experimental section, both the RMS deviation and a visual comparison of experimental and calculated band envelopes were used to assess the quality of the fit, but such means must necessarily contain an element of subjectivity. The high noise levels in the $\Delta v = 4$ spectra of the tetrafluorobenzenes (Fig. 22) also lead to considerable uncertainties in the associated linewidths. Thus the uncertainties in the linewidths for the five molecules with a single CH bond type are estimated to be $\leq$10%, and considerably <10% for the lower overtones. For the other three molecules, the linewidth uncertainties are estimated to be $\leq$20%, where the greater uncertainties are associated with the lower relative intensity peaks.

After these factors have been taken into account, there are still some significant features apparent. The increase in linewidth from $\Delta v = 3$ to $\Delta v = 4$ is considerably greater than the linewidth increase from $\Delta v = 4$ to $\Delta v = 5$ in all but one of the nine cases of resolved CH bond types (pentafluorobenzene excluded). In three of these cases, the linewidths decrease. The exception, where the linewidth continues to increase, involves the unresolved <u>meta</u> and <u>para</u> CH bonds of fluorobenzene. It is not unreasonable to conclude that

Table XXIX. Calculated Overtone Linewidths (cm^{-1}) of Gas Phase Fluorinated Benzenes

Molecule	Assignment	Δv			
		2	3	4	5
fluorobenzene	H(2)		52	89	103
	H(3),H(4)		54	85	121
1,2-difluorobenzene	H(3)		36	70	72
		31[a]			
	H(4)		50	98	78
1,3-difluorobenzene	H(2)		42	87	67
		31[a]			
	H(4)		34	92	91
	H(5)	46	45	73	88
1,4-difluorobenzene		13[b],17	39	80	101
1,3,5-trifluorobenzene		23	31	65	72
1,2,3,4-tetrafluorobenzene		31	63	81	
1,2,3,5-tetrafluorobenzene		26	35	100	
1,2,4,5-tetrafluorobenzene		11[b],11	40	66	
pentafluorobenzene[c]		19	33	38	50

[a]unresolved

[b]partly resolved doublet

[c]from Ref. 70

this increase is due in part to the increased energy spacing between the two inequivalent CH bond types at higher overtones.

The same trend was observed in the linewidths of the gas phase overtone spectra of benzene, at Δv = 3, 4 and 5[70]. With the exception of an anomalously large FWHM at Δv = 8, the linewidths decrease continually from Δv = 5 to 9. This narrowing was interpreted by Reddy, Heller, and Berry[70] as evidence of a sequential state-to-state intramolecular decay mechanism ($|v,0\rangle \rightarrow |v-1,1\rangle$), rather than a statistical mechanism in which increased line broadening follows the increase in the density of states. The gradual and steady increase in FWHM for pentafluoro- and pentadeuterobenzene was taken as an indication that a "quasi-continuum threshold" occurred between Δv = 2 and 3, instead of 5 and 6, as for benzene. More recently, Siebert et al.[102] have explained the narrowing in terms of a change in the efficiency of intramolecular vibrational energy distribution. The local mode state, $|v,0\rangle$ is coupled to states with one less quantum of local mode energy and two quanta of a CH in-plane wag, $|v-1,0;2\rangle$. These latter states are then coupled to the whole normal mode bath. The energy match between the "doorway" states and the pure local mode state changes throughout the overtone series. Thus, the density of these states in the energy region of interaction decreases from Δv = 5 to Δv = 9.

A similar decay mechanism could be operative in the fluorinated benzenes. Since the onset of narrowing is the same, or earlier than in benzene, the decrease in the density of "doorway" states may begin earlier. The CH in-plane bend vibrations in the fluorinated benzenes[103-107] are in roughly the same region as those of

benzene[108], 1000 to 1300 cm^{-1}. A much more detailed analysis, including data on the higher overtones, is required to obtain a more complete understanding of this problem.

g) $\Delta v = 2$ of the Tetrafluorobenzene

A doublet was observed in the $\Delta v = 2$ spectrum of 1,2,4,5-tetrafluorobenzene. There are three possible explanations for this occurrence: Fermi resonance between the pure local mode overtone with a combination involving one less quantum of CH stretch plus two quanta of CH bend (in-plane "wag"); splitting of the symmetrized $|2,0\rangle_{\pm}$ states; or rotational structure. After examination of the three possibilities, as discussed below, rotational structure appeared to be the most likely explanation.

The Fermi resonance interaction has been observed in the spectra of the dihalomethanes[28], in which the energy match between the two vibrations is quite good. The CH bending frequency in the tetrafluorobenzenes is quite low (1164 and 1125 cm^{-1} in the 1,2,4,5-isomer[104]) and therefore the energy matching would be poor. A better match in frequencies would occur with the ring deformation mode at 1534 cm^{-1}, but very similar frequencies are reported for analogous modes in the 1,2,3,4- and 1,2,3,5-isomers, for which no splitting at $\Delta v = 2$ is observed. Moreover, one of the factors involved in Fermi resonance is the bond-mode match[102], i.e., the CH bend and CH stretch modes are more likely to combine than modes involving other atoms, since a direct kinetic energy coupling can occur. The other small absorptions in the $\Delta v = 2$ spectra could possibly be assigned to combinations of CH-stretching and some other normal modes, but they are sufficiently small that they might also be due to impurities. One of the strongest arguments against the Fermi resonance explanation is the absence of lines at $\Delta v = 2$ which, based on their fundamental frequencies, appear equally likely to be present.

The second possibility is the lifting of the degeneracy of the symmetrized $|2,0\rangle_{\pm}$ states as described by Mortensen et al.[28] for the dihalomethanes. The initially degenerate states are described by eq. 4. There is coupling between the $|2,0\rangle_{+}$ and $|1,1\rangle$ states. The coupling term is evaluated spectroscopically as the splitting between the $|1,0\rangle_{\pm}$ states, which result from the direct coupling of the $|1,0\rangle$ and $|0,1\rangle$ states. The fundamental spectra of all three tetrafluorobenzenes have been fully analyzed[104] and thus the $|1,0\rangle_{+}$, $|1,0\rangle_{-}$ splitting is known. For 1,2,4,5-tetrafluorobenzene, the energies calculated for the $\Delta v = 2$ states are compared with the observed values:

	Calculated (cm^{-1})	Observed (cm^{-1})
$\|2,0\rangle_{+}$	6088	6081
$\|2,0\rangle_{-}$	6089	6089
$\|1,1\rangle$	6209	-

A coupling to the $|1,1\rangle$ state is insufficient to account for the observed splitting of 8 cm^{-1}. Furthermore, there is no evidence of the $|1,1\rangle$ absorption, predicted to lie at 6209 cm^{-1} (Fig. 20), yet it should have some intensity if it were coupled to the $|2,0\rangle_{+}$ state.

In the dihalomethanes, the two hydrogen atoms are bonded to the same carbon atom, and kinetic energy coupling is expected to predominate. In the tetrafluorobenzenes, the hydrogen atoms are bonded to different carbon atoms, and in the 1,2,4,5-isomer these carbons are farthest apart. The bandshapes in the spectra of the other two isomers at $\Delta v = 2$ are asymmetric, but no splitting can be seen clearly (Fig. 20). The overtone bands can be deconvoluted as the sum of two peaks, but in the absence of distinct shoulders such deconvolutions are not too reliable. Thus, there does not appear to be much to support the explanation of the splitting as the separation of the $|2,0\rangle_{\pm}$ states.

The third and most likely possibility is that the bandshapes in all three molecules are due to residual rotational structure. The gas phase fundamental spectra of all three molecules show rotational structure[104], and the linewidths at $\Delta v = 2$ are sufficiently narrow for it to be observed. The $\Delta v = 2$ spectrum of 1,4-difluorobenzene is very similar to that of 1,2,4,5-tetrafluorobenzene, and once again it is interpreted as residual rotational structure.

ii) Toluene and the Xylenes

a) Introduction to the Problem

The liquid phase overtone spectra of toluene and the xylenes are well documented in the literature. The spectral resolution of the aryl and alkyl CH-stretch overtone vibrations was reported by Ellis in 1928[31] and by Freymann in 1932[48] and 1933[4]. Relative intensities of the overtones of the two CH bond types were investigated by Kempter[5] in 1940, and by Suhrmann and Klein[6] a year later. Hayward and Henry[13] analyzed the spectra from $\Delta v = 3$ to 7 in terms of the local mode model. A doublet in the methyl region in ortho-xylene was interpreted as rotational structure. Nakagaki and Hanazaki[51,52] analyzed the methyl region of several methyl-substituted aromatic and heterocyclic molecules. They observed that doublets in the methyl region corresponded to the existence of high barriers to internal rotation. The methyl doublet peaks were assigned to CH oscillators locked into inequivalent positions in the molecule. The same explanation had been used previously by McKean and co-workers[109-113] in the assignment of the $\bar{\nu}_{CH}^{iso}$ spectra of molecules with methyl groups in asymmetric environments. The $\bar{\nu}_{CH}^{iso}$ (methyl) spectrum of toluene has recently been studied in some detail[114-117], (vide infra).

In spite of the great amount of attention paid to these molecules, there is still some controversy regarding the structure of toluene, and, in particular, the relative lengths of the CH bonds. Conflicting results were produced in two different electron diffraction studies[118,119], one predicting the methyl CH bonds were shorter, and the other, longer, than the aryl CH bonds. Detailed microwave analysis[120] failed to provide an unambiguous structure because of the

complexity of the spectra and the fact that a full substitution structure was not examined. The aryl CH bonds were found to be 0.01 Å shorter than the methyl.

As has been noted earlier in this report, it appears that for molecules of this size the use of ab initio molecular orbital calculations in conjunction with the overtone spectra can provide the most accurate description of the differences among CH bonds. The ab initio optimized geometry of toluene, at the 4-21G level, has been published by Boggs et al.[46] The aryl CH bonds were predicted to be 0.01 Å shorter than the alkyl, and the ring was found to be slightly asymmetric.

The gas phase overtone spectra of toluene and the xylenes at $\Delta v = 3, 4$ were recorded for this work, initially to study the frequency shifts in the aryl region, because the methyl group is a weak sigma electron donor, in contrast to the nitro group and the halogens. The methyl regions also proved to be of interest. The spectra appear in Figures 29-32. There is reduced collision broadening in the gas phase, and it is possible to observe much more structural detail. With the aid of the optimized geometry data[46], it was possible to assign almost all the peaks unambiguously.

The methyl group in toluene moves between two possible extreme conformations (Fig. 33), with the unique CH bond either planar or orthogonal to the ring. Both these conformations were optimized by Boggs et al.[46] The literature values of both optimized geometries were used in the MONSTERGAUSS program at the 4-21G level to obtain the Mulliken population analyses, as an aid to understanding the variations in the CH bond lengths. The peak assignments and molecular orbital calculations are discussed in the following sections.

Figure 29

The CH-stretching overtone spectra of toluene (lower spectrum) and ortho-xylene (upper spectrum) in the gas phase, 86°C, in the region of $\Delta v = 3$. 9.75 m pathlength; recorded on the Beckman 5270; single scan of each spectrum.

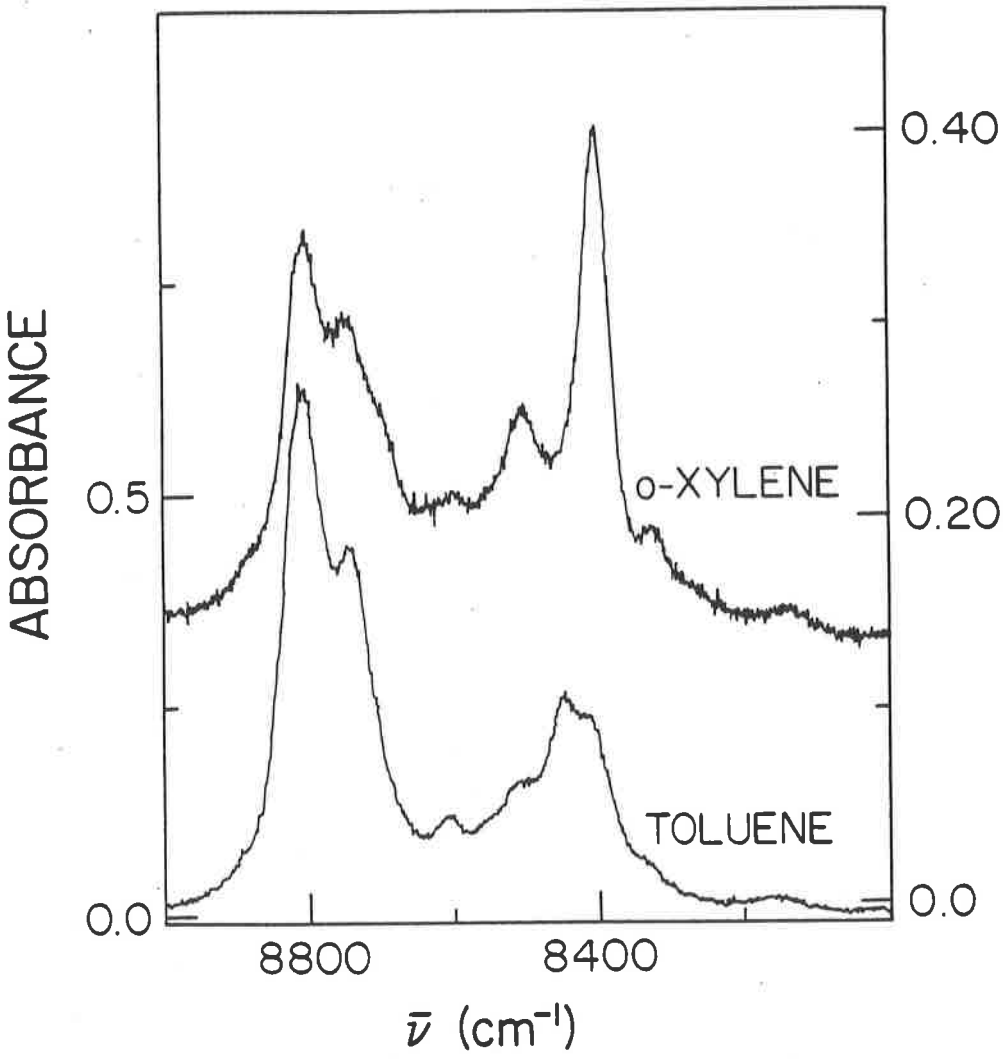
ABSORBANCE
0.5
0.0
0.40
0.20
0.0
o-XYLENE
TOLUENE
8800
8400
$\bar{\nu}$ (cm^{-1})

Figure 30

The CH-stretching overtone spectra of meta-xylene (lower spectrum) and para-xylene (upper spectrum) in the gas phase, 86°C, in the region of $\Delta v = 3$. 9.75 m pathlength; recorded on the Beckman 5270; single scan of each spectrum.

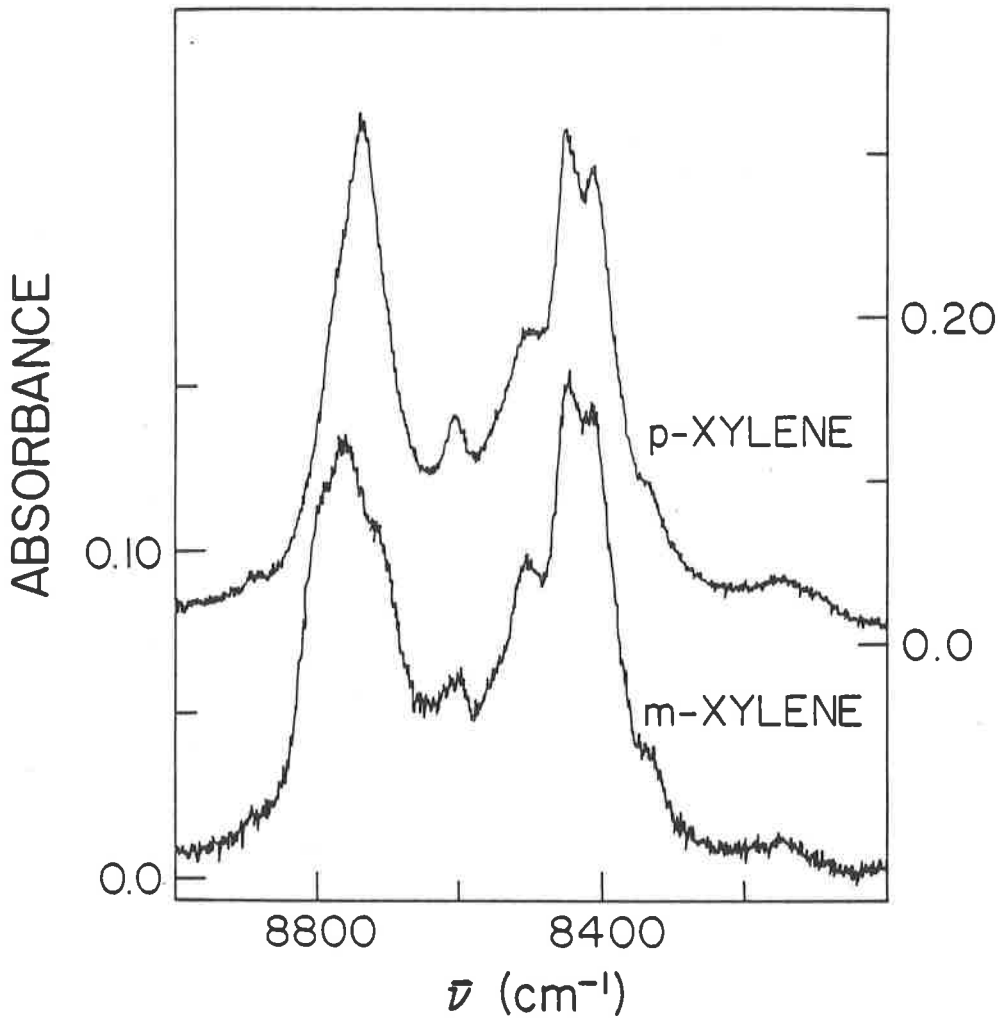
ABSORBANCE
0.20
0.10
0.0
0.0
p-XYLENE
m-XYLENE
8800
8400
$\bar{\nu}$ (cm^{-1})

Figure 31

The CH-stretching overtone spectra of toluene, sum of 10 scans (lower spectrum) and ortho-xylene, sum of 7 scans (upper spectrum) in the gas phase, 86°C, in the region of $\Delta v = 4$. 9.75 m pathlength; recorded on the Beckman 5270.

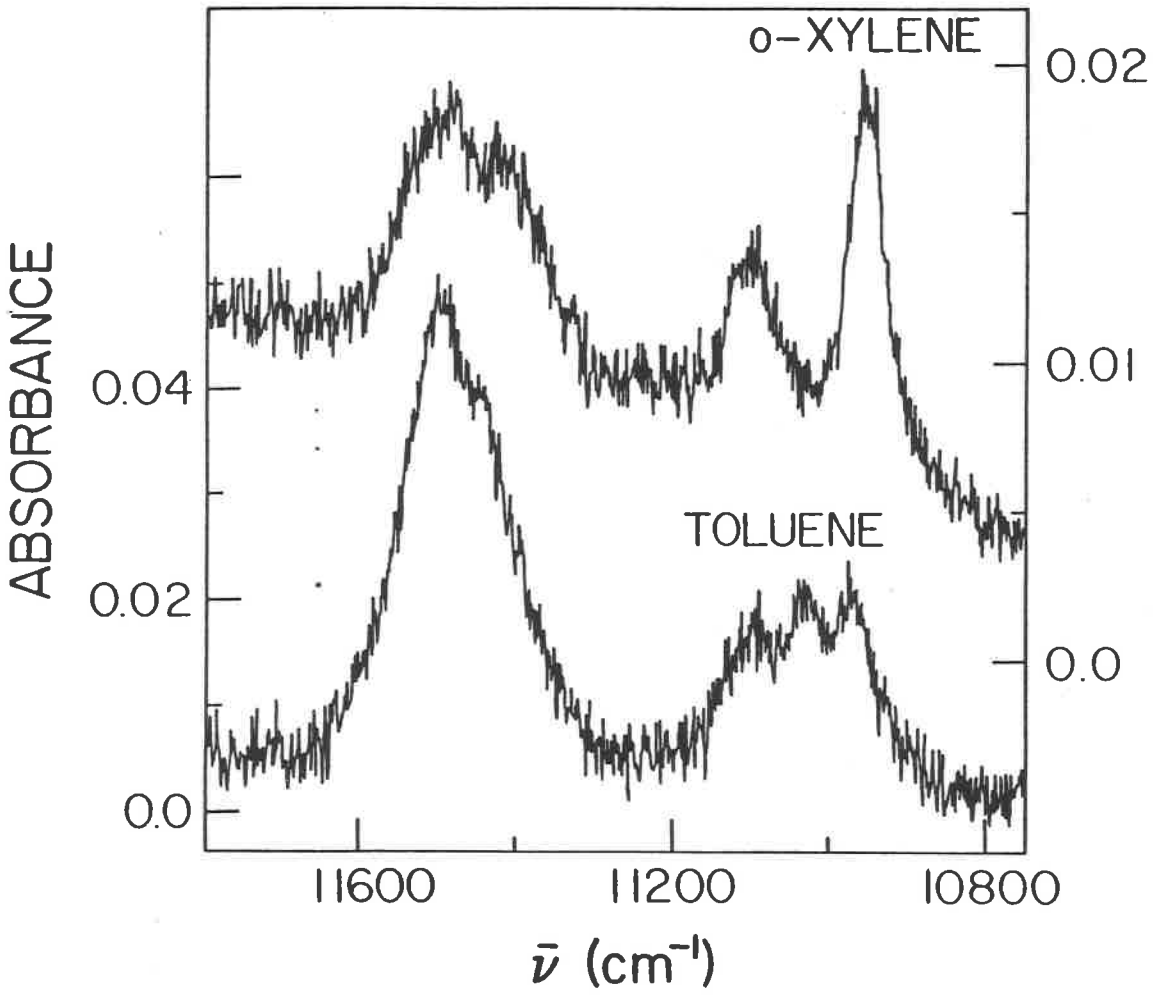
o-XYLENE
TOLUENE
ABSORBANCE
0.04
0.02
0.0
0.02
0.01
0.0
11600
11200
10800
$\bar{\nu}$ (cm^{-1})

Figure 32

The CH-stretching overtone spectra of meta-xylene, sum of 7 scans (lower spectrum) and para-xylene, sum of 4 scans (upper spectrum) in the gas phase, 86°C, in the region of $\Delta v = 4$. 9.75 m pathlength; recorded on the Beckman 5270.

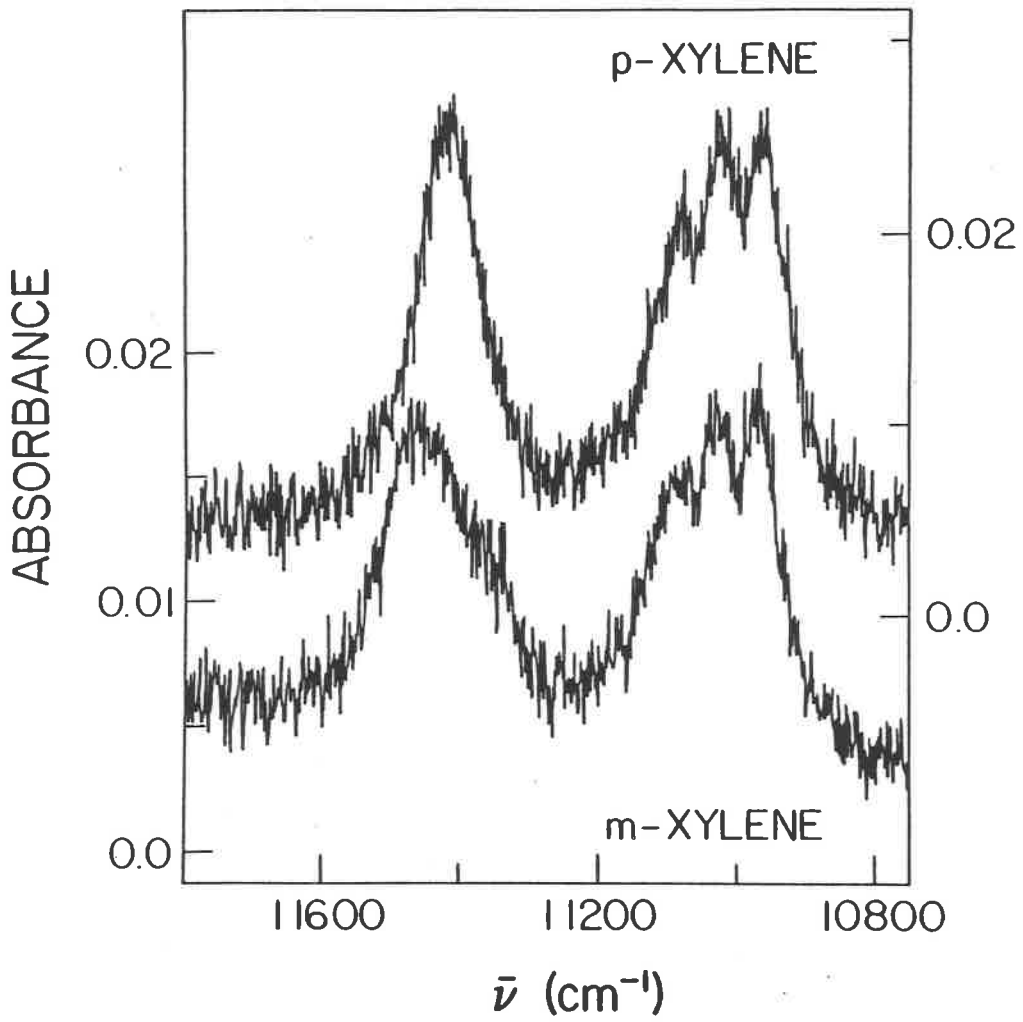
p-XYLENE
m-XYLENE
ABSORBANCE
0.02
0.01
0.0
0.02
0.0
11600
11200
10800
$\bar{\nu}$ (cm^{-1})

Figure 33

Labelling of atoms in toluene; planar and orthogonal conformations of the methyl group.

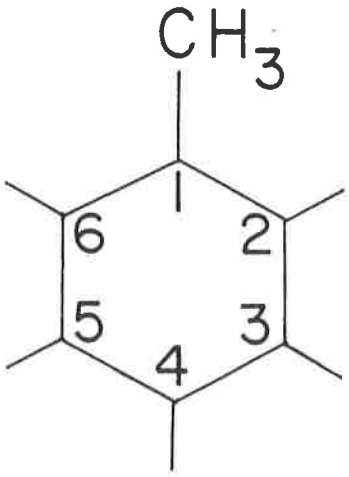

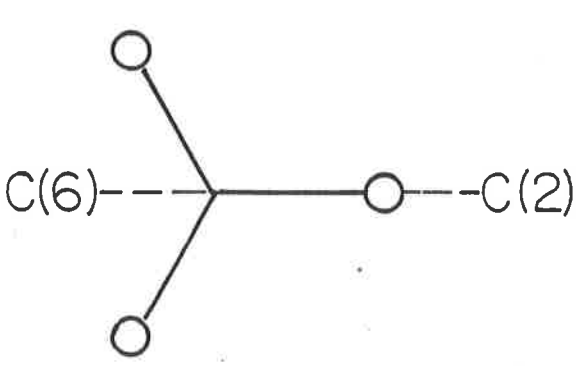

Planar

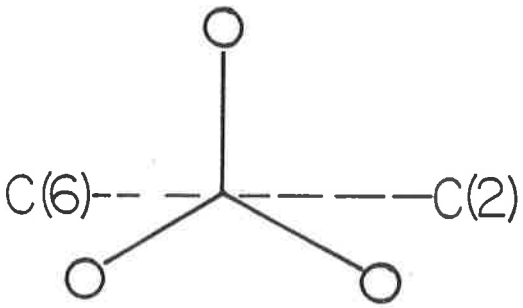

Orthogonal

b) Aryl CH Bonds

Regardless of the orientation of the methyl group, the two aryl CH bonds ortho to the substituent are predicted to be 0.001 Å longer than those meta or para to it, according to the 4-21G calculations. The CH bonds meta or para to the substituent are predicted to be unchanged from those in benzene. This result is also expected qualitatively on the basis of the sign and magnitude of σ_I for this molecule, which is small and positive (+0.02→0.06)[63] indicating its role as a weak sigma electron donor. The only effect expected is a slight lengthening of the CH bonds ortho to the substituent, with little or no effect at the meta and para positions.

The $\Delta v = 3$ and 4 spectra of toluene and the xylenes (Fig. 29-32) were decomposed with the band fitting program, and the peak positions, assignments and relative areas are listed in Table XXX. All the spectra contain two major absorption regions separated by several hundred cm^{-1}. The higher frequency region corresponds to excitation of the aryl CH bonds. Assignment of the methyl CH overtones is discussed in the next part of this section.

A partially resolved doublet appears in the aryl region of the toluene overtone spectra. The smaller, low frequency peak is assigned to the two CH oscillators ortho to the substituent, and the higher frequency peak to those meta and para. The ratio of the peak areas is about 3:2, high to low frequency. Thus, the aryl region in toluene is similar to those of fluoro- and nitrobenzene, except that proximity to the substituent produces a lengthening of the CH bond, and a shift to lower frequencies.

Table XXX. Calculated Peak Positions (cm^{-1}) and Relative Peak Areas[a] at Δv = 3, 4 and 5 for Benzene[b], Toluene and the Xylenes in the Gas Phase

Δv	Assignment	Benzene	Toluene	o-Xylene	m-Xylene	p-Xylene
3	Aryl (m,p,m+p)	8786	8806	8805	8797	
			(2.9)	(1)	(1.0)	
	(o,o+m,o+p)		8734	8740	8754	8731
			(2.0)	(1)	(1.8)	
	(o+o)				8703	
					(1.0)	
	Methyl 0°		8506	8498	8500	8499
			(1.0)	(1.0)	(1.0)	(1.0)
	free[c]		8445		8443	8442
	60°		8401	8399	8400	8400
			(1.5)	(1.8)	(2.0)	(1.6)
4	Aryl (m,p,m+p)	11498	11496	11502		
					11456	
			(2.9)	(1.1)	(2.8)	
	(o,o+m,o+p)		11423	11405		11411
			(2.0)	(1.0)		
	(o+o)				11349	
					(1.0)	
	Methyl 0°		11087	11098	11091	11080
			(1.0)	(1.0)	(1.0)	(1.0)
	free[c]		11018		11020	11016

Table XXX (cont'd)

Δν	Assignment	Benzene	Toluene	o-Xylene	m-Xylene	p-Xylene
	60°		10959	10951	10957	10950
			(1.0)	(1.8)	(1.4)	(1.3)
5[b]	Aryl (m,p)	14072	14061			
			(3)			
	(o)		13962			
			(2)			
	Methyl 0°		13555			
	free[c]		13473			
	60°		13409			

[a]Relative areas for peaks of a given bond type are given in brackets.

[b]from Ref. 70

[c]see text

The aryl regions of the ortho-, meta- and para-xylenes exhibit partially resolved doublet, triplet and singlet structures, respectively. The CH bonds in these molecules are analogous to those of the three difluorobenzenes, except for the reversal of the substituent effect, and the assignment is straightforward. The ratio of the peak areas is about 1:1 for ortho-xylene and 1:2:1 for meta-xylene.

The $\Delta v = 5$ gas phase spectrum of toluene was published recently by Reddy et al.[70], and the positions of the peak maxima are used with those in Table XXX to calculate the local mode parameters. These values, with uncertainties and correlation coefficients, are given in Table XXXI.

The large uncertainty in the parameters for the ortho CH bonds arises from the difficulties in decomposing the partially resolved shoulder, especially at $\Delta v = 4$. The value of X for the ortho CH bonds is just slightly smaller than that for the meta and para CH bonds. This is the ordering expected on the basis of steric hindrance, since these bonds are crowded by the presence of the methyl group in a manner similar to that which occurs in the methyl substituted butanes[24] and pentanes[23].

Table XXXI. Local Mode Parameters of Toluene from Gas Phase Overtone Spectra

Assignment		ω (cm^{-1})	X (cm^{-1})	r
Aryl	CH(2)	3091±9	$-59.5\pm2.2_5$	-0.99927
	CH(3),CH(4)	3120.0±0.6	-61.6±0.1	-0.99999
Methyl	CH(0°)	3021±3	-62.2±0.8	-0.99992
	CH(free)	2996.5±0.7	-60.2±0.2	-0.99999
	CH(60°)	2978±3	-59.3±0.8	-0.99989

c) Methyl CH Bonds

The methyl group in toluene, and similarly in meta- and para-xylene, is nearly a free rotor because of the low barrier[120,121]. The six-fold barrier to internal rotation in toluene, as measured by microwave spectroscopy[120], is 0.059 kJ/mole. The 4-21G calculations[46] predicted that the orthogonal conformation (Fig. 33), with one CH bond perpendicular to the ring plane, would be 0.013 kJ/mole more stable than the planar. A change in the methyl CH bond length of about 0.003 Å during internal rotation was also predicted. The CH bond was found to be shortest when lying in the plane of the ring, increasing to a maximum at 90° to the ring plane.

When the optimized geometries were run with the MONSTERGAUSS program at the 4-21G level (Pople[37]) the planar conformer was predicted to be more stable by 0.22 kJ/mole. The difference in the results lies in the use of slightly different orbital exponents and coefficients in the two programs (Ch. 2(v)(b)). Although the energy ordering is reversed, such differences lie within the uncertainty limits of these calculations.

Because the spectra of ortho-xylene are the least complex, both in terms of numbers of peaks and assignment, they are discussed first. The barrier to internal rotation in ortho-xylene is quite large (6.3-9.2 kJ/mole)[122-124]. According to the microwave spectroscopy data[122], the spectra are consistent only with a symmetric planar conformation, not one which is geared. The nuclear relaxation study[123] found a V_0 of 9.2 kJ/mole, but did not indicate the barrier components. The barrier was decomposed into a small V_3 and a large V_6, chiefly because the low temperature heat capacity study by Wulff[124] seemed to

be incompatible with a large V_3. The V_6 barrier was then assumed to imply a geared minimum energy conformer. STO-3G[125] calculations with full geometry optimization of six possible conformers predicted the most stable conformer would be the same as that found by the microwave study

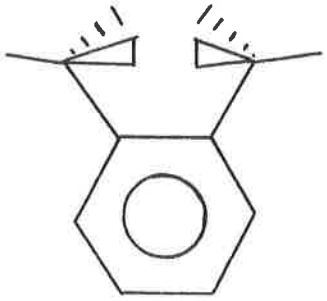

for which the barrier height is 4.8 kJ/mole, and the potential is three-fold along the minimum energy pathway. Because of the high barrier, the methyl groups are essentially locked into the minimum energy conformation on the near IR time scale. If the microwave spectra and STO-3G calculations are correct, then only two CH bond types in the ratio of 2:1 are expected. As with the 4-21G calculations on toluene[45], the STO-3G calculations on ortho-xylene predicted a gradual lengthening of the CH bond on rotation from 0° to 90° to the ring plane. Thus the overtones of the two in-plane CH bonds are expected to appear at a higher frequency than those of the four out-of-plane CH bonds. The spectra in Figures 29 and 30 display precisely this pattern. From the separation of 99 cm^{-1} at $\Delta v = 3$ and 147 cm^{-1} at $\Delta v = 4$, a difference in bond lengths of 0.003 Å is predicted (eq. 11), exactly in agreement with the difference predicted for the in-plane

(0°) and out-of-plane (60°) CH bonds in the STO-3G calculations on ortho-xylene[125], and 4-21G on toluene[46], (Tables XVIII and XIX).

In connection with this assignment, it is noted that the overtone spectra of hexamethylbenzene[126] in $CC\ell_4$ were observed to be partially resolved doublets. The ratio of the peak areas was 2:1, low to high frequency peak. At the time that these spectra were reported, the bond length-frequency shift correlation had not been established for the overtone spectra, nor had molecular orbital calculations been done. The minimum energy conformer was taken to be an orthogonal form, in which the CH bonds perpendicular to the ring alternate up and down

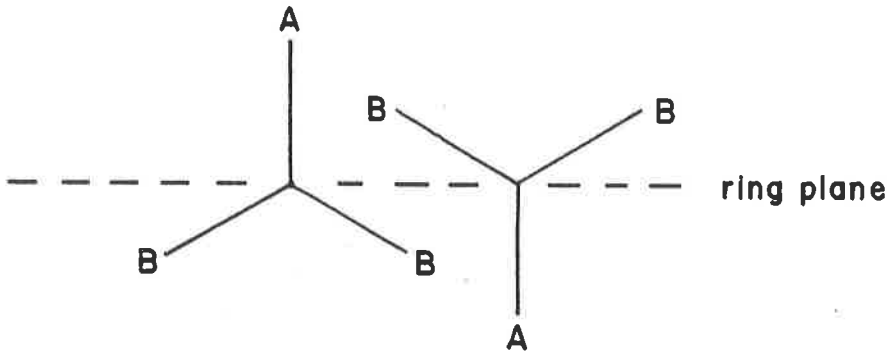

yielding six CH bonds of type A, and twelve of type B. This is the minimum energy conformer at low temperatures[127], but at room temperature, at which the overtone specta were recorded, the minimum energy conformer is uniformly planar, and geared

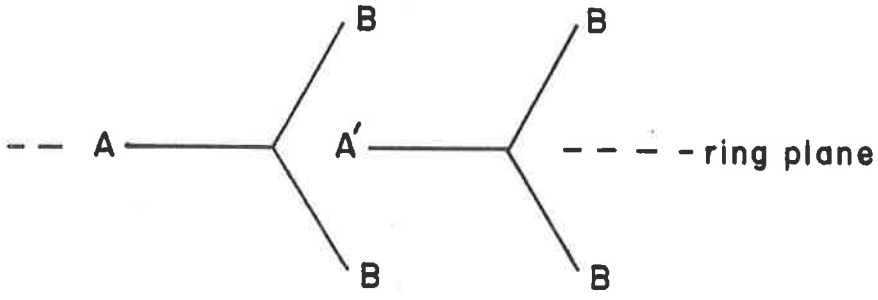

with the same 2:1 ratio of bond types. Since in fact it is the high frequency peak which has half the intensity of the low frequency peak in the hexamethylbenzene spectra, the spectra do correspond to the geared conformation. From the positions of the peaks, the difference in bond lengths is about 0.006 Å (eq. 11, and ref. 126), or twice that found in ortho-xylene. It appears that it is the in-plane bond which is significantly shortened, while the out-of-plane bonds are about the same as those in ortho-xylene. If one views the representation of the planar conformer of hexamethylbenzene (above) as the geared, planar ortho-xylene, then the CH bond labelled A' is predicted to be shorter than the one labelled A, according to the STO-3G calculations[126]. This appears to reflect steric crowding, which would also be operative in the hexamethylbenzene, and would account for the excessive decrease in the in-plane CH bond lengths.

A decrease in X for the in-plane CH bond might also be anticipated, since this parameter is sensitive to steric crowding. Only $\Delta v = 3$ and 4 were recorded for the hexamethylbenzene, so it is not possible to evaluate the differences in X values. From $\Delta v = 3$ and 4 only[126], approximate values of $-56.8\ cm^{-1}$ (in-plane) and $-61.8\ cm^{-1}$ (out-of-plane) are found. Obviously, the higher overtones must also be recorded in order to establish the proper values, but the initial trends are of the right magnitude.

The reassignment of the hexamethylbenzene spectra yields results which now conform closely to those found for the ortho-xylene:

- the planar conformer is the most stable at room temperature
- the in-plane CH bonds are shorter than the out-of-plane

bonds, and their overtones appear at a higher frequency

- the in-plane CH bond is shifted to a higher frequency than that in ortho-xylene, i.e., it is significantly shortened, because of the steric restrictions imposed by the "gearing".

To return now to the methyl regions in the spectra of toluene and the meta- and para-xylenes, first, it can be seen that these are essentially identical apart from the increased relative intensity in the disubstituted molecules (Fig. 29-32, Table XXX). There are three major peaks at each overtone. At $\Delta v = 3$, additional lower intensity peaks can be seen. These can probably be safely assigned to combinations involving two quanta of CH-stretching and two quanta of CH-bending. Such combinations are also present at $\Delta v = 2$, and have been assigned in the fundamental spectra[116,117]. Of these three major peaks, the positions of those at the highest and lowest frequencies are almost identical to those of ortho-xylene. This correspondence suggests that these peaks arise from methyl groups in the planar conformation. It is not possible to confirm this on the basis of the ratio of the calculated peak areas, (Table XXX), since it is difficult to determine such values accurately for overlapping peaks. However, the lower frequency peak is consistently larger for all three molecules at $\Delta v = 3$, and for meta- and para-xylene at $\Delta v = 4$. This would be consistent with the results for ortho-xylene, durene[128], and hexamethylbenzene.

The central peak is not accounted for by this assignment, and other causes must be considered. The first possibility is the existence of Fermi resonance between the CH stretch overtones and some

combination, similar to those discussed previously. Such peaks must "tune in" and "tune out" of resonance through the overtone series because of the different anharmonicities of the bending and stretching modes. Both the energy splitting and the relative intensities should change at each overtone. This is not observed at $\Delta v = 3$ or 4, or at $\Delta v = 5$ [70]. In fact, the central methyl peak can be fitted extremely well to eq. 3 (Table XXXI), and the relative intensities do not vary much.

Another possible explanation of this peak is the presence of a second minimum energy conformation, as suggested by Reddy et al.[70] This seems unlikely on two grounds. First, the molecular orbital calculations indicate that the potential varies smoothly with internal rotation, and there is no obvious alternative minimum energy conformer. Second, the CH bond length also varies smoothly and continuously with internal rotation, and increases as it goes from 0° to 90° to the ring plane. There is no conformation which would render all three CH bond lengths equivalent, yet only a single peak appears in the spectra. This is interpreted as being due to a single CH bond type, with r_{CH} intermediate between r_{CH} (0°) and r_{CH} (60°). A third possibility is that the peaks are due to rotational structure, and correspond to P, Q and R branches. Rotational structure is observed in the $\bar{\nu}_{CH}^{iso}$ (methyl) fundamental spectrum[116,117], but the P-R separation is about 10 cm^{-1}, and would not account for the 100 cm^{-1} separation of the outer peaks at $\Delta v = 3$.

The most likely explanation is that the central peak is due to CH-stretching overtones of CH oscillators on freely rotating methyl groups. At 86°C there is a large population of methyl groups in

rotational levels above the barrier. The rapid internal rotation would mean the three CH bonds would be essentially equivalent, and only a single "average" peak would be observed. This interpretation is supported by several facts and observations.

1) The central peak is observed only in the spectra of molecules where there is a very low barrier to internal rotation. Work is in progress on the gas phase spectra of the fluorotoluenes[129], but preliminary results show that the triplet is present in the methyl region of the spectra of meta- and para-fluorotoluene, but only the doublet, again similar to that in ortho-xylene, is observed for ortho-fluorotoluene. Thus the presence or absence of a central peak coincides with the absence or presence of a sizeable barrier to methyl internal rotation, for seven molecules.

2) The size of the central peak in the methyl region of toluene seems to show a temperature dependence. The spectrum at $\Delta v = 5$[70] was obtained at room temperature, while those at $\Delta v = 3$ and 4 were obtained at 86°C. There is a decrease in the relative intensity of the central peak compared to the two outer peaks in the room temperature spectrum. This decrease would correspond to a decrease in the population of the rotational levels above the barrier. More extensive studies on the temperature dependence of these spectra should be very informative.

3) Cavagnat and Lascombe[116] have examined the $\bar{\nu}^{iso}_{CH}$ spectra of $C_6D_5CHD_2$ and CHD_2NO_2, further to the work of McKean et al. on methyl groups in asymmetric environments[109-113]. In the gas phase $\bar{\nu}^{iso}_{CH}$ spectrum of $C_6D_5CHD_2$, two absorptions were observed. The major one showed considerable rotational structure and was assigned to a CH

oscillator on a freely rotating methyl. The second was a smaller single peak, about 14 cm^{-1} below the first. This was assigned to a CH on a methyl group which was below the rotational barrier, and hence locked into the minimum energy conformation. Cavagnat and Lascombe assumed that Boggs calculations[46] were correct, and assigned the orthogonal as the minimum energy conformer. They then assigned the low frequency peak to a methyl CH perpendicular to the ring. This would be in accordance with the work reported here, in that the molecular orbital calculations predict that the CH bond is longest when perpendicular to the ring, and the frequency/bond length correlation would then place it at the lowest frequency. This author disagrees with the assignment of Cavagnat and Lascombe, in part. The second peak could well be a "locked" CH oscillator, however the minimum energy conformer appears to be planar. In that case, the low frequency peak would correspond to the methyl CH at 60° to the ring plane. There should be little difference to the energy of the minimum upon interchanging H and D, so that absorptions corresponding to CH oscillators in both the 0° and 60° positions should appear, with that at 60° having twice the statistical weight.

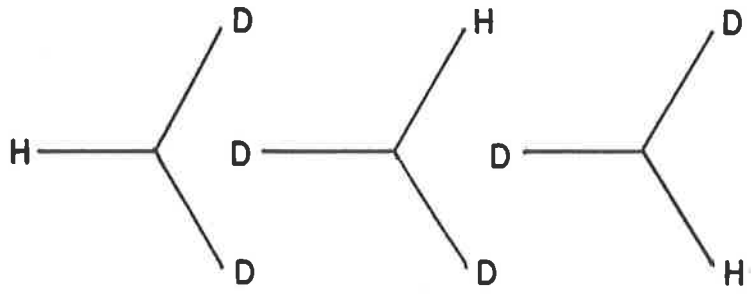

If the orthogonal conformation were the minimum, one would expect an absorption from the CH oscillator at 30° to the ring plane. This would have twice the statistical weight of the perpendicular position, and appear at a higher frequency, yet no such absorption is observed. Of the two, the planar assignment is more plausible. At $\Delta v = 3$ and 4, a similar interpretation then applies: the highest and lowest frequency peaks arise from excitation of methyl CH oscillators in the minimum energy conformation, at 0° and 60° to the ring, and the central peak from excitation of freely rotating methyl CH oscillators.

4) The splitting between the two peaks in the $\bar{\nu}^{iso}_{CH}$ spectrum is 14 cm^{-1}. The splitting between the lowest frequency and central peaks in the toluene overtone spectra is 44 cm^{-1} at $\Delta v = 3$ and 59 cm^{-1} at $\Delta v = 4$, just three and four times this difference.

5) The ab initio values of r_{CH} (methyl) are a function of the dihedral angle θ, and vary as $\sin^2\theta$. This is expected since the bond length change is due to the influence of the benzene pi system, (vide infra). The classically averaged bond length value is

$$r_{CH}\ (avg) = r_{CH}(0°) + \frac{\int_0^{\pi} \sin^2\theta\, d\theta}{\int_0^{\pi} d\theta}\, dr \qquad (14)$$

where r_{CH} (0°) is 1.0818 Å (uncorrected ab initio value) and dr is 0.0032 Å, the variation from 0° to 90°. This yields a value of 1.094_4 Å for r_{CH}(avg), after correction to spectroscopic lengths. The bond length associated with the central peak on the basis of frequency shift is 1.094_6 Å.

6) Because of the correlation between $\bar{\nu}$ and r_{CH}, it might be anticipated that a distribution over all possible r_{CH} should be observed for a freely rotating methyl group. The central peak is relatively narrow. This situation would be analogous to that which occurs in NMR couplings[130] and ESR hyperfine[131] splittings also involving freely rotating methyl groups. In both cases, a quantum mechanical treatment demonstrates that the ensemble average $\langle \sin^2\theta \rangle$ must be calculated before the value of the observable can be predicted. This latter will correspond to the average over the distribution, and not to the whole range of values within the distribution. The quantum mechanical average can be approximated by the classical average, as calculated in point (5) above.

There is a difficulty with regard to point (2) above. Given that the barrier is so low, a significant change in the central peak intensity on going from 300K to 360K might not be anticipated. In their study on the effect of internal rotation on the CH-stretching vibration, Cavagnat and Lascombe[116] calculated that the barrier to free rotation was about 20 cm^{-1} (29 J/mole) at v = 0, but about 60 cm^{-1} (87 J/mole) at v = 1 for $C_6D_5CHD_2$. The increase is presumably due to the magnitude of the excursion of the excited CH oscillator. It can be postulated that the barrier to internal rotation would be even higher for a methyl rotor in which a single CH bond was highly vibrationally excited, and thus a temperature dependence in the central peak intensity would exist.

d) r_{CH}^{LM} and Correlation with Ab Initio Parameters

r_{CH}^{LM}, Experimental and Ab Initio Bond Lengths

The CH bond lengths were calculated from the observed frequency shifts. The results for toluene are given in Table XXXII along with those from previous measurements. The excellent agreement between r_{CH}^{LM} and r_{CH}^{4-21G} has already been discussed in the fluorobenzene section, and the toluene data were included in the correlations, Tables XIX and XX. The uncertainties in the electron diffraction data are greater than the small variations predicted by the 4-21G calculations, and greater than the uncertainties in the other experimental techniques. From the remaining data it is seen that the methyl CH bonds are definitely about 0.01 Å longer than the aryl CH bonds. The slight increase in the aryl CH bond length at the ortho position was not observed in the microwave, in fact the results were just the reverse. It should be noted that while the microwave spectral uncertainties were estimated at ±0.002 Å, this was only a partial substitution structure. The final results were obtained with the assumption that the ring was a regular hexagon, in contrast to most of what is known about substituted benzene rings[134], and the molecular orbital calculations. The authors acknowledged that the results were strongly influenced by this assumption, and that the structure which they arrived at could not be considered complete. Finally, the usefulness of microwave spectra in the determination of CH bond lengths has been questioned recently[83], as was mentioned in the discussion of the structure of fluorobenzene.

It is not possible to confirm the assignment of the methyl CH bonds to the planar conformation on the basis of the bond length data

Table XXXII. Calculated and Experimental CH Bond Lengths (in Å) for Benzene, Methane, and Toluene (References are given in brackets)

Molecule	Assignment	4-21G (45)[a]			Electron Diffraction		Microwave	Raman	IR	Over-tones
		r_{calc}	r_e	r_o	$r_g(116)$	$r_g(117)$	$r_o(118)$	r_o	r_o^{iso}	r_o^{LM}
Benzene		1.0721	1.077 (43)	1.084				1.084±0.005 (132)	1.084	1.084
Methane		1.0815	1.086	[1.093][b]				1.0939_7 (133)	1.092	
Toluene	Aryl CH(2)	1.0728		1.085	1.11±0.01	1.117±0.005	1.078±0.002			1.086
	CH(3)	1.0723		1.084	1.11±0.01	1.117±0.005	1.083±0.002			1.084
	CH(4)	1.0719		1.084	1.11±0.01	1.117±0.005	1.074±0.002			1.084
	CH(5)	1.0724		1.084	1.11±0.01	1.117±0.005	1.083±0.002			1.084
	CH(6)	1.0733		1.085	1.11±0.01	1.117±0.005	1.078±0.002			1.086
	Methyl									
	CH(0°)	1.0818	1.0865	$[1.093_5]$[b]	1.10±0.02	1.137±0.005	1.09±0.01		1.097	1.093

Table XXXII (cont'd)

Molecule	Assignment	4-21G (45)[a]			Electron Diffraction		Microwave	Raman	IR	Over-tones
		r_{calc}	r_e	r_o	$r_g(116)$	$r_g(117)$	$r_o(118)$	r_o	r_o^{iso}	r_o^{LM}
	CH(60°)	1.0839	1.0886	$[1.095_6]$[b]	1.10±0.02	1.137±0.005	1.09±0.01		1.097	1.096

[a]For the "planar" configuration. The numbering of the atoms is taken from Ref. 46.

[b]Numbers in square brackets were not actually reported, but are determined from the calculated values in the standard way, as devised in Ref. 46

only. The variation in length is extremely small and an uncertainty of ±0.001 Å could change the assignment from planar to orthogonal.

r_{CH}^{LM} (aryl) and P^{Basis}

The values of P^{STO-3G} and P^{4-21G} for toluene, planar and orthogonal, were listed in Tables XVIII and XIX respectively. These data points were included in Fig. 23, 24 and 26, and in the correlations in Table XX. While the values of the parameter for the aryl CH bonds in toluene, at 4-21G, were close to those of benzene, they did not correlate as well as the fluorobenzene data. The parameter is now re-examined in the light of this failure. The bond length/population parameter correlation has been derived with many assumptions. The "ionic" contribution is measured only as a difference, although to deal with it more accurately an expression of the form $\frac{(q_1)(q_2)}{r^2}$, where q_1 and q_2 are the charges and r is the distance between them is required[90]. The aim in devising the parameter was to obtain some insight into the changes in population which went with the changes in bond length, and not to quantitatively define the bondlength. Therefore the results remained consistent as long as the neglected terms were small and constant. This was true for the fluorobenzene series, but possibly would not hold for a variety of substituents. The methyl group is significantly different from fluorine in that the pi electron donation is made possible by the interaction of the "quasi-pi" methyl orbital and the aromatic ring. This is dependent on methyl group orientation, and for any but the "planar" conformer, the methyl and ring pi orbitals contain sigma electron contributions. Thus the interpretation is less clear-cut than for fluorine substitution. Non-bonded terms are larger at the

4-21G than at the STO-3G level, but are still neglected. In these calculations the C(1)-H(2) and C(3)-H(2) terms vary from those in benzene by 0.003 or 0.004 millielectrons, a variation which is about the same order of magnitude as some of the changes in the terms of eq. 13.

A breakdown of the Mulliken electron population into sigma and pi terms for toluene is compared to that of benzene in Table XXXIII. There is a slight increase in the sigma electron population at the ortho ring hydrogens, regardless of methyl group orientation. There is also a slight increase in the ortho CH bond order term. Both of these changes reflect the sigma electron donating property of the methyl group, just as the increase in q_{π}^{C} at the ortho and para positions reflects its capacity to donate pi electrons. In the planar conformer, the in-plane methyl CH lies near CH(2), thus CH(2) and CH(6) differ slightly. In either case, there is a decrease in q_{σ}^{C} which compensates in part for the increase in q_{π}^{C}. Both the q_{σ}^{C} and q_{π}^{C} changes alternate around the ring.

The fact that the ortho hydrogens are slightly less positive and the ortho carbons are about the same as in benzene suggest that the increase in bond length is matched by a decrease in the ionic contribution to the bond strength. Overall, however, these changes are all on the order of a few millielectrons, much smaller than the variations observed in the fluorobenzenes.

The relationship between r_{CH}^{4-21G} and P^{4-21G} for the two toluene geometries, the fluorinated benzenes, and benzene is shown in Figure 34. The points for toluene cluster just below benzene and the correlation is poorer. In this case, the parameter cannot be

Table XXXIII. Mulliken Population Analysis of Toluene, Planar and Orthogonal[a], and Benzene[b] at 4-21G, Aryl Only

Molecule	Atom	Position	Electron Population (e^-)			
			σ	π	Total ($\sigma+\pi$)	Bond Order (C-H)
Benzene	C		4.4425	0.7327	5.1752	
	H		0.4251			0.7972
Toluene	C	2	4.4038	0.7570	5.1608	
(planar)		3	4.4390	0.7250	5.1635	
		4	4.4289	0.7504	5.1793	
		5	4.4324	0.7247	5.1571	
		6	4.4240	0.7553	5.1793	
	H	2	0.4296			0.8003
		3	0.4282			0.7961
		4	0.4271			0.7977
		5	0.4282			0.7967
		6	0.4293			0.8036
(orthogonal)	C	2	4.4136	0.7566	5.1702	
		3	4.4351	0.7247	5.1598	
		4	4.4291	0.7506	5.1797	
	H	2	0.4297			0.8021
		3	0.4283			0.7964
		4	0.4270			0.7977

[a]optimized geometries from Ref. 46

[b]optimized geometries from Ref. 44

Figure 34

Relationship between the CH bond lengths (aryl only) in benzene, fluorinated benzenes and toluene (planar and orthogonal), obtained from geometry optimization at the 4-21G level, and a bond strength parameter derived from the corresponding electron population analysis.

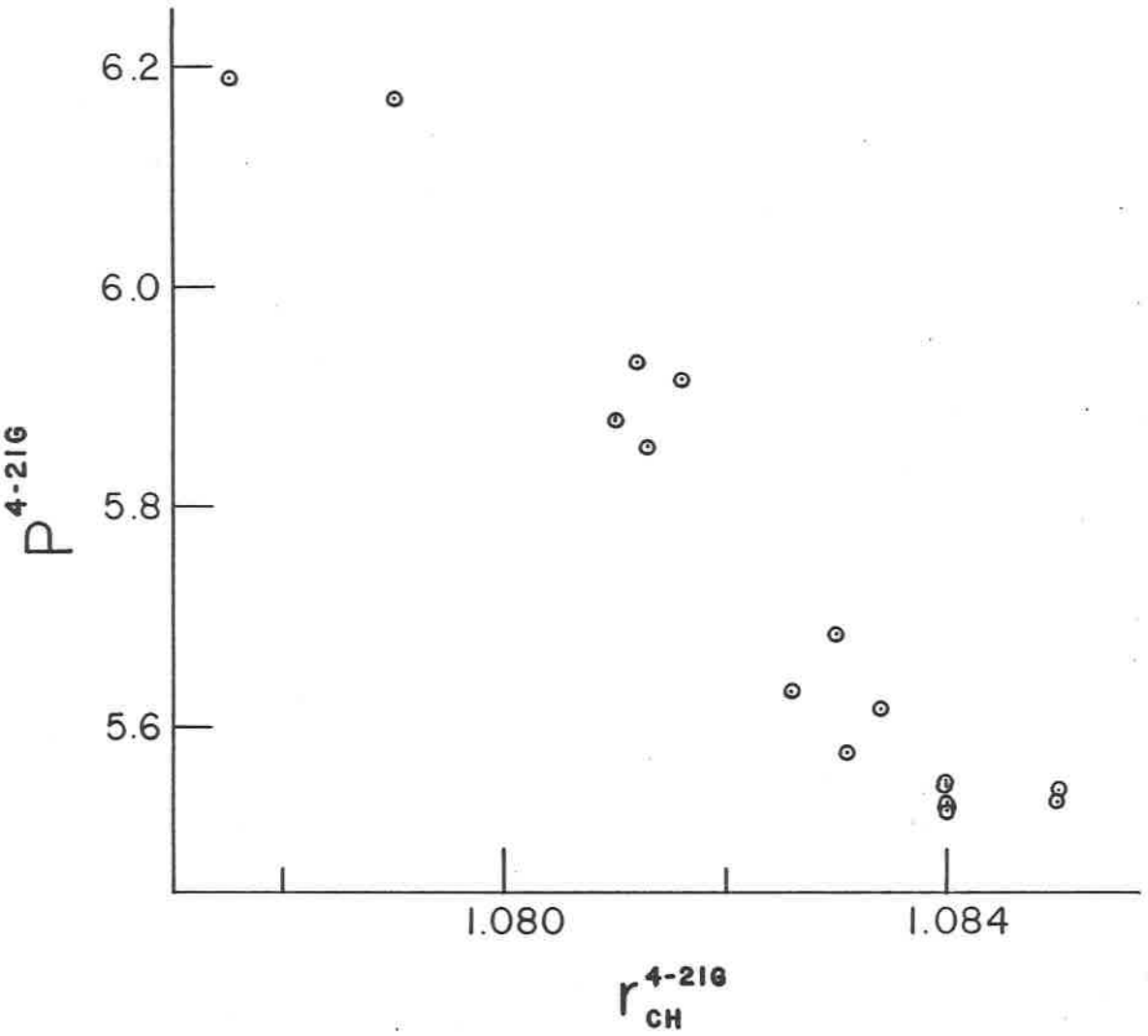
6.2
6.0
5.8
5.6
P 4-21G
1.080
1.084
r CH 4-21G

interpreted as simply as it was for the fluorinated benzenes, because of the inherent assumptions and its qualitative nature.

The STO-3G calculations on ortho-xylene predicted that the aryl CH bonds would be the same as in benzene, (Table XVIII). The difference between the value of P^{STO-3G} at the 3 and 4 positions is again only a few millielectrons. The changes in the sigma and pi populations are similar to those at the 4-21G level for toluene. This is probably the best that can be expected for the calculations at the STO-3G level.

r_{CH}^{LM} (methyl) and P^{Basis}

The parameter values calculated for the methyl CH bonds in toluene at 4-21G could not be related to those for the aryl CH bonds, but the variations were internally consistent. They could be readily understood in terms of a hyperconjugative interaction between the methyl group and the ring. The relevant atomic electron populations and bond order terms are shown in Figure 35 for the four calculated orientations to the ring. The non-bonded terms between the methyl hydrogen and the ring carbon atoms are listed in Table XXXIV. The variations in the populations and in r_{CH}^{4-21G} (methyl) show the expected $\sin^2\theta$ dependence (Fig. 36) for the interaction of an individual methyl CH bond and the benzene ring.

Ermler and Mulliken[135] recently used a large contracted basis set to examine hyperconjugation in toluene and the toluenium ion. Only a standard, non-optimized geometry was used, for the orthogonal conformer, and methyl hydrogens were not considered individually. They showed that hyperconjugation was evident in the four pi or quasi-pi

Figure 35

Electron population on the methyl hydrogen (diagonal term from the Mulliken population analysis matrix) and bond order term, for dihedral angle θ = 0°, 30°, 60° and 90°, in toluene, 4-21G optimized geometry.

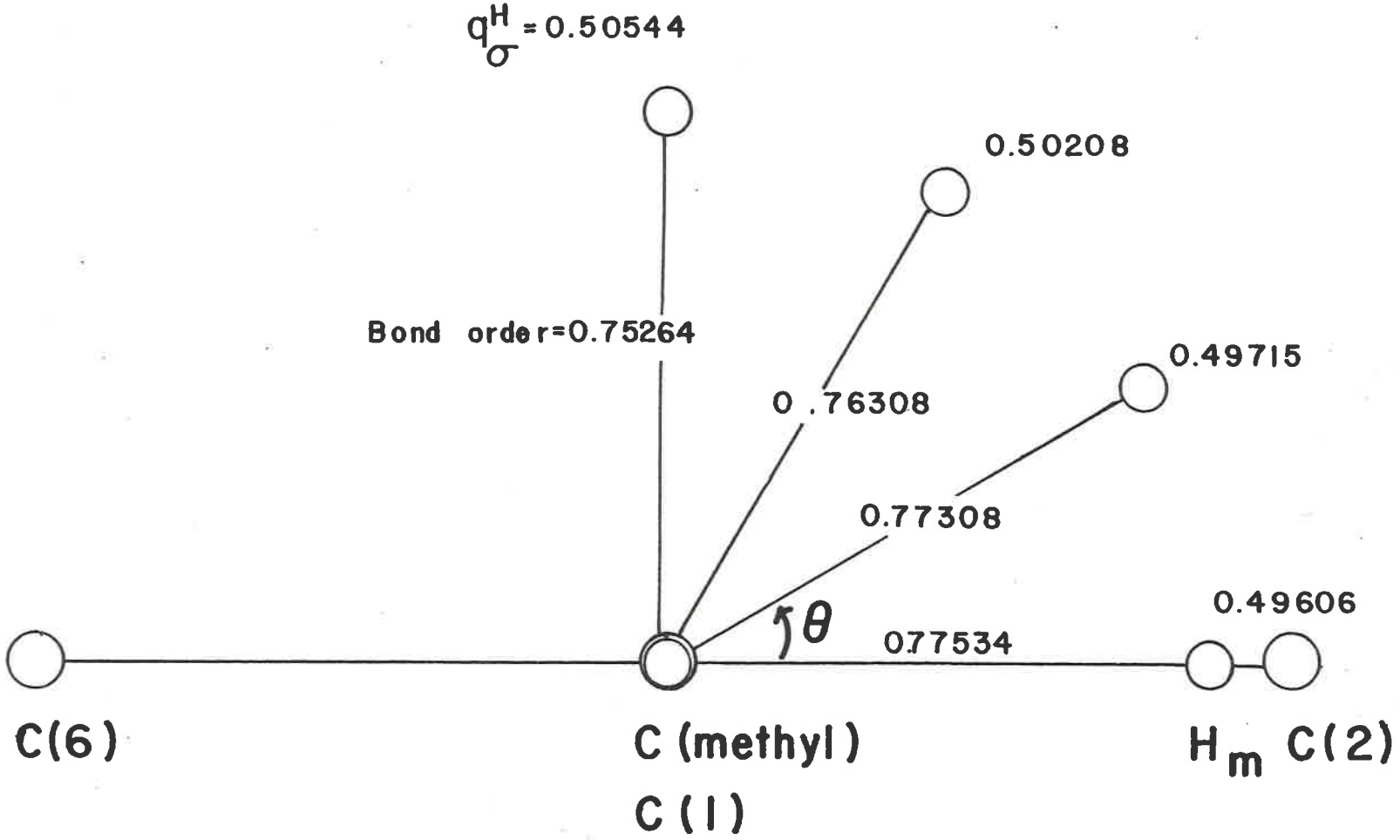
q^H_σ = 0.50544
0.50208
Bond order=0.75264
0.49715
0.76308
0.77308
θ
0.49606
0.77534
C(6)
C (methyl)
C (1)
H_m C(2)

Table XXXIV. Mulliken Electron Population Analysis on Toluene at 4-21G (Planar and Orthogonal): Non-bonded Terms (e^-) between Methyl Hydrogen and Ring Carbons

Carbon Position	Type	θ (degrees)[a]				Total Change
		0	30	60	90	(0°→90°)
1	σ	-0.04985	-0.04775	-0.04272	-0.04035	
	π	0.0	-0.00265	-0.00865	-0.01184	
	Total	-0.04985	-0.05040	-0.05137	-0.05219	-0.00234
2	σ	-0.00022	-0.00035	-0.00003	0.00108	
	π	0.0	-0.00055	-0.00154	-0.00169	
	Total	-0.00022	-0.00090	-0.00151	-0.00061	-0.00039
3	σ	0.00021	0.00015	0.00003	-0.00004	
	π	0.0	0.00002	0.00003	0.00001	
	Total	0.00021	0.00017	0.00006	-0.00003	-0.00024
4	σ	0.0	0.0	0.0	0	
	π	0.0	0.0	0.00001	0.00001	
	Total	0.0	0.0	0.00001	0.00001	0.00001
5	σ	-0.00006	-0.00006	-0.00006	-0.00004	
	π	0.0	0.0	0.0	0.00001	
	Total	-0.00006	-0.00006	-0.00006	-0.00003	-0.00003
6	σ	0.00267	0.00250	0.00199	0.00110	
	π	0.0	-0.00025	-0.00095	-0.00169	
	Total	0.00267	0.00225	0.00104	-0.00059	-0.00326

[a]Dihedral angle to ring as shown in Fig. 35

Figure 36

Variation in methyl CH related terms with dihedral angle θ, from ab initio geometry optimization of toluene at the 4-21G level.

Top curve: optimized CH bond length

Upper trio: Methyl H - ring C(1) shared electron population:

σ — — —, π ----, Total ———

Lower trio: Methyl H - ring C(2) shared electron population:

σ — — —, π ----, Total ———

Bottom curve: bond strength parameter dervied from Mulliken population analysis

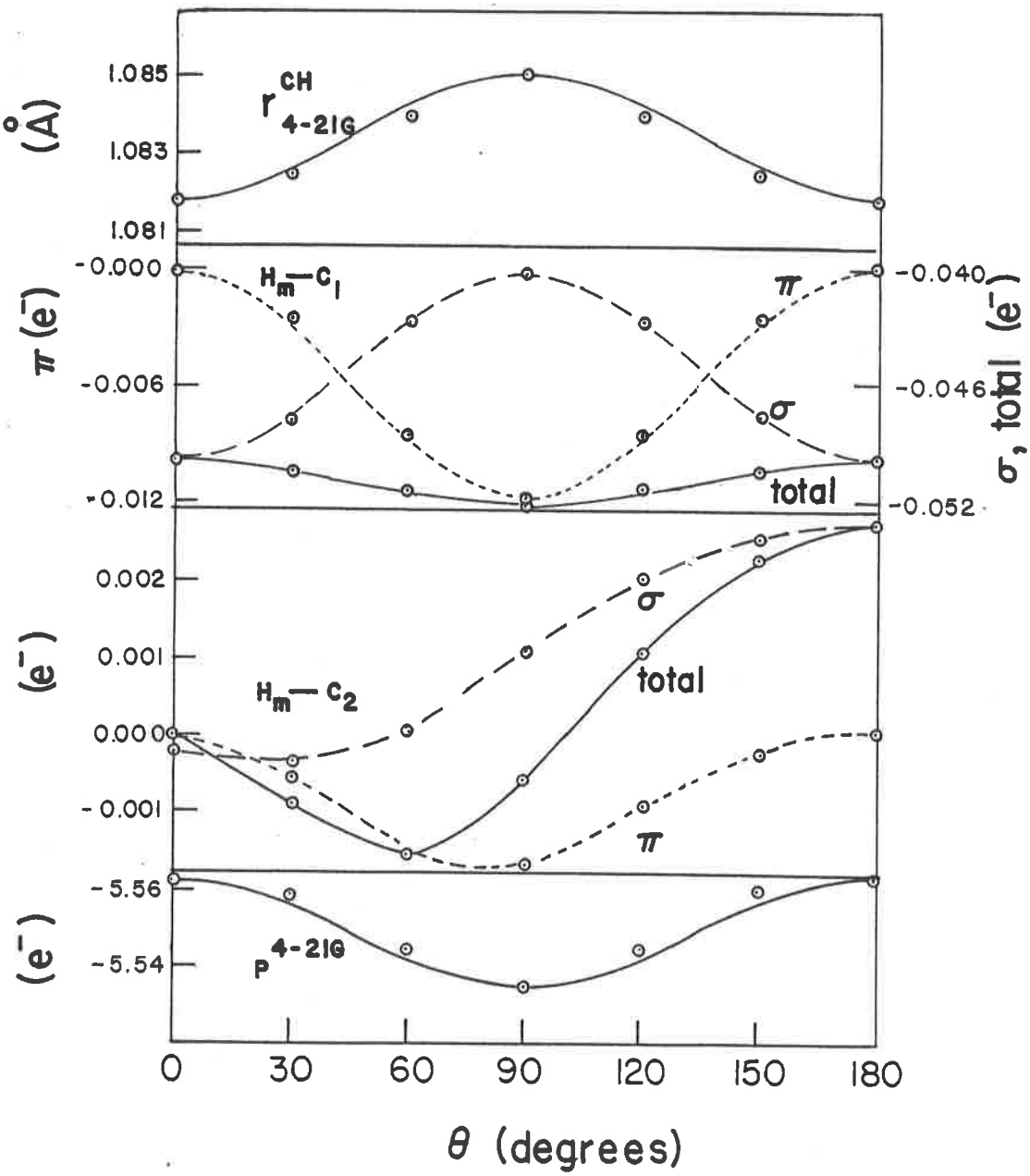
1.085
1.083
1.081
Å
$r^{CH}_{4\text{-}21G}$
-0.000
-0.006
-0.012
$H_m - C_1$
π
σ
total
π (e⁻)
-0.040
-0.046
-0.052
σ, total (e⁻)
0.002
0.001
0.000
-0.001
$H_m - C_2$
σ
total
π
(e⁻)
-5.56
-5.54
$P^{4\text{-}21G}$
(e⁻)
0
30
60
90
120
150
180
θ (degrees)

molecular orbitals involving the methyl group and the carbon $2p_y$ (π) orbitals. The interaction between the methyl group and the ring was primarily antibonding (i.e., antibonding in three of the four molecular orbitals). In the 4-21G calculations performed for this work, the antibonding interaction was again evident, both in the molecular orbitals and the electron populations. The detailed analysis of the non-bonded terms between the methyl hydrogen and the carbon atoms (Table XXXIV, Fig. 36) shows that this antibonding is maximum for a CH bond perpendicular to the ring. It is interesting to note that the changes in the sigma framework tend to oppose this.

The electron population on the hydrogen atom, (Fig. 35) increases from the 0° to the 90° position. Since the population on the carbon remains constant, there is a decrease in the ionic contribution to the parameter, (eq. 13), as the dihedral angle changes from 0° to 90°. The bond order term between methyl carbon and hydrogen also decreases as it moves from 0° to 90°. The parameter thus changes with the bond length (Table XIV, Fig. 36) although it appears that non-bonded interactions are also important in the bond length variation.

The variation in P^{4-21G} can also be viewed as a further effect of hyperconjugation. The simple picture which emerges is that the methyl group as a whole is in an antibonding relationship to the benzene pi system. The involvement of an individual methyl CH bond is zero when it lies in the ring plane, and at a maximum when at 90° to it, where the bond is weakened and slightly longer.

It is not possible to determine where the electron density is transferred, from these calculations. The change in electron density

at any ring atom is always the sum of the contributions from all three hydrogens, which remains constant by symmetry. The calculated molecular orbitals could be transformed to localized molecular orbitals, so that the overlap between a given methyl CH bond and the other atoms could be examined.

Alternative theoretical descriptions of methyl hyperconjugation and the effects of an asymmetric environment have received some attention in recent years. Pross, Radom and Riggs[136] used perturbation molecular orbital theory to qualitatively describe methyl hyperconjugation in terms of a "trans-lone pair"[137] effect. The latter is a widely used explanation for the decrease in the average or isolated CH stretching frequency of groups attached to atoms with a lone pair of electrons. Within this interpretation the weakening of a CH bond is said to arise from the donation of electron density from the occupied lone pair orbital into an unoccupied antibonding orbital of the trans CH bond. Alternatively the occupied methyl quasi-pi orbital could donate electron density into an unoccupied lone pair orbital on a neighbouring atom. Flood, Pulay and Boggs[138] have suggested that bond-bond repulsion and bond-lone pair repulsion are the important factors. For H—C---X—H interactions, where X is an atom possessing a lone pair, the bond-lone pair repulsion would predominate. Both interpretations have been found to be useful in explaining the tilt of the methyl group and the bond length changes, however they neglect any possible changes within the sigma bond framework. The analysis presented in this report offers an alternative description which includes hyperconjugation as an antibonding interaction, as well as the changes in the sigma bond framework.

iii) Cyclohexadienes

a) Introduction to the Problem

The gas phase overtone spectra of 1,3- and 1,4-cyclohexadiene were recorded for the regions corresponding to Δv = 3, 4 and 5. The analysis of these spectra provides another demonstration of the usefulness of the overtone frequency plus ab initio calculation technique for resolving structural problems.

Microwave spectroscopy studies[139,140] have shown that the 1,3-cyclohexadiene structure is non-planar with C_2 symmetry and an angle of 17.5 ± 2° between the ethylene planes. Electron diffraction studies[141-143] also support this structure. The barrier to inversion has been measured at 13.5 kJ/mole from Raman spectra[144].

The 1,4-cyclohexadiene molecule is probably planar, according to vibrational[145], rotational Raman[146], NMR[147], and electron diffraction[148] studies, however in the latter a planar structure was assumed. Another electron diffraction study[141] predicted non-planarity, with the minimum in a boat conformer. Far IR[149] spectra also indicated the possibility of non-planarity.

Ab initio molecular orbital calculations[150] with full geometry optimization and a split-valence basis set predicted that the 1,4-isomer would be planar and the 1,3-isomer would be puckered. Furthermore, the methylene CH bonds in the latter molecule were predicted to be inequivalent, in a manner similar to the axial and equatorial CH bonds in cyclohexane. In the latter molecule the two inequivalent CH bonds give rise to a partially resolved doublet in the overtone spectra[31,32]. Because of the high barrier to inversion, the 1,3-isomer should be locked into its minimum energy conformation on the near IR time scale.

Three different overtone series should appear in the spectra of the 1,3-isomer, two at low frequencies corresponding to the two different pairs of methylenic CH bonds, and one at a much higher frequency corresponding to the four ethylenic CH bonds. If the 1,4-isomer is planar, only two CH bond types would be present: ethylenic and methylenic. If it is non-planar, three types are expected, since the methylenic CH bonds would not be equivalent. The relative intensities of the peaks might not reflect the number of CH oscillators since the overtone peaks of the axial and equatorial oscillators in cyclohexane[56], and the aryl and alkyl CH oscillators in toluene[5], are not comparable on a per hydrogen basis.

b) Peak Positions, Assignments and Local Mode Parameters

Figures 37-42 show Δv = 3, 4 and 5 of 1,3- and 1,4-cyclohexadiene in the gas phase at 86°C. Calculated peak positions, assignments, and local mode parameters are listed in Table XXXV.

The non-planar structure of 1,3-cyclohexadiene can readily be deduced from the presence of three different absorptions at each overtone. The high frequency ethylenic peak appears in the same spectral region as the overtones of benzene. The overtones of the two inequivalent methylenic CH bonds are well resolved. It can similarly be deduced that the 1,4-cyclohexadiene molecule is planar, since only two major absorptions occur at each overtone region. The high frequency peak again corresponds to the four equivalent ethylenic CH oscillators. The single low frequency absorption corresponds to the four equivalent methylenic oscillators. The latter peak falls part way between the two methylenic absorptions of 1,3-cyclohexadiene.

The local mode parameters for all the ethylenic CH bonds are comparable to those of benzene. The magnitude of the anharmonicity constant is quite large for all the methylenic CH bonds. There is a precedent for this in the n-alkanes[57] for which the value of X ranges from -62 to -68 cm^{-1}. The numbers are still rather suspect, owing to the poor correlation coefficient for CH(5) in 1,3-cyclohexadiene and the existence of doublets at Δv = 5 for CH(3) in the 1,4-isomer, and Δv = 3 for CH(5') in the 1,3-isomer, since each appears in only one of the three overtones. For CH(3) of 1,4-cyclohexadiene, the band centre was found to give an excellent correlation with the other two overtones. For CH(5') in 1,3-cyclohexadiene, the lower frequency peak gave the best correlation with the peak maxima at Δv = 4 and 5, but

Figure 37

The CH-stretching overtone spectrum of 1,4-cyclohexadiene in the gas phase, 86°C, in the region of $\Delta v = 3$. Pathlength, 9.75 m; recorded on the Beckman 5270; single scan.

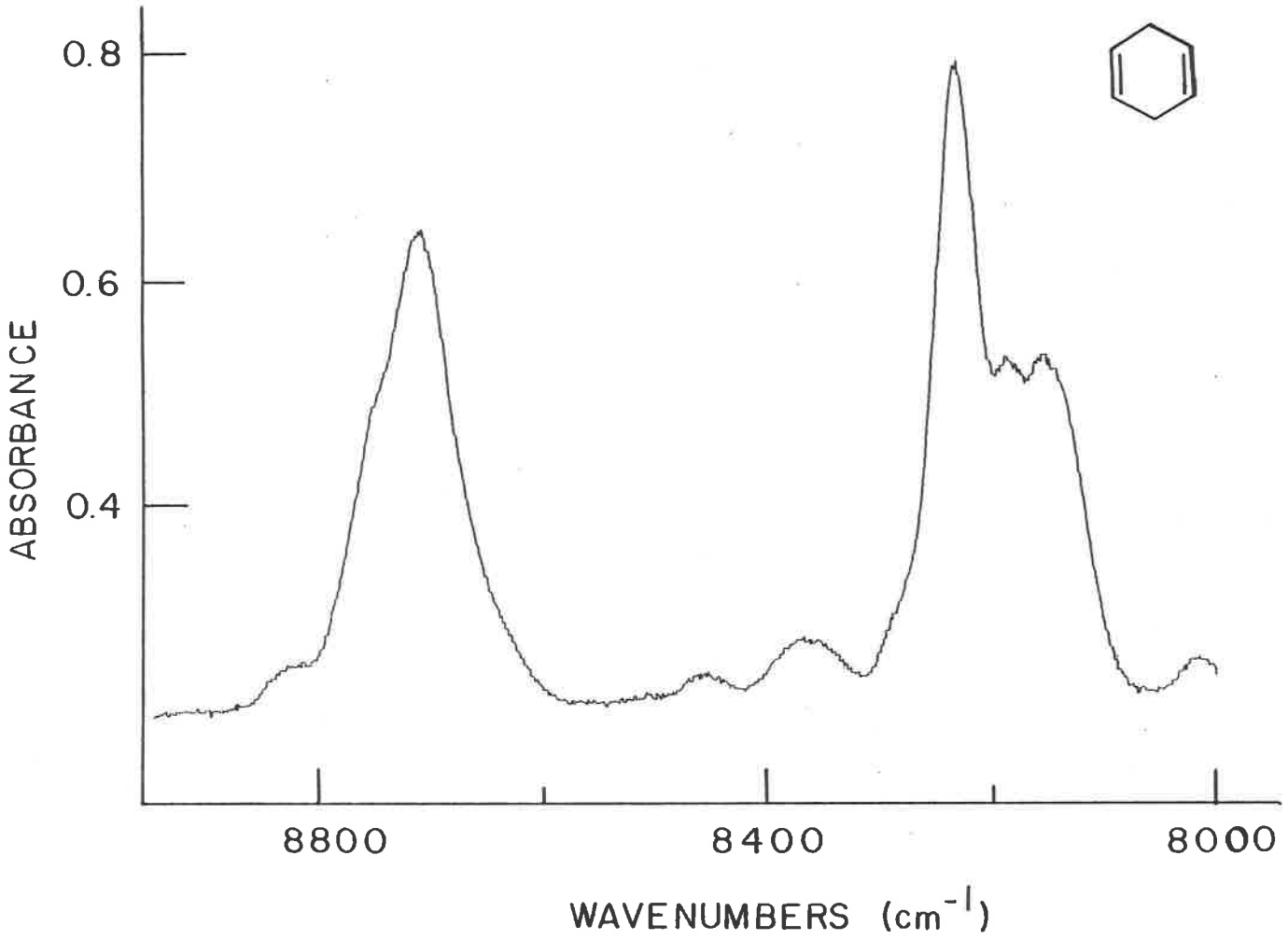
0.8
0.6
0.4
ABSORBANCE
8800
8400
8000
WAVENUMBERS (cm⁻¹)

Figure 38

The CH-stretching overtone spectrum of 1,4-cyclohexadiene in the gas phase, 86°C, in the region of $\Delta v = 4$. Pathlength, 9.75 m; recorded on the Beckman 5270; sum of 2 scans.

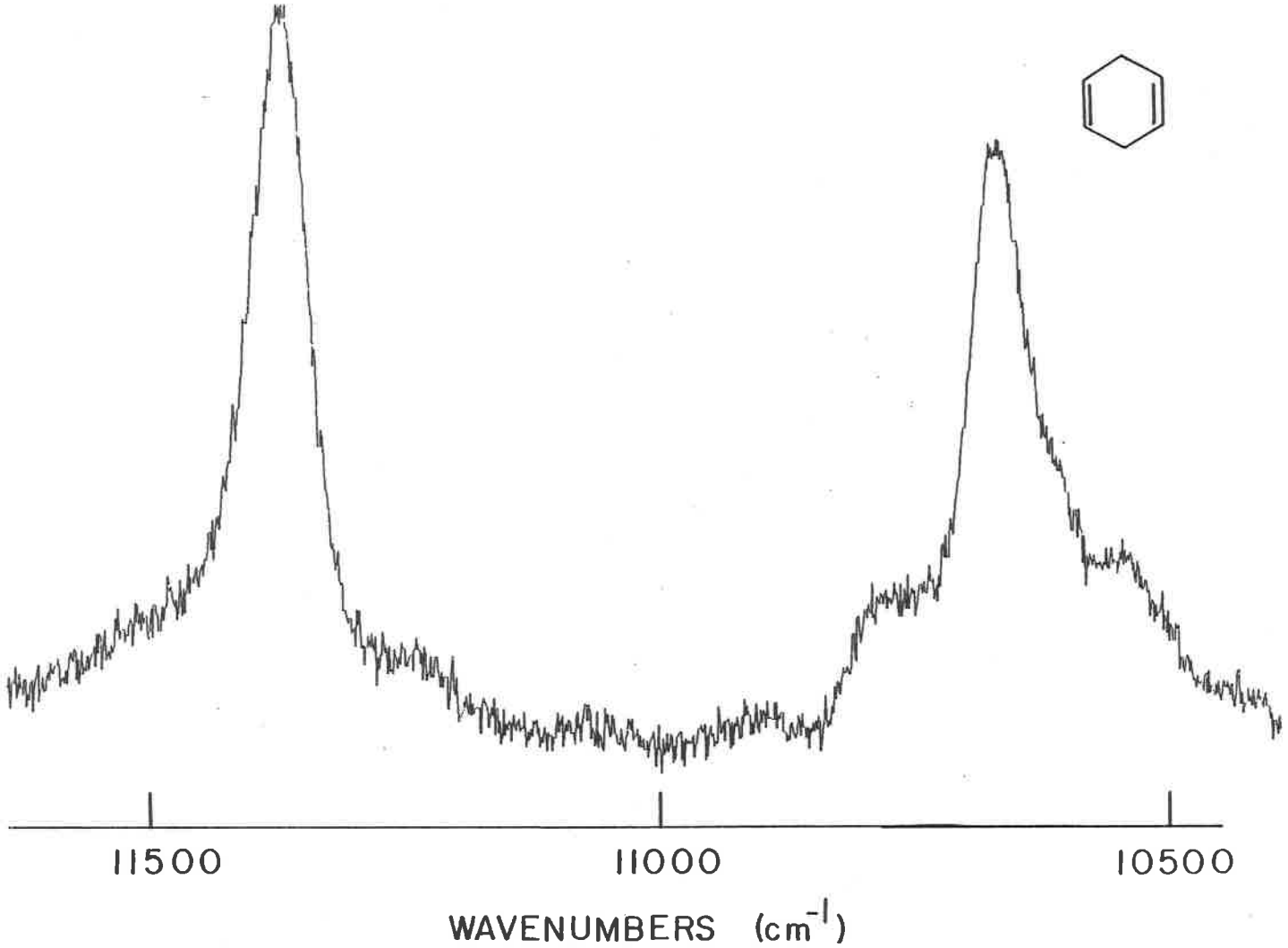
11500
11000
10500
WAVENUMBERS (cm⁻¹)

Figure 39

The CH-stretching overtone spectrum of 1,4-cyclohexadiene in the gas phase, 86°C, in the region of $\Delta v = 5$. Pathlength, 9.75 m; recorded on the Beckman 5270; sum of 7 scans.

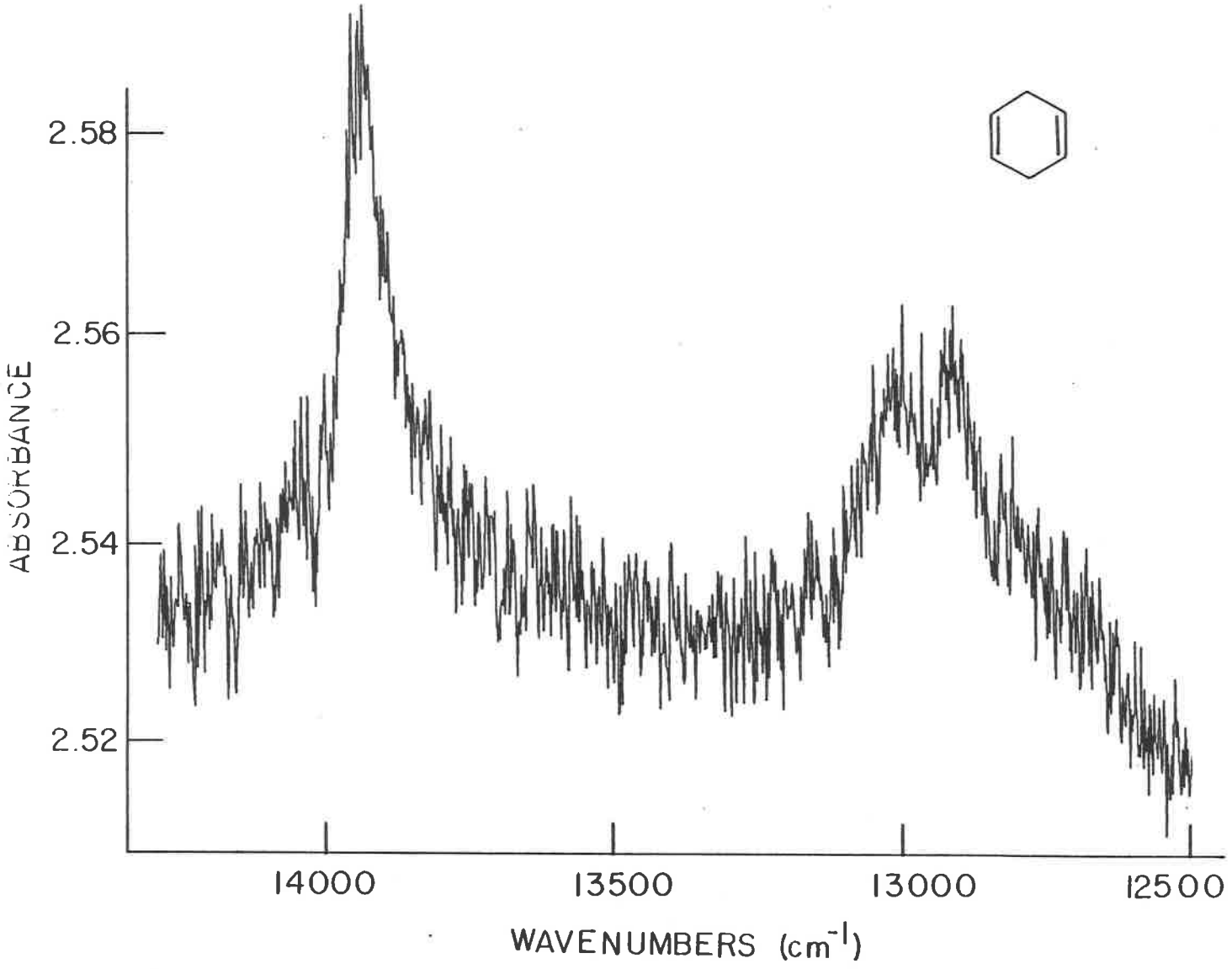
2.58
2.56
2.54
2.52
ABSORBANCE
14000
13500
13000
12500
WAVENUMBERS (cm⁻¹)

Figure 40

The CH-stretching overtone spectrum of 1,3-cyclohexadiene in the gas phase, 86°C, in the region of $\Delta v = 3$. Pathlength, 8.25 m; recorded on the Beckman 5270; single scan.

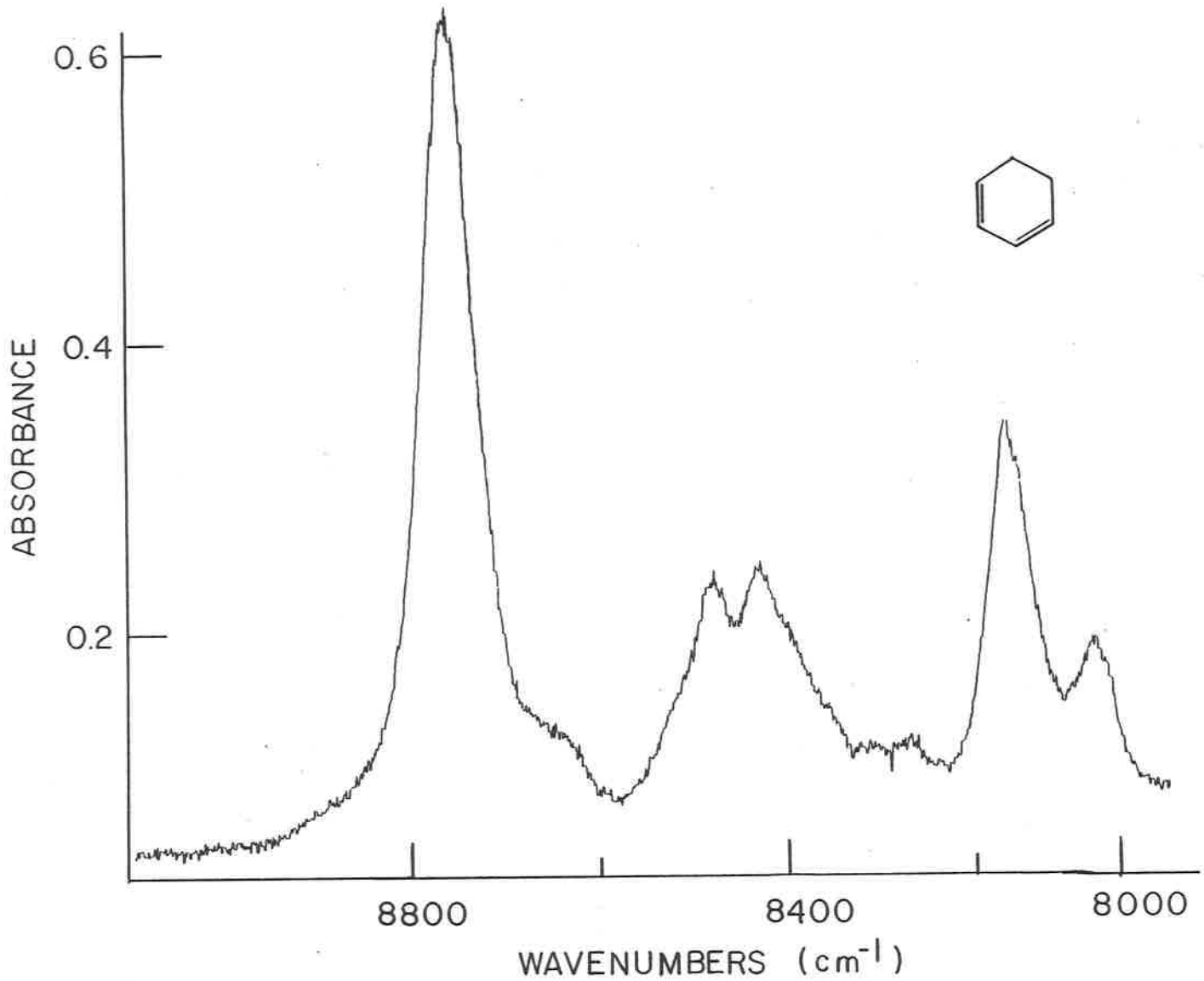
0.6
0.4
0.2
ABSORBANCE
8800
8400
8000
WAVENUMBERS (cm⁻¹)

Figure 41

The CH-stretching overtone spectrum of 1,3-cyclohexadiene in the gas phase, 86°C, in the region of $\Delta v = 4$. Pathlength, 8.25 m; recorded on the Beckman 5270; single scan.

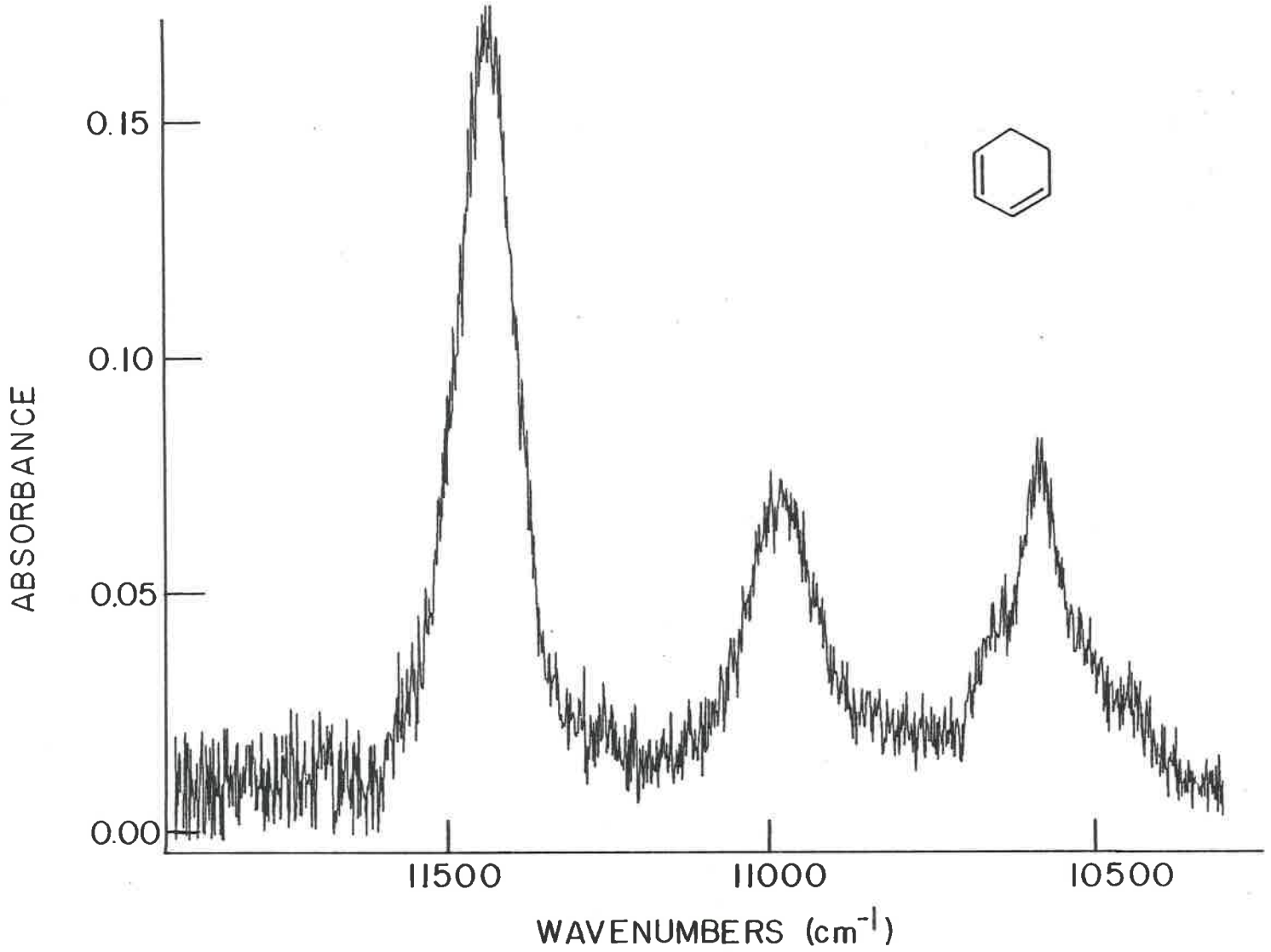
0.15
0.10
0.05
0.00
ABSORBANCE
11500
11000
10500
WAVENUMBERS (cm^{-1})

Figure 42

The CH-stretching overtone spectrum of 1,3-cyclohexadiene in the gas phase, 86°C, in the region of $\Delta v = 5$. Pathlength, 8.25 m; recorded on the Beckman 5270; sum of 6 scans.

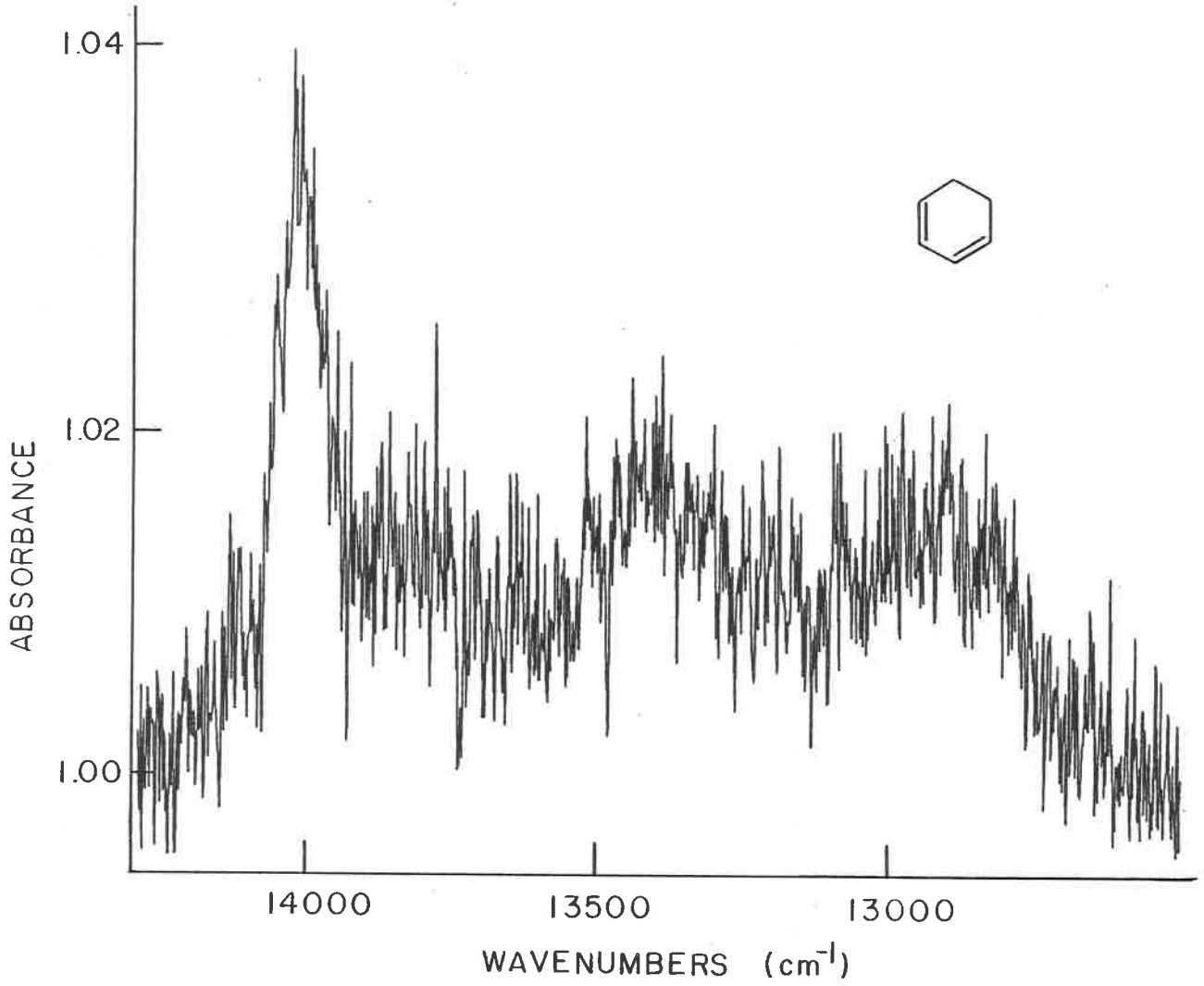
1.04
1.02
1.00
ABSORBANCE
14000
13500
13000
WAVENUMBERS (cm⁻¹)

Table XXXV. Calculated Peak Positions, Assignments and Local Mode Parameters from Gas Phase Overtone Spectra of 1,3- and 1,4-Cyclohexadiene

Molecule	Assignment	Δv	$\bar{\nu}_{max}$ (cm^{-1})	ω (cm^{-1})	X (cm^{-1})	r
1,4-cyclo-	CH(1)	3	8705	3081	-59.6	-0.99997
hexadiene		4	11371			
		5	13912			
	CH(3)	3	8227	2969	-75.6	-0.99999
		4	10668			
		5	12955[a]			
1,3-cyclo-	CH(1),CH(2)	3	8768	3104	-60.7	-0.99988
hexadiene		4	11441			
		5	14006			
	CH(5')	3	8428[b]	2990	-60.5	-0.99993
		4	10989			
		5	13440			
	CH(5)	3	8170	2936	-71.6	-0.9989
		4	10583			
		5	12900			

[a]Centre of doublet

[b]Lower frequency peak in doublet, chosen for best fit.

because of the poor quality of the spectrum at $\Delta v = 5$, there is a good deal of uncertainty associated with these parameters.

From the spectra at $\Delta v = 4$, (Fig. 38 and 41), the relative peak intensities do roughly follow the number of inequivalent CH bonds. The ratio of the calculated peak areas is 1.2:1.0 for the ethylenic to methylenic peaks in 1,4-cyclohexadiene, and about 2:1:0.75 for CH(1):CH(5'):CH(5) bond types in 1,3-cyclohexadiene. The linewidths are between 70 and 100 cm^{-1}, comparable to those of the fluorinated benzenes in Table XXIX.

c) r_{CH}^{LM} and r_{CH} (ab initio)

The shift in the position of the overtone maximum relative to benzene[70] was determined for each oscillator, at each overtone. The bond lengths were calculated from eq. 11, and averaged over the three overtones to yield r_{CH}^{LM}. The results are listed in Table XXXVI, along with the ab initio and other experimental values. The ab initio bond lengths are the ones calculated in the geometry optimization[150]. The authors employed a split valence basis set which was not 4-21G but which was not otherwise identified. The authors suggested that the correction to obtain comparable r_o values should be similar to that for the 4-21G basis set (+0.012 Å).

The correlation between r_{CH}^{LM} and r_{CH} (ab initio) is not as good as that found for the fluorinated benzenes and toluene. This is due at least in part to the difficulties with the spectra. There is greater uncertainty for these numbers (probably a few thousandths of an Angstrom), however the assignment is still straightforward. The r_{CH}^{LM} values provide the only experimental evidence that the methylenic CH bonds in 1,3-cyclohexadiene are inequivalent. As predicted by the ab initio calculations, all four ethylenic bonds are found to be equivalent, and about the same as in benzene. The four methylenic CH bonds in 1,4-cyclohexadiene are equivalent from which it may be concluded that the molecule is indeed planar.

Table XXXVI. CH Bond Lengths (Å) in 1,3- and 1,4-cyclohexadiene from Experimental and Ab Initio Studies. References in Brackets

Molecule	Assignment	r_{CH}^{LM}	Ab Initio (150) r_{CH}^{calc} [Corrected][a]	Electron Diffraction r_a (141)	r_e	r_g (143)	Microwave r_o (139)
1,3-cyclohexadiene	CH (1)(2)(3)(4)	1.083	1.071 [1.083]	1.082	1.107 (142)	1.099	1.086±.015
	CH (5')	1.095	1.081 [1.093]	1.096	1.14 (142)	1.111	1.10±.015
	CH (5)	1.104	1.086 [1.098]	1.096	1.14 (142)	1.111	1.10±.015
1,4-cyclohexadiene	CH (1)(2)(4)(5)	1.081_2	1.072 [1.084]	1.079	1.103 (148)		
	CH (3) (6)	1.102_7	1.088 [1.100]	1.096	1.114 (148)		

[a]Values corrected to r_o according to Ref. 150, in square brackets.

iv) Anisole

The liquid phase CH-stretching overtone spectra of anisole were recorded for Δv = 3-6 (Fig. 43, 44), and deconvoluted. Because of the high boiling point (154°C), it was only possible to obtain Δv = 2, and 3 (Fig. 45) in the gas phase. The value of σ_I for this substituent has been measured as 0.23 to 0.34[63]. The resonance parameter is also quite large (-0.43 to -0.45)[63], so that the group behaviour should be similar to that of fluorine.

The minimum energy conformer of anisole has all the heavy atoms co-planar[151-155]. The methoxy group lies cis to the ring C(1)-C(2) bond, and the methyl group is staggered with respect to the ring. The barriers to methyl and methoxy internal rotation are related, and are large, >10 kJ/Mole[151-155].

The geometry of anisole was optimized at the STO-3G level. The aryl CH(2) bond was shortened (Table XVIII) although this may not be significant; the uncertainty in aryl CH bond lengths is large at this level (Table XX). In the methyl group, the in-plane CH bond is predicted to be shorter than the CH bonds 60° above and below the ring plane. It is interesting to note that the STO-3G calculations consistently agree with the 4-21G calculations on toluene[46], on this point. The methyl CH bond is shortest when it lies in the ring plane, and increases to a maximum at 90° to the ring plane for anisole, 2-methoxypyridine[95] (several conformations), ortho-xylene[125] (6 conformations) and ortho-fluorotoluene[129]. Thus while the bond length correlation may be poor, the distinction between in-plane and out-of-plane CH bonds, due to hyperconjugative interactions, does appear at this level of computation.

Figure 43

The CH-stretching overtone spectra of liquid phase anisole, at room temperature, in the region of $\Delta v = 3$, 2 cm pathlength (lower spectrum) and $\Delta v = 4$, 10 cm pathlength (upper spectrum). Recorded on the Beckman 5270; single scan at each overtone.

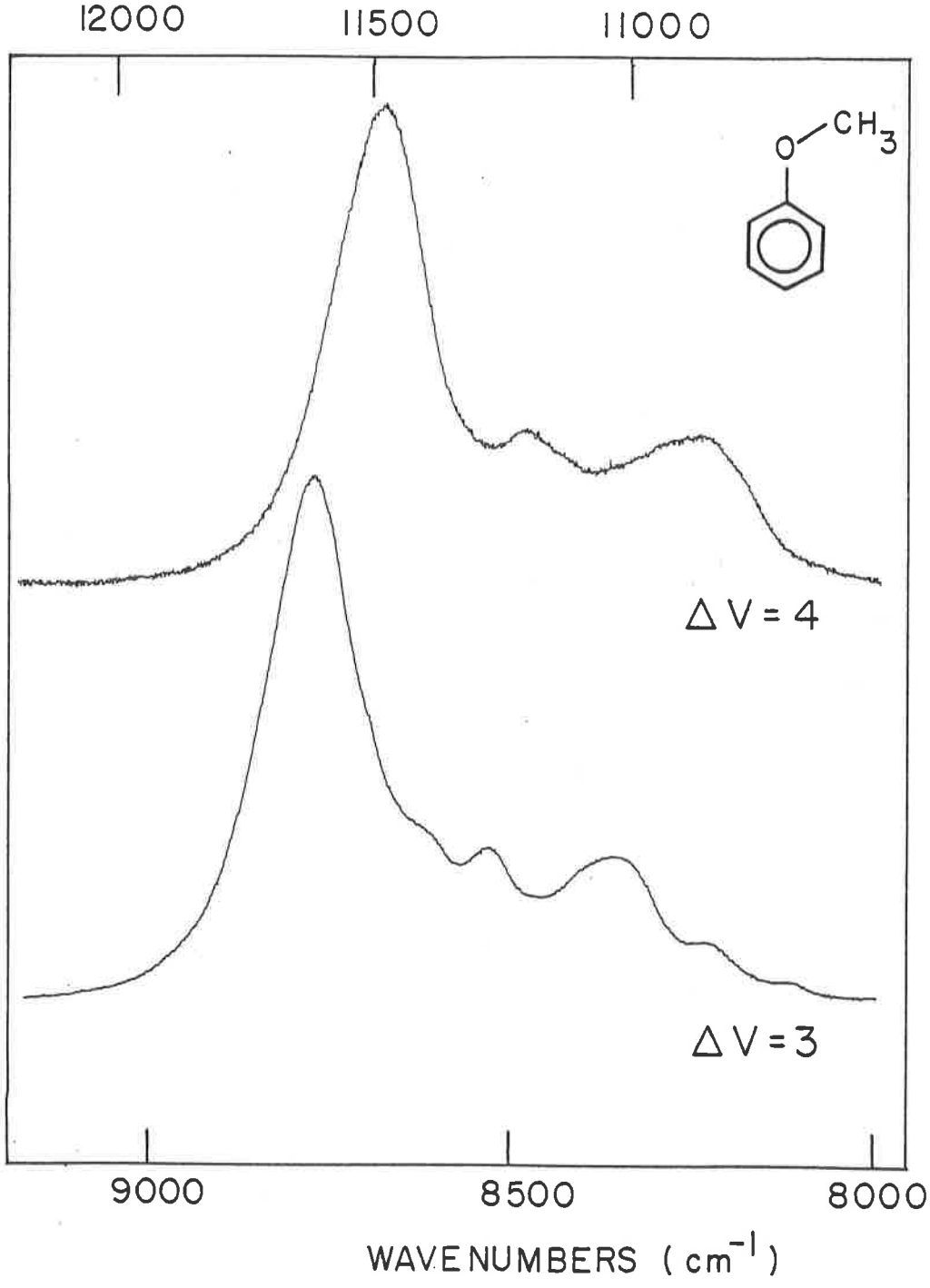
12000
11500
11000
O
CH3
ΔV = 4
ΔV = 3
9000
8500
8000
WAVE NUMBERS (cm-1)

Figure 44

The CH-stretching overtone spectra of liquid phase anisole, at room temperature, in the region of $\Delta v = 5$ (lower spectrum) and $\Delta v = 6$ (upper spectrum), 10 cm pathlength; recorded on the Beckman 5270; single scan at $\Delta v = 5$, sum of 6 scans at $\Delta v = 6$.

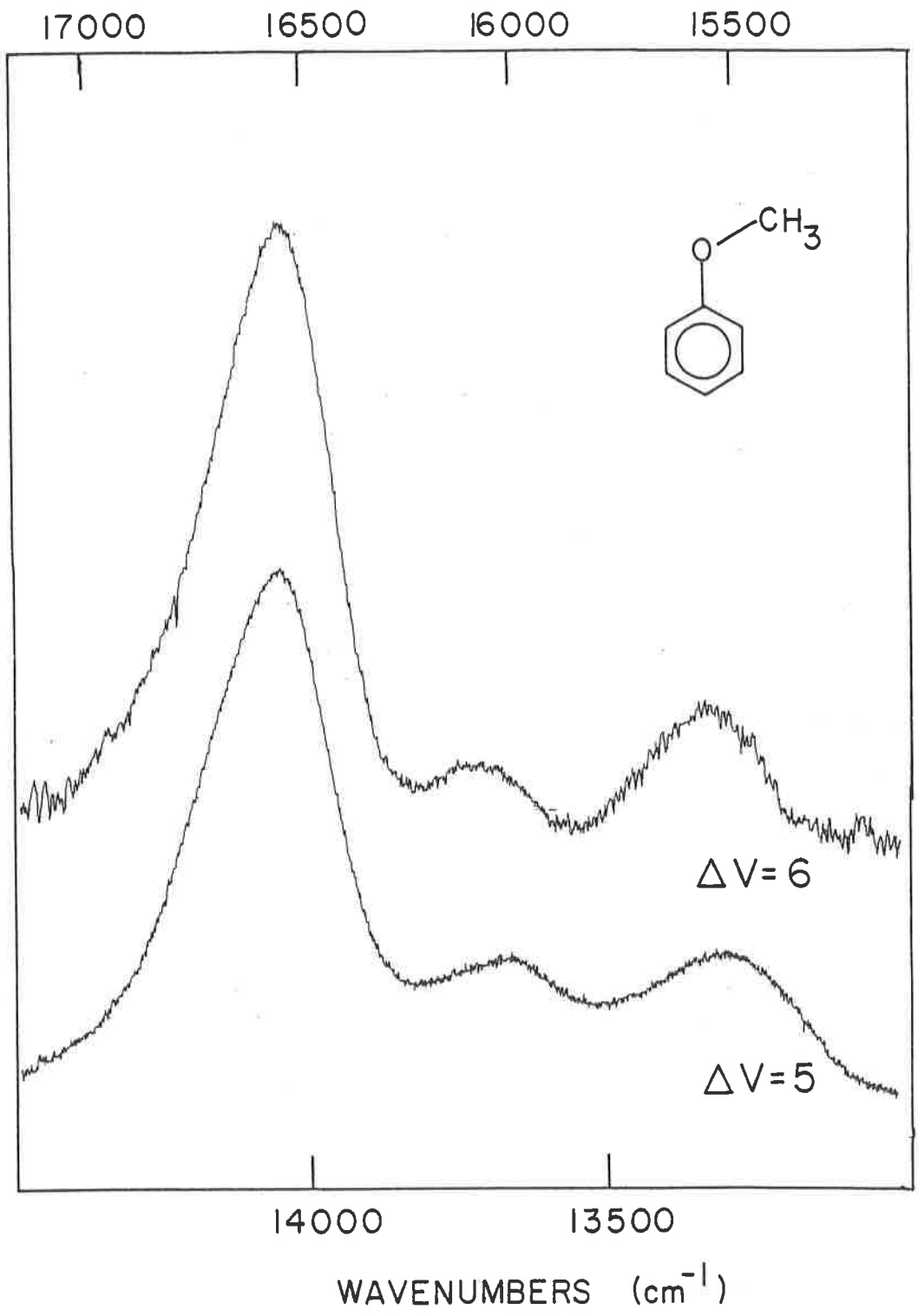
17000
16500
16000
15500
CH3
ΔV=6
ΔV=5
14000
13500
WAVENUMBERS (cm-1)

Figure 45

The CH-stretching overtone spectrum of anisole in the gas phase, 86°C, in the region of $\Delta v = 3$. Pathlength, 0.75 m; recorded on Beckman 5270; single scan.

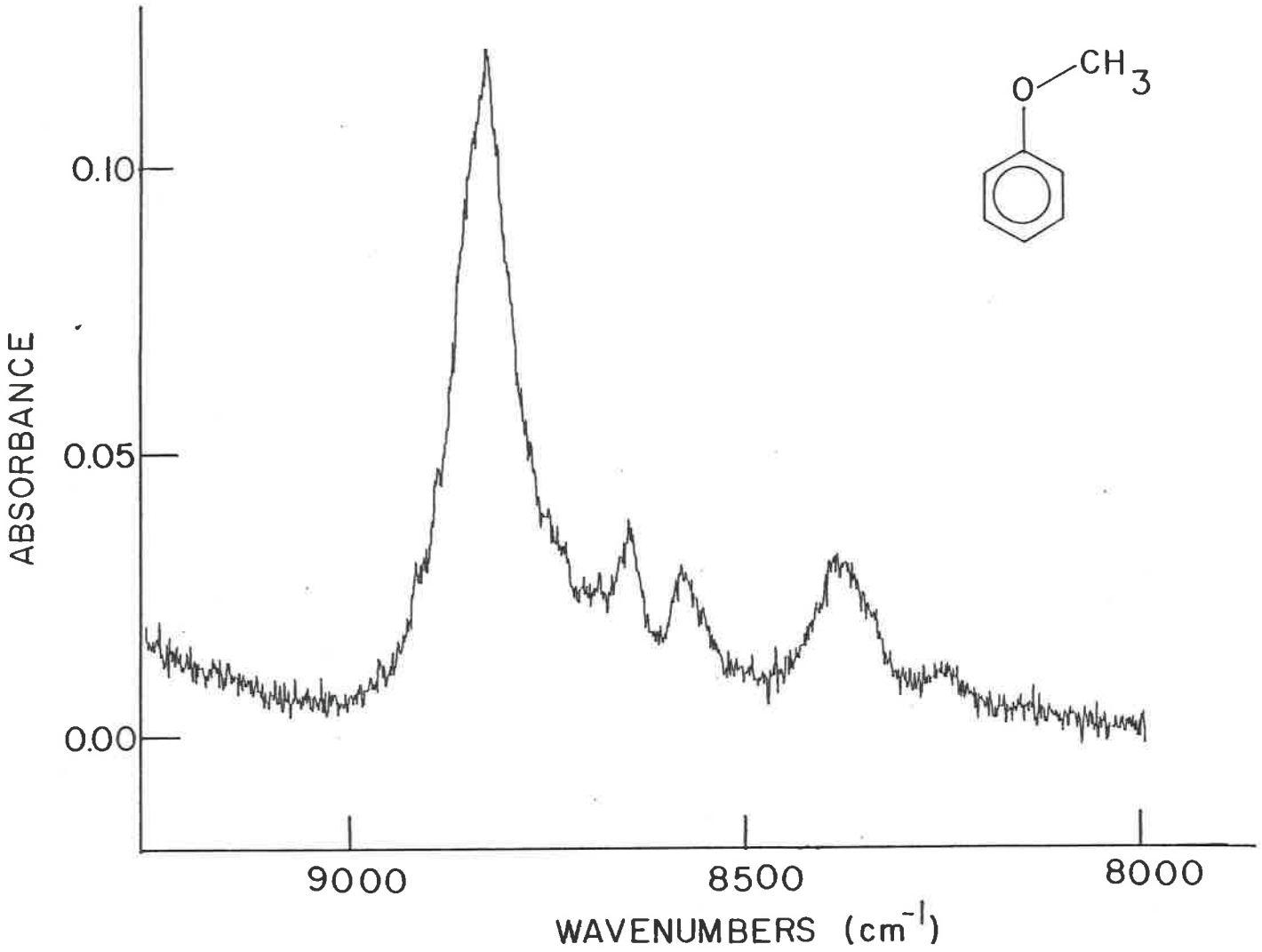
ABSORBANCE
0.10
0.05
0.00
9000
8500
8000
WAVENUMBERS (cm⁻¹)
O
CH3

a) Peak Positions,Assignments and Local Mode Parameters

The results of the band fit procedure appear in Table XXXVII along with the assignments and local mode parameters. The liquid phase spectra are fairly complex, and the lines are broad. It does appear that the inequivalent methyl CH bonds are resolved, but there are other absorptions present, and the local mode parameters reveal the uncertainty of the assignment. It is possible that the other lines are due to Fermi resonance interactions or to the presence of other conformers.

The gas phase spectrum at $\Delta v = 3$ does not clarify the situation greatly. Several peaks are well resolved but gas phase spectra at higher overtones are needed to confirm the assignments. The aryl region shows only a single major absorption but the linewidth (about 80 cm^{-1}) is considerably larger than those of the fluorinated benzenes (Table XXIX), and may contain contributions from various slightly inequivalent oscillators. There is no evidence of a high frequency absorption corresponding to the aryl CH(2) bond, so that the extreme shortening predicted by the STO-3G calculations may be an artifact. The optimization was done sequentially with the GAUSSIAN70 program and it was difficult to minimize. It was for these reasons that the correlation between r_{CH}^{LM} and the STO-3G parameters were checked both with and without the anisole data (Table XX).

Table XXXVII. Peak Positions, Assignments and Local Mode Parameters from the Liquid Phase CH Overtone Spectra of Anisole

Assignment	Δv	$\bar{\nu}_{max}$ (cm^{-1})	ω (cm^{-1})	X (cm^{-1})	r
Aryl	3	8794	3106	-58.7	-0.99968
	4	11482			
	5	14051			
	6	16534			
Methyl CH (0°)	3	8543	3020	-57.4	-0.99999[a]
	4(?)	11202	3027	-58.3	-0.998[b]
	5	13662			
	6	16057			
CH (60°)	3	8398	3005	-68.2	-0.99990
	4	10932			
	5	13309			
	6	15574			

[a]Correlation with Δv = 3, 5 and 6 only

[b]Correlation with Δv = 3, 4, 5 and 6

v) α, α, α-trifluorotoluene: Peak Positions and Comparison with Fluorobenzene and Toluene

The gas phase spectra of α, α, α-trifluorotoluene were recorded for $\Delta v = 3$ and 4 (Fig. 46). The σ_I value for this molecule is fairly large (0.41 to 0.45)[63] while σ_R is positive and close to zero (0.0 to 0.11)[63]. The two spectra were decomposed, but of course it was not possible to calculate local mode parameters. Geometry optimizations were not performed.

At both overtones, the band envelope was decomposed as the sum of two major peaks. The low frequency peak was the more intense, at about 70% of the total area. There is no strong evidence for the presence of very inequivalent CH bonds, since the separation of the calculated peaks was 50 cm^{-1} at $\Delta v = 3$ and 60 cm^{-1} at $\Delta v = 4$, which suggests a bond length difference of 0.001 to 0.0015 Å at most, if these peaks are actually due to inequivalent CH bonds. This is quite different from the results from fluorobenzene and toluene where inequivalent CH bonds were well resolved (Fig. 14, 29, 31). It is possible that it is the absence of a resonance type of interaction that leaves the aryl CH bonds so little changed in α, α, α-trifluorotoluene. In fluorobenzene, the molecular orbital calculations indicated that it was the pi electron donating properties as well as the sigma electron withdrawal that produced the significant shortening of the ortho CH bonds. Unfortunately the α, α, α-trifluorobenzene molecule is too large to be optimized at the 4-21G level, with MONSTERGAUSS.

Figure 46

The CH-stretching overtone spectra of gas phase α, α, α-trifluorotoluene in the region of $\Delta v = 3$, single scan (lower spectrum) and $\Delta v = 4$, sum of 4 scans (upper spectrum). Recorded on the Beckman 5270; 12.75 m pathlength.

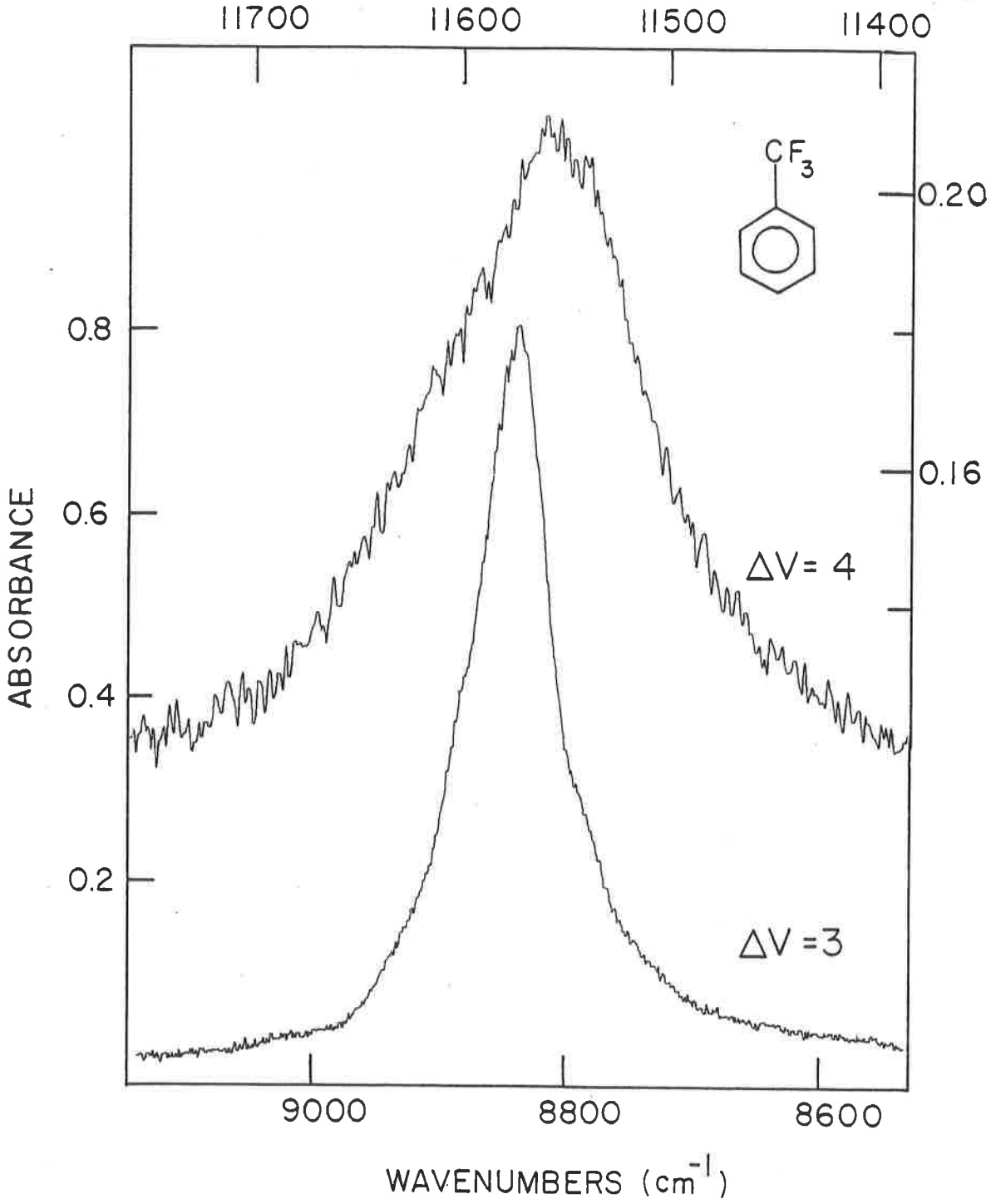
11700
11600
11500
11400
CF3
0.20
0.16
0.8
0.6
0.4
0.2
ABSORBANCE
ΔV= 4
ΔV =3
9000
8800
8600
WAVENUMBERS (cm-1)

CHAPTER 5

SUMMARY

The higher overtones of the CH-stretching vibrations have been used as a probe of the variations in CH bond length and strength in molecules containing a range of CH bond types. Conformationally and structurally inequivalent CH bonds give rise to partially resolved peaks in the overtone spectra. These spectra have been interpreted in terms of the local mode model[3,12,13,15-19], according to which all of the vibrational quanta are effectively localized in a single CH oscillator. The local mode parameters ω, the local mode frequency, and X, the local mode anharmonicity were determined for all spectrally resolved peaks, or for band maxima.

In the liquid phase overtone spectra of nitrobenzene, a partially resolved doublet was observed at each overtone, due to the differences between the CH bonds ortho, and those meta and para to the substituent. The assignment of the higher frequency peak to the ortho CH oscillators was confirmed by a partial deuteration study.

The liquid phase CH-stretching overtone spectra of nineteen halogen substituted benzenes from mono- to penta-substitution were recorded in the regions corresponding to Δv = 2-7. There was no evidence of inequivalent CH oscillators in the overtone lineshape nor did computer-assisted curve decomposition produce results which could be interpreted as such evidence. Two factors did suggest that inequivalent CH bonds, such as were found in nitrobenzene, did exist. First, the FWHM corresponded to the number of inequivalent CH oscillators anticipated, decreasing in the order: mono-, meta-di-> ortho-di-> para-di-, sym-tri- and penta-substituted. Second, the frequency shift of the overtone maxima for the di-substituted molecules was always meta > para >> ortho, a pattern which can be

understood with the assumption that the frequency shift depends on the proximity of the CH bond to the substituent.

A decrease in the magnitude of X was observed for molecules in which all or most of the CH bonds were sterically hindered by a bulky substituent: 1,3- and 1,4-dibromobenzene, 1,3,5-trichloro- and 1,3,5-tribromobenzene, 1,2,4,5-tetrachlorobenzene and the ortho CH oscillators of nitrobenzene.

The shift in the position of the overtone maximum with respect to that of benzene[55], $\Delta\bar{\nu}$ (cm^{-1}), was plotted against the value of σ_I, the inductive part of the Hammett sigma, for all molecules, at each overtone. The σ_I parameter provides an empirical measure of the sigma electron donating or withdrawing power of the substituent, at the meta and para positions, and has been shown to correlate with $\Delta\bar{\nu}$ at $\Delta v = 6$ for some mono- and di-substituted benzenes[53,54]. The correlation found in this work was only moderately good; for each level of substitution, mono-, di-, tri-, etc., the frequency shift increased more rapidly than the change in σ_I suggested, for the four halogens. There was also a scatter in the data for the disubstituted molecules, which depended on the position of the substituents (1,2- 1,3- or 1,4-) as noted above. It was found that the value of $\Delta\bar{\nu}$ for the meta + para peak in nitrobenzene correlated exactly with the overall least squares fit, while the value of the ortho peak was shifted well above the line. All of the above observations were attributed to the enhanced effect of the substituent(s) on the CH bonds ortho to them , an effect which cannot be accounted for by σ_I.

The dissociation energies were calculated from the local mode parameters, with either the Morse[68] or the Lippincott-Schroeder[69]

potential. There was little correlation between D_e and σ_I with either method. This was due in large part to the magnitude of the uncertainties of the local mode parameters.

The overtones of eight fluorobenzenes: mono, 1,2-, 1,3-, and 1,4-di-, 1,3,5-tri, 1,2,3,4-, 1,2,3,5-, and 1,2,4,5-tetrafluorobenzene, were obtained in the gas phase for Δv = 2-5. Peaks corresponding to inequivalent CH oscillators were observed in the spectra of the mono-, 1,2- and 1,3-disubstituted molecules. As expected from the small size of the substituent, there was no evidence, from the magnitude of X, of a decrease in anharmonicity due to steric crowding. Based on the excellent correlation between $\bar{\nu}_{CH}^{iso}$ [20] (fundamental vibrational frequency of an isolated CH bond in an otherwise deuterated molecule), or $\bar{\nu}$ (Δv=6), with the CH bond length, r_{CH}^{LM} (bond length calculated from the shift in the position of the overtone maxima) was calculated for all resolved peaks.

Molecular orbital calculations at the STO-3G and 4-21G levels were carried out for the molecules above. At the STO-3G level, full geometry optimizations were performed for all eight molecules. At 4-21G, literature[44,45] values for the optimized geometries of the mono-, 1,3-di- and 1,3,5-trisubstituted molecules were used for single calculations. Geometry optimizations at the 4-21G level were carried out for 1,2- and 1,4-difluorobenzene. A bond strength parameter, p^{Basis}, the sum of "ionic" plus "covalent" terms from the Mulliken population matrix[90,94], was devised in order to investigate the relationship between the changes in the electron population distribution and CH bond length. A number of other molecules were also optimized at the STO-3G or 4-21G level. The correlation between

r_{CH}^{LM} and r_{CH}^{STO-3G} or P^{STO-3G} was significant over a range of 0.02 Å in r_{CH}, but poor for the aryl CH bonds alone. At the 4-21G level, the correlation was excellent between r_{CH}^{LM} and r_{CH}^{4-21G}, ($r = 0.99$ for 22 data points). The correlation between r_{CH}^{LM} (aryl) and P^{4-21G} was also excellent. According to the definition of P^{Basis}, the increase in "ionic" strength was the most significant factor to correlate with the bond length decrease.

The problems in the correlation with σ_I were shown to derive mainly from two sources: the presence of unresolved inequivalent CH bond types in the liquid phase spectra, and the enhanced effect of a substituent on the CH bonds ortho to it. In contrast, the parameter, P^{Basis}, is additive up to tetra-substitution, and applies at the ortho, meta and para positions.

Doublets in the $\Delta v = 2$ spectra of 1,4-di- and 1,2,4,5-tetrafluorobenzene were attributed to residual rotational structure.

The aryl and methyl CH oscillators gave rise to well resolved absorption maxima at $\Delta v = 3, 4$ of toluene and the xylenes in the gas phase. Absorptions due to inequivalent aryl CH oscillators were partly resolved. The pattern was analogous to that of the corresponding fluorobenzenes, except that proximity to the CH_3 group results in an increase in CH bond length.

Of the two well resolved peaks in the methyl region of ortho-xylene, the higher frequency peak was assigned to the two CH bonds in the plane, and the lower frequency peak to the four CH bonds at 60° to the plane of the ring. This assignment is in agreement with the microwave spectra[122] and recent STO-3G geometry optimized[125] predictions on the minimum energy conformer.

In toluene, meta and para-xylene, a triplet was observed in the methyl region. The central peak was assigned to vibrational excitation of CH bonds on a freely rotating methyl group. The two outer peaks were assigned to inequivalent CH bonds on methyl groups in the minimum energy conformation, taken to be planar. 4-21G, geometry optimized calculations on toluene[46] confirmed the assignment of the aryl CH bonds. Hyperconjugative interactions were interpreted from the molecular orbitals. Variations in the electron population within a methyl CH bond, during internal rotation, were found in the Mulliken population matrix, and P^{4-21G}. The methyl CH bond length increase during rotation from 0° to 60° to the ring plane occurs because of its increased involvement in the hyperconjugation.

The gas phase overtone spectra of 1,3- and 1,4-cyclohexadiene were recorded for $\Delta v = 3$ and 4. In the alkene region, the spectra of both molecules display only a single, narrow, symmetric absorbance. This confirmed the equality of the four alkene CH bonds in the 1,3-isomer, as predicted from experimental[139,141-143] and geometry optimized ab initio calculations[150]. Two other well resolved absorbances at $\Delta v = 3$, 4 and 5 of the 1,3-isomer were observed, in agreement with the molecular orbital calculations[150] which predict inequivalent methylene CH bonds with axial/equatorial character. Only a single methylene absorbance was observed in the spectra of the 1,4-isomer, so that all four methylene CH bonds must be equivalent. This is possible only for a planar conformation. Previous experimental studies[141,145-148] have disagreed on the planarity of this molecule, although the molecular orbital calculations[150] also predicted planarity.

The overtone spectra of anisole in the liquid phase, Δv = 3-6, and in the gas phase, Δv = 2, 3, were obtained. There was only slight evidence of inequivalent aryl CH bonds even in the gas phase spectra, in contrast to the range of 0.005 Å predicted by STO-3G calculations. In the gas phase, the aryl band was relatively broad and asymmetric, at Δv = 3. Two lower frequency absorptions in the liquid phase spectra were assigned to the vibrations of methyl CH bonds at 0° and 60° to the ring plane. STO-3G calculations predicted that the shorter bond would be in the 0° position. Further studies on both the cyclohexadienes and on anisole are required for a complete assignment of these spectra.

There was little evidence of inequivalent CH bonds in the gas phase spectra of α,α,α-trifluorotoluene at Δv = 3 or 4. This substituent does not interact strongly with the ring pi system. The latter interaction was very important in the bond length changes in the fluorinated benzenes.

With regard to the work presented here, it would be particularly interesting to pursue the question of hindered internal rotation, raised by the spectra of toluene, the xylenes and anisole. Spectra at higher overtones, in the gas phase, and at various temperatures should yield further information on the problem.

The most significant outcome of the work reported here has been the remarkable usefulness of the combined overtone and ab initio calculations, the $r_{CH}^{LM}/r_{CH}^{4-21G}$ relationship. That absorptions due to inequivalent CH bonds can be resolved in the CH-stretching overtone spectra has long been known[3-7,31,47-55]. The range over which the bond length/frequency shift relationship holds probably covers the

entire range of CH bond types. In this work it has been shown to extend over 0.02 Å. McKean's studies on $\bar{\nu}^{iso}_{CH}$, to which the overtone frequencies correspond clearly, is valid over a range of 0.04 Å[20]. There are many advantages to working in the overtone region rather than the fundamental: it is not necessary to obtain the deuterated species of the molecule in question, unknown changes introduced by deuteration are avoided, peaks due to Fermi resonance are readily identifiable in an overtone series, and the general problem of mixing among modes, although reduced in the $\bar{\nu}^{iso}_{CH}$ spectra, is virtually eliminated. The overtone series provide further information, in the parameter X, since it is sensitive to the local environment, especially steric crowding.

A further advantage of working in the overtone region as compared to, for example, NMR, is that the time scale of the experiment is extremely rapid. The usefulness of this fact in studying rapid conformational changes has been demonstrated[32,77]. The overtone frequency is apparently more sensitive to small (~0.001 Å) changes in the CH bond length than any other experimental method. Electron diffraction studies regularly report uncertainties of 0.005 to 0.01 Å. Microwave studies can be extremely sensitive, but full substitution structures for molecules of the size examined here, are infrequent, and the CH bond lengths are most subject to error[83]. It is reasonable to conclude that the combined use of the local mode analysis of overtone spectra, with the optimized geometries from split-valence basis set ab initio calculations, will assist greatly in resolving conformational and structural problems in molecules of this size.

References

1. G. Herzberg, "Infrared and Raman Spectra of Polyatomic Molecules", (D. Van Nostrand Co., Inc., Princeton, N.J., 1945).
2. E.B. Wilson, J.C. Decius, and P.C. Cross, "Molecular Vibrations", (McGraw-Hill Book Co., N.Y. 1955).
3. J.W. Ellis, Trans. Farad. Soc. 25, 888 (1929).
4. R. Freymann, Ann. de Phys. 10^{e} serie, t. XX, 243 (1933).
5. H. Kempter, Zeitschrift f. Physik, Bd 116, 1 (1940).
6. R. Suhrmann and P. Klein, Zeitschrift f. Physik. Chem. B50, 23 (1941).
7. R. Suhrmann, Angew. Chem. 62, 507 (1950).
8. W. Siebrand, J. Chem. Phys. 46, 440 (1967).
9. W. Siebrand, J. Chem. Phys. 47, 2411 (1967).
10. W. Siebrand and D.F. Williams, J. Chem. Phys. 49, 1860 (1968).
11. T.E. Martin and M. Kalantar, J. Chem. Phys. 49, 235 (1968).
12. B.R. Henry and W. Siebrand, J. Chem. Phys. 49, 5369 (1968).
13. (a) R.J. Hayward and B.R. Henry, J. Mol. Spec. 57, 221 (1975), and reference therein;
    (b) R.J. Hayward and B.R. Henry, Chem. Phys. 12, 387 (1976).
14. J.L. Duncan, D.C. McKean, P.D. Mallinson and R.D. McCullough, J. Mol. Spectry. 46, 232 (1973).
15. R. Wallace, Chem. Phys. 11, 189 (1975).
16. B.R. Henry, Acc. Chem. Res. 10, 207 (1977).
17. B.R. Henry, "Vibrational Spectra and Structure" Vol. 10, J. Durig. Ed.; Elsevier, Amsterdam, 1981, p. 269.
18. R.T. Lawton and M.S. Child, Mol. Phys. 40, 773 (1980).

19. B.R. Henry, A.W. Tarr, O.S. Mortensen, W.F. Murphy and D.A.C. Compton, J. Chem. Phys. 79,2583 (1983).

20. D.C. McKean, Chem. Soc. Rev. 7, 399 (1978).

21. J.S. Wong and C.B. Moore, J. Chem. Phys. 77, 603 (1982).

22. Y. Mizugai and M. Katayama, Chem. Phys. Lett. 73, 240 (1980).

23. W.R.A. Greenlay and B.R. Henry, Chem. Phys. Lett. 53, 325 (1978).

24. B.R. Henry and R.J.D. Miller, Chem. Phys. Lett. 60, 81 (1978).

25. B.R. Henry, M. A. Mohammadi and J.A. Thomson, J. Chem. Phys. 75, 3165 (1981).

26. R.L. Swofford, M.E. Long and A.C. Albrecht, J. Chem. Phys. 65, 179 (1976).

27. W.M. Gelbart, P.R. Stannard and M.L. Elert, Int. J. Quantum Chem. 14, 703 (1978).

28. (a) H.S. Moller and O.S. Mortensen, Chem. Phys. Lett. 66, 539 (1979).

(b) O.S. Mortensen, B.R. Henry and M.A. Mohammadi, J. Chem. Phys. 75, 4800 (1981).

29. R.W. Taft in "Steric Effects in Organic Chemistry", M.S. Newman, Ed., (Wiley, N.Y. 1956). Ch. 13.

30. R.W. Taft, J. Am. Chem. Soc. 75, 4231 (1953); R.W. Taft and I.C. Lewis, J. Am. Chem. Soc. 80, 2436 (1958).

31. J.W. Ellis, Phys. Rev. 32, 906 (1928).

32. B.R. Henry, I-Fu Hung, R.A. MacPhail and H.L. Strauss, J. Am. Chem. Soc. 102, 515 (1980).

33. R.D. Guthrie and D.P. Wesley, J. Am. Chem. Soc. 92, 4057 (1970).

34. R.P. Young and R.N. Jones, Natl. Res. Coun. Canada, Bull. No. 11, Ottawa, 1968. Program PC-138.

35. W.J. Hehre, W.A. Lathan, R. Ditchfield, M.D. Newton and J.A. Pople, Q.C.P.E. 10, 236 (1974).

36. M.R. Petersen and R.A. Poirier, MONSTERGAUSS, Dept. of Chemistry, University of Toronto, Toronto, Ontario, Canada (1981).

37. J.S. Binkley, R.A. Whiteside, R. Krishnan, R. Seeger, D.J. Defrees, H.B. Schlegel, S. Topiol, L.R. Kahn and J.A. Pople, GAUSSIAN80, Dept. of Chemistry, Carnegie-Mellon University, Pittsburgh, PA, U.S.A. (1980).

38. W.C. Davidon, Math. Programming 9 1 (1975) and W.C. Davidon and L. Nazareth, Technical Memos 303 and 306, Appl. Math. Div., Argonne National Laboratories, Argonne, Illinois, U.S.A.

39. P. Pulay, Mol. Phys. 17, 197 (1969).

40. W.J. Hehre, R.F. Steward and J.A. Pople, J. Chem. Phys. 51, 2657 (1969).

41. P. Pulay, G. Fogarasi, F. Pang and J.E. Boggs, J. Am. Chem. Soc. 101, 2550 (1979).

42. J.S. Binkley, J.A. Pople and W.J. Hehre, J. Am. Chem. Soc. 102, 939 (1980).

43. L. Schäfer, C. Van Alsenoy and J.N. Scarsdale, J. Mol. Struct. (THEOCHEM) 86, 349 (1982).

44. P. Pulay, G. Fogarasi and J.E. Boggs, J. Chem. Phys., 74, 3999 (1981).

45. J.E. Boggs, F. Pang and P. Pulay, J. Comput. Chem. 3, 344 (1982).

46. F. Pang, J.E. Boggs, P. Pulay and G. Fogarasi, J. Mol. Struct. 66, 281 (1980).

47. J. Barnes and W.H. Fulweiler, J. Am. Chem. Soc. 49, 2034 (1927).

48. R. Freymann, Comptes Rendus 194, 1471 (1932).

49. G. Allard, Comptes Rendus 194, 1495 (1932).

50. P. Barchewitz, Comptes Rendus 206, 512 (1938).

51. R. Nakagaki and I. Hanazaki, Chem. Phys. Lett. 83, 512 (1981).

52. R. Nakagaki and I. Hanazaki, Chem. Phys. 72, 93 (1982).

53. Y. Mizugai, M. Katayama, J. Am. Chem. Soc. 102, 6424 (1980).

54. Y. Mizugai, M. Katayama and N. Nakagawa, J. Am. Chem. Soc. 103 5061 (1981).

55. C.K.N. Patel, A.C. Tam and R.J. Kerl, J. Chem. Phys. 71, 1470 (1979).

56. H.L. Fang and R.L. Swofford, J. Chem. Phys. 73, 2607 (1980).

57. W.R.A. Greenlay and B.R. Henry, J. Chem. Phys. 69, 82 (1968).

58. M.S. Burberry and A.C. Albrecht, J. Chem. Phys. 71, 4631 (1979).

59. H.L. Fang and R.L. Swofford, J. Chem. Phys. 72, 6382 (1980).

60. R.A. Fisher and F. Yates, "Statistical Tables for Biological, Agricultural and Medical Research", 3rd ed., (Hafner Publishing Co., New York, 1948) p. 46.

61. K.M. Gough and B.R. Henry, J. Phys. Chem. 87, 3433 (1983).

62. M. Charton, Prog. Phys. Org. Chem. 13, 119 (1981).

63. O. Exner in "Correlation Analysis in Chemistry, Recent Advances", N.B. Chapman and J. Shorter, Eds., (Plenum Press, New York and London, 1978), Ch. 10.

64. R.D. Topsom, Prog. Phys. Org. Chem. 12, 1 (1976).

65. W.F. Reynolds, Prog. Phys. Org. Chem. 14, 165 (1983) and references therein.

66. T. Fujita and T. Nishioka, Prog. Phys. Org. Chem. 12, 49 (1976).

67. W.F. Reynolds, P. Dais, D.W. MacIntyre, R.D. Topsom, S. Marriott, E. von Nagy-Felsobuki and R.W. Taft, J. Am. Chem. Soc. 105, 378 (1983).

68. P.M. Morse, Phys. Rev. 34, 57 (1929).

69. E.R. Lippincott and R. Schroeder, J. Chem. Phys. 23, 1131 (1955).

70. K.V. Reddy, D.F. Heller and M.J. Berry, J. Chem. Phys. 76, 2814 (1982).

71. R.M. Badger, J. Chem. Phys. 2, 128 (1934).

72. R.M. Badger, J. Chem. Phys. 3, 710 (1935) and references therein.

73. R.M. Badger and S.H. Bauer, J. Chem. Phys. 5, 839 (1937).

74. H.J. Bernstein, Spectrochim. Acta 18, 161 (1962).

75. D.C. McKean and I. Torto, J. Mol. Struct. 81, 51 (1982).

76. D.C. McKean, private communication.

77. J.S. Wong, R.A. MacPhail, C.B. Moore and H.L. Strauss, J. Am. Chem. Soc. 86, 1478 (1982).

78. L. Schäfer, J. Mol. Struct. 100, 51 (1983) and references therein.

79. R.A. Whiteside, J.A. Binkley, R. Krishnan, D.J. Defrees, H.B. Schlegel and J.A. Pople, "Carnegie-Mellon Quantum Chemistry Archive", Carnegie-Mellon University, Pittsburgh, PA, U.S.A. 15213, (1980) p. 119.

80. J. Jokisaari, J. Kuonanoja, A. Pulkkinnen and T. Väänänen, Mol. Phys. 44, 197 (1981).

81. L. Nygaard, I. Bojesen, T. Pedersen and J. Rastrup-Andersen, J. Mol. Struct. 2, 209 (1968).

82. E.E. Babcock, R.C. Long Jr. and J.H. Goldstein, J. Mol. Struct. 74, 111 (1981).

83. D.C. McKean, J. Chem. Phys. 79, 2095 (1983).

84. P. Diehl and J. Jokisaari, J. Mol. Struct. 53, 55 (1979).

85. L. Pauling, H.D. Springer and K.J. Palmer, J. Am. Chem. Soc. 61, 927 (1939).

86. L. Pauling, "The Nature of the Chemical Bond" (Cornell University Press, Ithaca, N.Y., 1945) Ch. 8.

87. C.A. Coulson, "Valence" (Oxford University Press, 1953) Ch. 8.

88. C.A. Coulson, J. Phys. Chem. 56, 311 (1952), and references therein.

89. B.P. Stoicheff and G. Herzberg, Nature 175, 80 (1955).

90. R.S. Mulliken, J. Chem. Phys. 23, 2338 (1955).

91. H.A. Bent, Chem. Rev. 61, 275 (1961).

92. S.F. Boys in "Quantum Theory of Atoms, Molecules and the Solid State", (Academic Press, N.Y. 1966) p. 253.

93. C. Edmiston and K. Ruedenberg, Rev. Mod. Phys. 35, 457 (1953).

94. R.S. Mulliken, J. Chem. Phys. 23, 1833 (1955).

95. W.J.P. Blonski, F.E. Hruska and T.A. Wildman, private communication.

96. J.E. Boggs, D.C. McKean, private communication.

97. W.J. Hehre, L. Radom and J.A. Pople, J. Am. Chem. Soc. 94, 1496 (1972).

98. D. Steele and D.H. Whiffen, Trans. Farad. Soc. 56, 177 (1960).

99. S. Marriott and R.D. Topsom, J. Mol. Struct. 89, 83 (1982).

100. P.R. Wells, S. Erhensen and R.W. Taft, Prog. Phys. Org. Chem. 6, 147 (1968).

101. R.T.C. Brownlee, J. DiStephano and R.D. Topsom, Spectrochim. Acta 31A 1685 (1975).

102. E.L. Siebert, W.P. Reinhardt and J.T. Hynes, Chem. Phys. Lett. 92, 455 (1982).

103. A. Stojiljkovic and D.H. Whiffen, Spectrochim. Acta 12, 47 (1958).

104. J.H.S. Green and D.J. Harrison, Spectrochim. Acta 32A, 1185 (1976).

105. J.H.S. Green, W. Kynaston and H.M. Paisley, J. Chem. Soc. 473 (1963).

106. J.R. Nielsen, C.-Y. Liang and D.C. Smith, Disc. Farad. Soc. 9, 177 (1950).

107. V.J. Eaton and D. Steele, J. Mol. Spec. 48, 446 (1973).

108. D.H. Whiffen, Phil. Trans. Roy. Soc. London 248A, 131 (1955) and references therein.

109. D.C. McKean, Chem. Comm., 1373 (1971).

110. D.C. McKean, J.L. Duncan and L. Batt, Spectrochim. Acta 29A, 1037 (1973).

111. D.C. McKean, Spectrochim. Acta 31A, 861 (1975).

112. D.C. McKean and R.A. Watt, J. Mol. Spectry. 61, 184 (1976).

113. D.C. McKean, H.J. Becker and F. Bramsiepe, Spectrochim. Acta 33A, 951 (1977).

114. J.L. Breuil, D. Cavagnat, J.C. Cornut, M.T. Forel, M. Fouassier and J. Lascombe, J. Mol. Struct. 57, 35 (1979).

115. D. Cavagnat, J.C. Cornut and J. Lascombe, J. Chim. Phys. - Chim. Biol. 76, 341 (1979).

116. D. Cavagnat and J. Lascombe, J. Mol. Spectry. 92, 141 (1982), and references therein.

117. D. Cavagnat and J. Lascombe, J. Chem. Phys. 76, 4336 (1982).

118. T. Iijima, Z. Naturforsch. 32A, 1063 (1977).

119. R. Seip, Gy. Schultz, I. Hargittai and Z.G. Szabo, Z. Naturforsch. 32A, 1178 (1977).

120. W.A. Kreiner, H.D. Rudolph and B.T. Tan, J. Mol. Spectry. 48, 86 (1973).

121. K.S. Pitzer and D.W. Scott, J. Am. Chem. Soc. 63, 803 (1943); C.A. Wulff, J. Chem. Phys. 39, 1227 (1963).

122. H.D. Rudolph, K. Walzer and I. Krutzik, J. Mol. Spectry. 47, 314 (1973).

123. J. Haupt and W. Müller-Warmuth, Z. Naturforsch. 23A, 208 (1968).

124. C.A. Wulff, J. Chem. Phys. 39, 1227 (1963).

125. K.M. Gough, B.R. Henry and T.A. Wildman, unpublished results.

126. B.R. Henry and W.R.A. Greenlay, J. Chem. Phys. 72, 5516 (1980).

127. W.C. Hamilton, J.W. Edmonds, A. Tippe and J.J. Rush, Disc. Farad. Soc. 48, 192 (1969).

128. J.W. Perry and A.H. Zewail, J. Phys. Chem. 86, 5197 (1982).

129. M. Sowa, K.M. Gough and B.R. Henry, unpublished results.

130. W.J.E. Parr and T. Schaefer, Acct. Chem. Res. 13, 400 (1980).

131. P.B. Ayscough, M.C. Brice and R.E.D. McClung, Mol. Phys. 20, 41 (1971).

132. A. Langseth and B.P. Stoicheff, Can. J. Phys. 34, 350 (1956).

133. J. Herranz and B.P. Stoicheff, J. Mol. Spectry. 10, 448 (1963).

134. F.H. Allen, O. Kennard and R. Taylor, Acct. Chem. Res. 16, 146 (1983) and references therein.

135. W.C. Ermler and R.S. Mulliken, J. Am. Chem. Soc. 100, 1647 (1978).

136. A. Pross, L. Radom and N.V. Riggs, J. Am. Chem. Soc. 102, 2253 (1980).

137. L.J. Bellamy and D.W. Mayo, J. Phys. Chem. 80, 1217 (1976).

138. E. Flood, P. Pulay and J.E. Boggs, J. Am. Chem. Soc. 99, 5570 (1977).

139. S.S. Butcher, J. Chem. Phys. 42, 1830 (1965).

140. G. Luss and M.D. Harmony, J. Chem. Phys. 43, 3768 (1965).

141. H. Oberhammer and S.H. Bauer, J. Am. Chem. Soc. 91, 10 (1969).

142. G. Dallinga and L.H. Toneman, J. Mol. Struct. 1, 11 (1967).

143. M. Tratteberg, Acta Chem. Scand. 22, 2305 (1968).

144. L.A. Carreira, R.O. Carter and J.R. Durig, J. Chem. Phys. 59, 812 (1973).

145. H.D. Stidham, Spectrochim. Acta 21, 23 (1965).

146. B.J. Monostori and A. Weber, J. Mol. Spectry. 12, 129 (1964).

147. E.W. Garbisch, Jr. and M.G. Griffith, J. Am. Chem. Soc. 90, 117 (1968).

148. G. Dallinga and L.H. Toneman, J. Mol. Struct. 1, 117 (1967).

149. J. Laane and R.C. Lord, J. Mol. Spectry. 39, 340 (1971).

150. S. Saebo and J.E. Boggs, J. Mol. Struct. 73, 137 (1981).

151. T.A. Wildman, Ph.D. Thesis, University of Manitoba, Winnipeg, Manitoba (1982), and references therein.

152. H. Tylli and H. Konschin, J. Mol. Struct. 42, 7 (1977).

153. H. Tylli, H. Konschin and C. Grundfelt-Forsius, J. Mol. Struct. 55, 157 (1979).

154. H. Tylli, H. Konschin and C. Grundfelt-Forsius, J. Mol. Struct. 77, 51 (1981), and references therein.

155. T. Schaefer, T.A. Wildman and J. Peeling, J. Mag. Res. 56, (1984).

156. G.M. Korenowski and A.C. Albrecht, Chem. Phys. 38, 239 (1979).

157. D.F. Heller and S. Mukamel, J. Chem. Phys. 70, 463 (1979).

158. G.A. West, R.P. Mariella Jr., J.A. Pete, W.B. Hammond and D.F. Heller, J. Chem. Phys. 75, 2006 (1981).

159. J.H. Callomon, E. Hirota, K. Kuchitsu, W.J. Lafferty and A.G. Maki, Landolt-Börnstein, Neue Serie II/7, 1-14 (1976).

160. E.B. Wilson, Int. J. Quant. Chem.: Quant. Chem. Symp. 13, 5-14 (1979).

161. R.G. Snyder, A.L. Aljibury, H.L. Strauss, H.L. Casal, K.M. Gough and W.F. Murphy, unpublished results.